Engineering Aspects of Nitrification
with Immobilized Cells

Jan H. Hunik

Promotor: dr. ir. J.Tramper

Hoogleraar in de bioprocestechnologie

STELLINGEN

1 In onderzoek naar nitrificatie met vlokkig actief slib van Hanaki et al. (1990), wordt ten onrechte geen rekening gehouden met de diffusiesnelheid van zuurstof in deze vlokken.
K. Hanaki *et al.* in Water Research **24**, 289-296, 1990

2 De problemen van de intensieve veehouderij worden het best geïllustreerd door een massabalans van stikstof en fosfaat over Nederland.

3 Naast de door Coleman & Montgomery (1993) genoemde redenen voor het mislukken van onderzoeksprojecten in produktiebedrijven, moet het gemis aan onderzoekservaring in de bedrijfsleiding worden toegevoegd.
D.E. Coleman & D.C. Montgomery in Technometrics **35**, 1-12, 1993

4 Het koppelen van een natte zomer aan voorspellingen over klimaatsveranderingen als gevolg van menselijk handelen mist elke grond.

5 Het opzetten van stekels door egels en het op een congres presenteren van grote hoeveelheden wiskundige vergelijkingen leiden beide tot een communicatie-stoornis.

6 Het niveau waarop kennis tijdens congressen wordt uitgewisseld verbetert aanmerkelijk, indien wetenschappers een cursus volgen in het gebruik van audio-visuele hulpmiddelen.

7 Bovenstaande stelling wordt slechts ter harte genomen door wetenschappers die reeds in staat zijn een goede presentatie te geven.

8 De voortvarendheid waarmee gemeentes voetbalwedstrijden afgelasten is niet representatief voor de aanpak van andere gemeentelijke aangelegenheden.

9 Het wijdverbreid gebruik om bij koninklijk bezoek het interieur een verfbeurt te geven, leidt tot een voor hen ongewenste verhoogde blootstelling aan oplosmiddelen.

10 Een auto is niets anders dan een consumptie-artikel.

11 Zonder de vrolijke oogopslag kan het rennend zwijn in het Veluwelooplogo ten onrechte worden gezien als op de vlucht.

Stellingen behorende bij het proefschrift " Engineering aspects of nitrification with immobilized cells"

Jan H. Hunik

Wageningen, 3 december 1993

Jan H. Hunik

Engineering Aspects of Nitrification

with Immobilized Cells

VOORWOORD

Het gereed komen van dit proefschrift is ook de gelegenheid om iedereen die hier een bijdrage aan heeft geleverd te bedanken. Allereerst mijn vader en moeder die een belangrijke stimulerende invloed hebben gehad op mijn schoolloopbaan.

Uiteraard de sectie Proceskunde waar een prettige en stimulerende werksfeer heerste. Vanaf het eerste (natte) fietstochtje in de Ardennen tot de laatste werkbespreking voelde ik mij hier thuis. Het half 6 Loburg zal dan ook node gemist worden.

Hans Tramper, die naast waardevolle discussies over het onderzoek ook steun en toeverlaat was tijdens de minder wetenschappelijk perikelen rondom het onderzoek. Dankzij zijn onvoorwaardelijke steun was het mogelijk het proefschrift af te ronden. Bedankt coach!

Mijn kamergenoten en mede nitrificeerders René Wijffels, Imke Leenen, Vitor Santos en Ida Gunther.

De studenten in volgorde van opkomst: David Vertegaal, Harold Meijer, Gerrit-Jan Runia, Annemarie Rooden, Kees Bos, Joris van Rooij, Vitor Santos, Marijke van den Hoogen, Wiebe Jonsma, Ronald Kostanje, Peter van der Weij. Zonder jullie inbreng was dit proefschrift aanzienlijk dunner geweest.

Kees de Gooijer voor zijn modelmatige ondersteuning, Gerrit Meerdink voor de gezamelijke inspanning om de resonantie nozzel te doorgronden en Hedy Wessels die nu eenmaal de spil van de sectie is en waarmee naast de printer ook veel levenswijsheden werden gedeeld.

Het zwemploegje met Hans Tramper, Nettie Buitelaar, Anja Jansen, Albert van der Padt, Henk van Sonsbeek, René Wijffels, Joyce Kraus, Vitor Santos en Gerrit Heida. Zij zorgden voor de nodige ontspanning en zagen mijn gekrabbel uitgroeien tot een redelijke borstcrawl.

De medewerkers van de werkplaats, fotolocatie, tekenkamer en chemicaliën-magazijn.

Tot slot mijn huisgenootjes van de Hoogstraat 71^a die altijd hun willig oor leenden voor de (niet-)wetenschappelijke beslommeringen en deze in het juiste perspectief wisten te plaatsen tijdens de vele gezamelijken maaltijden.

Contents

1 INTRODUCTION

T he oxidation of ammonia via nitrite to nitrate by microorganisms of the *Nitrobacteracaea* family is generally known as nitrification (Watson, 1974):

$$NH_4^+ + 1.5\ O_2 \rightarrow NO_2^- + 2\ H^+ + H_2O$$
$$NO_2^- + 0.5\ O_2 \rightarrow NO_3^-$$
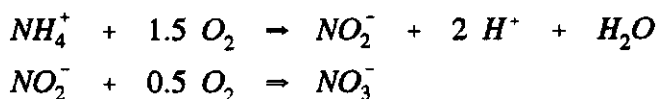
The microorganisms of this family are strictly autotrophs with the exception of a few *Nitrobacter winogradskyi* strains under anaerobic conditions (Bock et al., 1988). Autotrophic growth, i.e. with CO_2 as the only carbon source, results in a low biomass yield compared to heterotrophic microorganisms. Therefore, the nitrification process is characterized by a low growth rate of the nitrifying bacteria.

An increasing interest for the biological removal of ammonia from various waste streams has been the driving force to solve the problem of washout due to the low growth rate of these microorganisms. A characteristic value for the doubling time of nitrifying microorganisms at maximum growth rate is 15-30 h, which is long compared to a doubling time of 1.5-3 h for heterotrophic microorganisms isolated from wastewater treatment plants (Sharma & Ahler, 1977). The growth rate of nitrifying microorganisms decreases rapidly at more extreme conditions, i.e. high product and substrate concentrations. The biomass retention becomes increasingly important for nitrification processes at such unfavourable conditions. Several methods for biomass retention are applied, for example, attached growth and artificial immobilization.

Generally, attached growth of cells is achieved on a wide variety of support materials. An overview of the different support materials (silica, wood shavings, ceramic, porous brick, glass fibre, ion exchanger, PVC chips and porous glass) used for attached growth is given by Klein & Ziehr (1990). Artificial immobilization techniques include: flocculation, covalent bonding, cell to cell crosslinking, microencapsulation and entrapment in polymer matrices (Klein & Vorlop, 1985; Philips & Poon, 1988; Woodward, 1988; Klein & Kressdorf, 1989). The entrapment in polymer matrices with a high water content is by far the most frequently used technique. With this technique the cells are immobilized in the network of a polymer matrix. Substrates and products, on the other hand, are generally small enough to diffuse through this network.

The advantage of the attached growth is the spontaneous attachment of the cells to the support without the use of an additional apparatus. The advantages of artificial biofilms above attached growth biofilms is the fixed boundary between solid and liquid phase and the absence of biofilm detachment. The cell retention of entrapped cells will be better compared to cells growing in an attached growth biofilm (Klein & Ziehr, 1990). Here we will focus on the application of artificially immobilized nitrifying microorganisms. An overview of the available methods and the pros and cons are presented. Large-scale processes with immobilized cells require an immobilization procedure with sufficient capacity. Artificial immobilization methods for nitrifying microorganisms are evaluated and the scale up of a specific immobilization technique is discussed.

The theory and engineering tools for the cultivation of cells in two-phase systems consisting of a liquid and a gas phase is comprehensive. The theory for processes having a third phase with growing microorganisms is mainly derived from the theory for heterogeneous reactions used in chemical engineering; main reference is Levenspiel (1972). Applications of this theory for processes with immobilized cells are given by Venkatasubramanian et al. (1983), Moser (1988) and Riet & Tramper (1991). However,

the application of this theory to nitrification processes is scarce. Literature where a link is made between the different aspects - nitrification, immobilization, modelling and scale-up - is lacking. Models, methods for model validation, immobilization techniques, scale-up and some preliminary experiments with artificially immobilized pure cultures of *Nitrosomonas europaea* and *Nitrobacter agilis* are discussed here.

IMMOBILIZED-CELL PROCESSES

T he third phase with immobilized cells introduces an additional step for substrate transport. Compared to suspended-cell reactors a mass-transfer step between liquid phase and immobilized cells is introduced, see Figure 1.
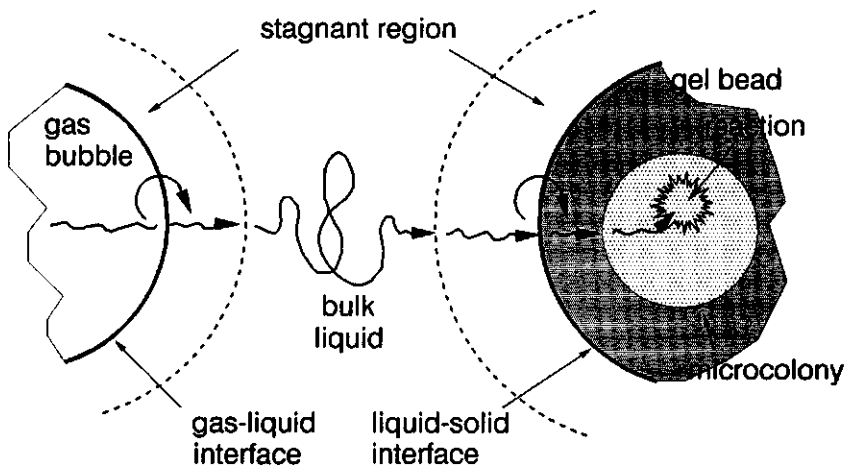

Figure 1   Transport of substrate from gas phase to immobilized cells.

Transport from the liquid to the solid-phase surface is described by a liquid-solid mass-transfer coefficient. In the solid phase both transport and consumption of substrate will take place. For an immobilized-cell process the growth rate of the cells is no longer the rate-limiting step, because of the high biomass retention. Introduction of a third phase is only then beneficial when mass transfer is a faster process than growth. A comparison between the time-scale of cell growth and mass transfer presented by Roels (1982) shows a 1000 fold faster rate for mass transfer compared to growth. Changing the rate-limiting step from growth to mass transfer can therefore be an advantage.

Models. The nitrification process with immobilized cells is complicated due to the relation between the microorganisms and the substrates involved. Oxygen is used by both microorganisms and ammonia is converted to nitrate via nitrite as intermediate. The nitrite-consuming microorganisms are strictly dependent on the nitrite production in the first step. This commensalistic relation together with the competition for oxygen, the development of gradients of biomass, oxygen, ammonia, nitrite and nitrate in the solid phase are hampering a better understanding of the immobilized-cell nitrification process. Modelling can be a helpful tool then. Models for immobilized-cell processes can be divided in steady-state and dynamic models. Steady-state models describe the nitrifying capacity and reactor concentrations at constant input values, such as substrate concentration and dilution rate. Examples of steady-state biofilm models with nitrifying and heterotrophic microorganisms are given by: Chen et al. (1989), Gujer & Boller (1989), Tanaka & Dunn (1982), Tanaka et al. (1981), Rittman & Manem (1992) and Wanner & Gujer (1984). In practice it is very unlikely that all input values are constant. The influent concentrations as well as the dilution rate of a nitrifying reactor will vary in time. This changes in input values can be described when dynamic models are used. Differences between dynamic and steady-state models and several methods for solving the mass balances of such a biological reactor are discussed by Billing & Dold (1988[a,b,c]). The advantage of a dynamic model is its capability to describe the nitrifying capacity and

reactor concentrations in transient state, which is of particular interest during the start-up phase. Also the influence of influent concentration or temperature changes on the process can be predicted. Dynamic biofilm models with nitrifying and heterotrophic microorganisms are presented by: Bryers (1988), Denac et al. (1983), Kissel et al. (1983) and Wanner & Gujer (1986). An example of a dynamic model for an artificially immobilized *Nitrobacter agilis* is presented by Gooijer et al. (1991) and Wijffels et al. (1991).

Model validation. Model validations can be divided into methods in which the overall reactor concentrations or conditions are measured as function of time and methods which follow the biofilm processes in the solid phase. Examples of the first methods, where the coarse of reactor concentrations as function of time is monitored, can be found in: Tanaka & Dunn (1982), Tanaka et al. (1981), Bryers (1988), Cour Jansen & Harremoës (1984), Williamson & McCarty (1976). Other examples are the measurement of overall fluorescence (Müller et al., 1988; Reardon et al., 1986) and NMR spectra (Lohmeijer-Vogel et al., 1990) in the reactor with immobilized cells.

The second methods are based on the determination of the concentration profiles in the biofilm as function of time. Examples: Lewandowski et al. (1991, 1993), Beer & Heuvel (1988), Beer et al. (1993), Hooijmans et al (1990[a]), and Hooijmans et al. (1990[b]), who all use microelectrodes to measure oxygen concentration profiles in different types of biofilms. The location of the solid-phase surface and the copying of reactor conditions in the measurement set-up are very important for the accuracy of the measurement with these microelectrodes. Another example is determination of biomass profiles in the biofilm. A detailed investigation of the biomass composition and distribution in such biofilms is an important aspect in biofilm research (Christensen et al., 1989). Artificially immobilized pure cultures of cells offer the possibility to determine such a biomass distribution in biofilms. Several methods for the determination of such biomass profiles are used. Examples of techniques based on the fixation of gel beads and cross-sectioning

5

of these beads are: a scanning microfluorimetry technique used by Monbouquette et al. (1990) for immobilized *Zymomonas mobilis* cells; a toluidine-blue staining method for artificially immobilized *Nitrobacter agilis* by Wijffels et al. (1991). Examination of biofilm growth on a solid support is done with a radiolabelling technique of thin biofilm slices by Bryers & Banks (1990).

The second method is advantageous for the study of biofilm processes, because the processes inside the biofilm can be investigated. Microelectrodes provide a fast and accurate substrate profile when the reactor situation is copied correctly. The latter is however the difficult part. The measurement of biomass profiles does not have such problems and can be very accurate, but has the disadvantage to be very laborious.

ARTIFICIAL IMMOBILIZATION OF NITRIFYING BACTERIA

A n overview of artificial-immobilization techniques available for a wide variety of cells is given by Scott (1987) and Klein & Vorlop (1985). So far nitrifying microorganisms are only artificially immobilized by entrapment in various matrices; no examples of cell cross-linking and encapsulation in membrane-surrounded microcapsules can be found. Table I gives an overview of entrapped nitrifying microorganisms. Three methods are used for entrapment: thermo-gelation, ionotropic gelation and polymerization.

Thermo-gelation. The thermo-gelation with a temperature-controlled phase transition requires low ion concentrations. This low ion concentration makes thermo-gelation with for instance agar a suitable method for experiments with microelectrodes in nitrifying biofilms (Beer & Heuvel 1988, Beer et al. 1990). High ion concentrations would interfere with the microelectrodes. The immobilization in an agar gel however yields a mechanical weak gel. The disadvantage of such a weak gel is not relevant for

6

laboratory studies, but large-scale applications in reactors with much turbulence, i.e. shear, are for that reason unlikely.

Ionotropic gelation. Table I shows that immobilization of nitrifyers with an ionotropic-gelation technique is applied most often. Two types of gels are mainly used: alginate stabilized with Ca^{2+} and κ-carrageenan stabilized by K^+. These types of gelling material offer sufficient mechanical stability and a mild immobilization procedure. Ionotropic gels offer the possibility to produce small spheres of a uniform diameter with the resonance nozzle (Hulst et al., 1985; Hunik & Tramper, 1993).

The characterization of cell viability, growth, substrate-consumption rate and influence of diffusion is extensively done for both immobilized *Nitrosomonas europaea* and *Nitrobacter agilis* cells (Ginkel & Tramper, 1983; Tramper et al., 1985; Tramper & Man, 1986; Tramper & Grootjen, 1986; Wijffels & Tramper, 1989; Wijffels et al.,1990). An illustrative example of the growth of microcolonies and subsequent development of a biofilm in the outer layer of the gel beads is shown by Neerven et al.(1990). It is valid to assume that the immobilized cells have the same intrinsic kinetics as free cells, which is shown with the substrate affinity at different cell concentrations in the gel beads and various gel-bead diameters (Ginkel & Tramper, 1983; Tramper et al., 1985; Tramper & Man, 1986). Diffusion-limited transport of substrate is apparently masking the intrinsic kinetics.

Polymerization. The advantage of polymerization as immobilization technique is the independence of the Ca^{2+} or K^+ concentration in the wastewater. The disadvantage of the polymerization with PEG , acrylamide or epoxy is the rather hostile environment for the bacteria during immobilization. Sumino et al.(1992) report a loss in activity of more than 90 %. Also Tanaka et al.(1991) describe activity losses of more than 95% for acrylamide and epoxy-immobilized cells.

Table 1   *Immobilization methods used for (de)nitrifying bacteria*

method	organism(s)	reference
thermo-gelation		
agar	*Nitrobacter agilis*	Wijffels et al. (1991)
ionotropic gelation		
alginate	*Nitrosomonas europaea*	Ginkel et al. (1983)
alginate	(de) nitrifyers	Tramper (1984), Lewandowski et al. (1987), Tramper et al. (1985)
alginate	*Nitrobacter agilis*	Tramper & Man (1986), Tsai et al. (1986)
carrageenan	*Nitrosomonas europaea*	Wijffels et al. (1989), Neerven et al. (1990)
carrageenan	*Nitrobacter agilis*	Tramper & Grootjen (1986), Wijffels et al. (1990), Gooijer et al. (1990), Gooijer et al. (1991), Gooijer et al. (1992)
carrageenan	(de)nitrifyers	Santos et al. (1992)
polymerization		
polyvinylalcohol (PVA)	active sludge	Hashimoto & Furukawa (1986)
PVA	(de)nitrifyers	Myoga et al. (1991), Asano et al. (1992), Asano et al. (1992), Hitachi (1988), Wildenauer et al.(1992)
PVA, chitosan	*Nitrosomonas europaea*	Kokufuta et al. (1982), Kokufuta et al. (1987), Kokufuta et al. (1988)
polyethyleenglycol (PEG), acrylamide, epoxy	(de)nitrifyers	Tanaka et al. (1991)
PEG, acrylamide	nitrifyers	Sumino et al. (1992)
urethane	nitrifyers	Sumino et al. (1992)
silicone, alginate, epoxy	nitrifyers	Wilke & Vorlop (1990)
silica	nitrifyers	Petersen et al. (1991)

Immobilization in PEG also shows a low cell survival; Tanaka et al.(1991) report an activity loss of 85-95% for PEG-immobilized cells after immobilization but nevertheless a stable nitrification process for 60 days.

Several procedures are developed to overcome the high activity losses and some promising techniques are presented. Sumino et al.(1992) present an immobilization by urethane polymerization using a macromolecular coagulant. The activity losses are limited to 60-90%. Long-term (120 d) experiments are carried out with these urethane immobilized nitrifying bacteria. An alternative immobilization method is presented by Kokufuta et al. (1982), Kokufuta et al. (1987), Kokufuta et al. (1988). They use tri-methyl-ammonium chitosan iodide for the aggregation of the cells in the culture broth and subsequently added PVA-sulphate to form a stable complex with the aggregates. Only short-term (800 h) experiments are presented, which show growing *Nitrosomonas europaea* cells. Myoga et al.(1991), Asano et al.(1992[a]. 1992[b]) describe an immobilization method with PVA in which the cells are mixed with 20% polymer solution and subsequently frozen at -20 to -80 °C. They present no results about the cell survival after immobilization, but stable nitrification was carried out for 70 days. Myoga et al. (1991) show that immobilization of active sludge, instead of pure cultures, in PVA was beneficial for steady-state nitrifying capacity. Another method is given by Wildenauer et al. (1992) who added 20 % w/v sugar or glycerol to the PVA solution before immobilization. A possible explanation could be that both sugar and glycerol solutions as well as the active sludge do not enhance the nitrifying capacity itself but create more space in the PVA-matrix for nitrifying bacteria. This additional space for the cells in the matrix is then responsible for the increased nitrifying capacity.

Prospects of artificially immobilized cells. The potential applications of artificially immobilized nitrifying microorganisms for wastewater treatment are based on the separation of biomass retention and liquid retention, resulting in higher ammonia removal rates (Tramper, 1984; Tramper, 1987; Lewandowski et al., 1987; Wijffels et al.,1990). It is also shown that *Nitrobacter agilis* cells immobilized in alginate are less affected by inhibitory compounds (Tsai et al., 1986). An interesting example of artificial immobilization is the possibility to create an inner and outer layer with different species

9

of microorganisms in them. This method with *Nitrosomonas europaea* at the outside and *Pseudomonas denitrificans* inside is presented by Santos et al. (1992) for the integration of the nitrification and denitrification process.

Immobilization in ionotropic gels is most suitable for biofilm studies. The stabilization of ionotropic gels by either Ca^{2+} or K^+ ions is a disadvantage for application in wastewater. Polymerization offers stable gels, but scale up of the polymerization technique is not yet fully developed. Therefore, ionotropic gelation seems to be the most convenient method currently available.
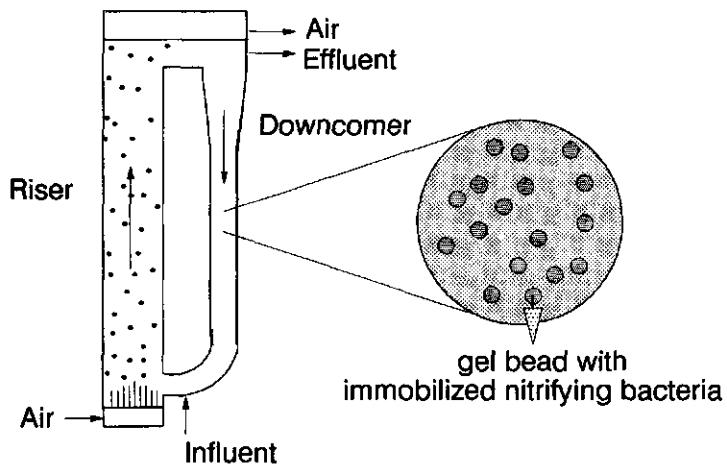

Figure 2   *Air-lift loop reactor.*

10

BIOREACTORS

M echanically stirred-tank reactors are not suitable for immobilized-cell processes due to the high local shear forces at the impeller. Small-scale experiments (170 cm^3) with epoxy-carrier beads with immobilized *E. coli* cells show increased abrasion with increased stirrer speed (Klein & Eng, 1979). The breakage of nylon microcapsules in a turbine reactor (318 cm^3) was proportional to the stirrer speed (Poncelet & Neufeld, 1989). The local shear forces around the stirrer and the tip speed of the impeller will increase drastically with increased reactor scale. An alternative for mechanically stirred reactors is the air-lift loop reactor. (Figure 2)

Gas sparging at the bottom of the riser and gas liquid separation at the top of the reactor is the origin of a density difference between riser and downcomer. This density difference is the driving force for liquid circulation in the reactor. In this way sufficient mixing and mass transfer without stirring can be achieved. The principles and theoretical aspects of air-lift loop reactors are described by Chisti (1989) and Verlaan (1987).

SCALE UP

A pplication of immobilized cells for nitrification implies scale-up of the process. Translation of bench-scale experiments to production scale of more than 100 m^3 requires design rules and extension of immobilization methods. Scale-up of bioprocesses aims at a constant physical and chemical environment for the microorganisms independent of the volume of the reactor. It is obvious that it is not possible to derive scale-up rules, which keep all these chemical and physical parameters constant. Small-scale experiments and careful evaluation of the large-scale design should reveal those physical and chemical parameters, which are important at large scale.

11

The currently used techniques for immobilization are sufficient for the bench-scale experiments, but not amenable for large-scale applications. High-capacity immobilization methods are therefore necessary for pilot and production-scale nitrification processes with immobilized cells. Besides high production capacity also spherical shape and uniform size of the gel beads are required.

Scale up of immobilization methods. Dripping of the aqueous κ-carrageenan gel solution in a stirred potassium chloride solution is the easiest procedure for cell immobilization. A productivity of 0.2 $dm^3.h^{-1}$ (Hulst et al., 1985) and 0.43 $dm^3.h^{-1}$ (Schmidt, 1990) can be realized. Scale up is done by multiplication of the dripping equipment, i.e. more syringes. Higher production rates of immobilized cells are also achieved with two other methods: dispersion in air or liquid and extrusion of the gel solution. With the dispersion-in-air method the κ-carrageenan gel is dispersed in air by a rotating-disk atomizer and collected in a hardening solution (Ogbonna et al. 1989, 1991). A production rate of 1.05 $dm^3.h^{-1}$ is reported for this method. For the dispersion in liquid the gel is dispersed by stirring in an non-aqueous continuous phase. Hardening is achieved by changing the temperature of this continuous phase (Castillo et al., 1992; Audet and Lacroix, 1989). The procedure is shown to work batch-wise in a 1.5-dm^3 vessel. With the extrusion technique the gel solution is pressed through a small orifice at such a flow rate that a jet is formed (Hulst et al., 1985). An improvement of the extrusion technique resulted in a production of 27.6 $dm^3.h^{-1}$ (Hunik & Tramper, 1993). The dispersion and extrusion technique are both amenable to further scale up. However, Audet and Lacroix (1989) and Ogbonna et al. (1991), who themselves use the dispersion technique, mention that gel beads made with the extrusion technique of Hulst et al. (1985) are more uniform and reproducible.

Scale-up strategy. Large-scale applications of bioprocesses need the reproduction of laboratory-scale experiments at pilot or production scale. Trial and error together with the extrapolation of reactor volume are among the most straight-forward methods for

12

scale up. Several rules-of-thumb methods are also used and are based on maintaining a constant value for a specific parameter, for example: power to volume ratio, gas-liquid oxygen transfer, tip speed of the impeller, O_2- tension, and gas-flow rate per reactor volume (Sweere et al. 1987, Hubbard 1987). This constant-parameter method implicitly assumes that the parameter is related to the rate-limiting step of the process. The constant-parameter method is widely used in the fermentation industry, which is primarily dealing with bioprocesses having two phases, i.e. a gas phase and a liquid phase with suspended cells. A more mechanistic approach, based on characteristic times, to determine the rate-limiting step of such two-phase bioprocesses is proposed by Sweere et al. (1987), Roels (1983) and Moser (1988). This regime analysis is based on a careful evaluation of all transport and conversion processes that take place.

Establishing the rate-limiting step in immobilized-cell processes is more difficult, due to the introduction of the a solid third phase. Regime analysis is used by Schouten et al. (1986) to compare the reactor design of immobilized *Clostridium* cells in a fluidized-bed and a gas-lift reactor. The effect of immobilization on the cells was neglected and the regime analysis was limited to the processes in the gas and liquid phase. The theory for the regime analysis needs an extension, which is described by Hunik et al. (1993) for dealing with cells immobilized in a third phase, for which the effects of immobilization can not be neglected.

APPLICATION OF CO-IMMOBILIZED PURE CULTURES

I mmobilization of pure cultures of *Nitrosomonas europaea* and *Nitrobacter agilis* is mainly restricted to immobilization in alginate and κ-carrageenan gels (Table 1). In a series of well controlled experiments (Ginkel et al. 1983, Tramper & Man 1986, Tsai et al. 1986, Wijffels et al. 1989, Tramper & Grootjen 1986, Wijffels et al. 1991) the effects of immobilization on *Nitrosomonas europaea* and *Nitrobacter agilis* are presented

13

with respect to growth, pH effects, substrate affinity, inhibitory effects and storage stability. A next and logical step to achieve overall conversion of ammonia to nitrate is the co-immobilization of *Nitrosomonas europaea* and *Nitrobacter agilis* (Wijffels et al. 1990, Hunik & Tramper 1990). An alternative for the immobilization of pure cultures is the immobilization of active sludge, a mixture of heterotrophic microorganisms, nitrifying microorganisms and inert organic material from wastewater-treatment plants (Tramper et al. 1985, Tramper 1987). The advantages of the immobilization of pure cultures compared to the immobilization of active sludge, however, are numerous: no incorporation of heterotrophs in the gel beads, the possibility to concentrate the pure cultures before immobilization, reduction of the amount of gel beads needed for nitrification.

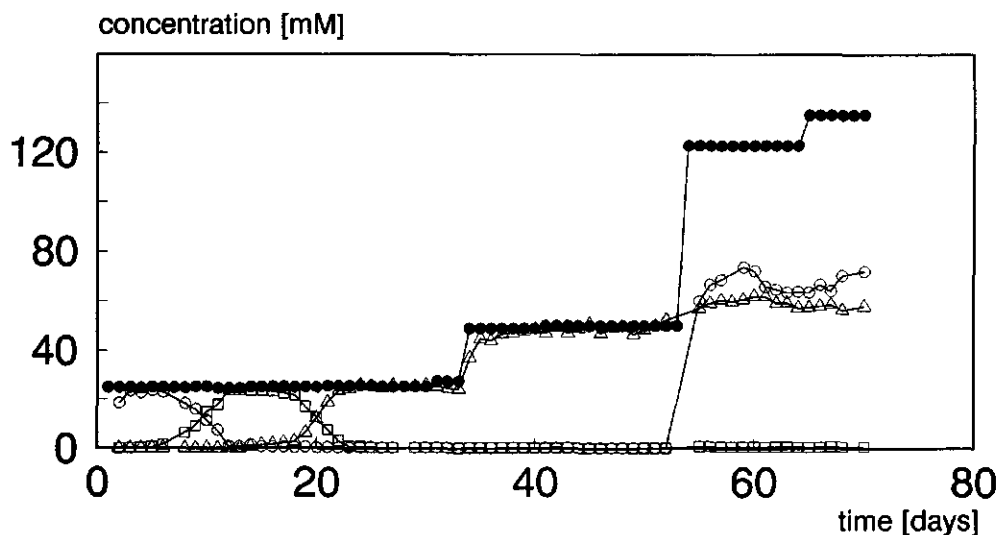

Figure 3   *Influent NH_4^+ (—●—) and effluent NH_4^+ (—○—), NO_2^- (—□—), NO_3^- (—△—) concentrations in an 3.3 dm³ air-lift loop reactor with co-immobilized N. europaea and N. agilis. The liquid dilution rate is 1.2 * 10⁻⁵ s⁻¹.*

Two examples of small-scale experiments with co-immobilized *N. europaea* and *N. agilis* cells are shown in Figure 3 and 4. In the experiment shown in Figure 3 the ammonium concentration was step-wise increased. At day 52 it can be observed that the ammonium was not completely converted to nitrate and nitrite accumulation occurred. The maximum nitrification capacity was thus reached, but the limiting factor could not be derived from this experiment. Reactor concentrations or maximum biomass concentration could be both responsible for this.
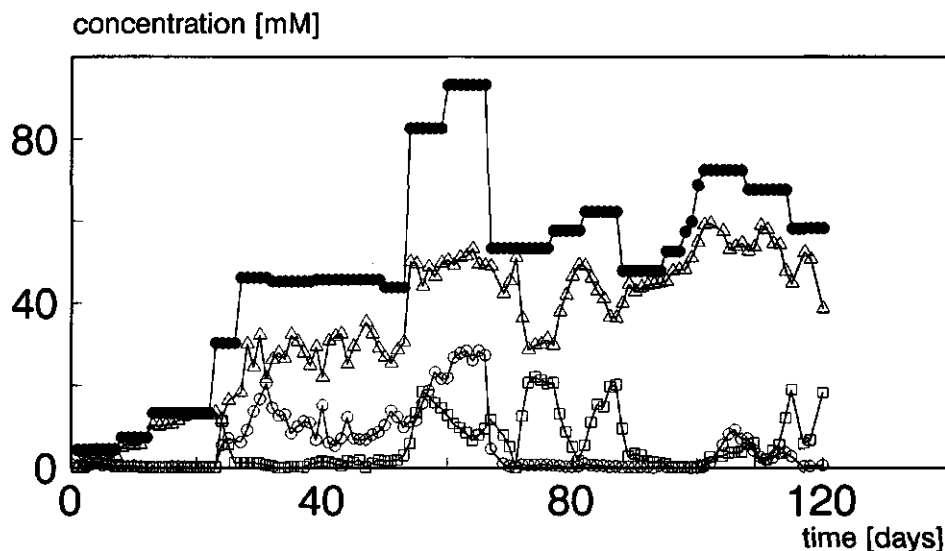
concentration [mM]

Figure 4   *Influent NH_4^+ (—●—) and effluent NH_4^+ (—○—), NO_2^- (—□—), NO_3^- (—△—) concentrations in an 3.3 dm³ air-lift loop reactor with co-immobilized N. europaea and N. agilis. Liquid dilution rate is 3.7 * 10⁻⁵ changing to 1.9* 10⁻⁵ s⁻¹ and the influent concentration was doubled at day 54.*

A second experiment shown in Figure 4 was done. After 50 days a steady state ammonia conversion was reached. At that moment the influent concentration is doubled and the dilution rate reduced to half the steady-state value, so that the total amount of ammonium offered per unit of time is the same. After this change in reactor conditions accumulation of nitrite occurred. The substrate and product concentrations seem thus to be important for a nitrification process with immobilized cells. The influence of high substrate and product concentrations on *N. europaea* and *N. agilis* is therefore important for the application of immobilized nitrifying cells in concentrated wastestreams. Furthermore the balance between the ammonia and nitrite oxidizing cells seems to be very delicate and nitrite accumulation can easily occur.

OUTLINE OF THE THESIS

C hapters 1 to 7 in this thesis can be read as independent articles. The coherence of the chapters 2 to 7 is demonstrated in this Introduction. In chapter 2 and 3 the kinetics of, respectively, *N. europaea* and *N. agilis* are described with emphasis on extreme conditions. An improved method for immobilization with ionotropic gels, including the theoretical background, is presented in chapter 4. In chapter 5 a method for the determination of biomass profiles for co-immobilized *N. europaea* and *N. agilis* in one gel bead is given. Chapter 6 presents a dynamic model for nitrification with immobilized cells of *N. europaea* and *N. agilis*, with experimental validation. A strategy for the scale-up of this process is presented in chapter 7. The last chapter contains a short general discussion of this thesis.

REFERENCES

Asano H, Myoga H, Asano M, Toyao M (1992) A study of nitrification utilizing whole microorganisms immobilized by PVA-freezing method. Wat Sci Tech 26:1037-1046.

Asano H, Myoga H, Asano M, Toyao M (1992) Nitrification treatability of whole microorganisms immobilized by PVA-freezing method. Wat Sci Tech 26:2397-2400.

Audet P, Lacroix C (1989) Two-phase dispersion process for the production of biopolymer gel beads: effect of various parameters on bead size and their distribution. Process Biochem 2:217-226.

Beer D de, Heuvel JC van den (1988) Gradients in immobilized biological systems. Analytica Chimica Acta 213: 259-265

Beer D de, Heuvel JC van de, Sweerts JPRA (1990) Microelectrode studies in immobilized biological studies. In: Physiology of immobilized cells. Bont JAM de, Visser J, Mattiasson B, Tramper J (eds) Elsevier science publishers, Amsterdam, the Netherlands, 613-624.

Beer D de, Heuvel JC van den, Ottengraf SPP (1993) Microelectrode measurements of the activity distribution in nitrifying bacterial aggregates. Appl Environ Microbiol 59:573-579.

Billing AE, Dold PL (1988) Modelling techniques for biological reaction systems. 1. Mathematical description and representation. Water SA 14:185-192.

Billing AE, Dold PL (1988) Modelling techniques for biological reaction systems. 1. Modelling of the steady state case. Water SA 14:193-206.

Billing AE, Dold PL (1988) Modelling techniques for biological reaction systems. 1. Modelling of the dynamic case. Water SA 14:207-218.

Bock E, Wilderer PA, Freitag A (1988) Growth of *Nitrobacter* in absense of dissolved oxygen. Wat Res 22:245-250.

Bryers JD (1988) Modeling biofilm accumulation. In: Bazin MJ; Prosser JI (ed). Physiolological models in microbiology, vol 2. CRC Press, Boca Raton Fl, USA, 109-144.

Bryers JD, Banks MK (1990) Assessment of biofilm ecodynamics. In: Physiology of immobilized cells. Bont JAM de, Visser J, Mattiasson B, Tramper J (eds) Elsevier science publishers, Amsterdam, the Netherlands, 49-61.

Castillo E, Ramírez D, Casas L, López-Munguía A (1992) A two-phase methode to produce gel beads. Application in the design of a whole cell β-galactosidase catalyst. Appl Biochem Biotech 34/35:477-486.

Chisti MY (1989) Airlift bioreactors, Elsevier Science Publishers, Essex, England.

Chen GH, Ozaki H, Terashima Y (1990) Modelling of the simultaneous removal of organic substances and nitrogen in a biofilm. Wat Sci Tech 21:791-804.

Christensen FR, Holm Kristensen G, Cour Janssen J la (1989) Biofilm structure - an important and neglected parameter in waste water treatment. Wat Sci Tech 21:805-814.

Cour Jansen J la, Harremoës P (1984) Removal of soluble substrates in fixed films. Wat Sci Tech 17:1-14.

Denac M, Uzman S, Tanaka H, Dunn IJ (1983) Modeling of experiments on biofilm penetration effects in a fluidized bed nitrification reactor. Biotechnol Bioeng 25:1841-1861.

Ginkel CG van, Tramper J, Luyben KChAM, Klapwijk A (1983) Characterization of *Nitrosomonas europaea* immobilized in calcium alginate. Enzyme Microb Technol 5: 297-303.

Gooijer CD de, Wijffels RH, Tramper J (1990) Modelling the growth of immobilized *Nitrobacter agilis* cells. In: Physiology of immobilized cells. Bont JAM de, Visser J, Mattiasson B, Tramper J (eds) Elsevier science publishers, Amsterdam, the Netherlands, 355-360.

Gooijer CD de, Wijffels RH, Tramper J (1992) Dynamic modeling the growth of immobilized nitrifying bacteria: biofilm development. In: Biofilms, Science and Technology. Eds. LF Melo et al. Kluwer Academic Publishers, the Netherlands, 291-296.

Gooijer CD de, Wijffels RH, Tramper J (1991) Growth and substrate consumption of *Nitrobacter agilis* cells immobilized in carrageenan: part 1. Dynamic modeling, Biotechnol Bioeng 38: 224-231.

Gujer W, Boller M (1989) A mathematical model for rotating biological contactors. In: Proceedings of the technical advances in bioreactors conference, Nice, CFRP-AGHTM Paris. 69-89.

Hashimoto S, Furukawa K (1987) Immobilization of activated sludge by PVA-boric acid method Biotechnol Bioeng 39: 52-59.

Hitachi Plant engineering and construction (1990) Bioreactor for nitrogen removal. Bioprocess Eng 5:188

Hooijmans CM, Briasco CA, Huang J, Geraats SGM, Barbotin JN, Thomas D, Luyben KChAM (1990[a]) Measurement of oxygen concentration gradients in gel-immobilized recombinant *Escherichia coli*. Appl Microbiol Biotechnol 33:611-618.

Hooijmans CM, Geraats SGM, Niel EWJ van, Robertson LA, Heijnen JJ, Luyben KChAM (1990[b]) Determination of growth and coupled nitrification/denitrification by immobilized *Thiosphaera pantotrofa* using measurement and modelling of oxygen profiles. Biotech Bioeng 36:931-939.

Hubbard DW (1987) Scale-up strategies for bioreactors. In: Biotechnology Processes, Scale-up and mixing. Ho CS, Oldshue JY (eds) American Institute of Chemical Engineers, New York, USA, 168-184.

Hulst AC, Tramper J, Van 't Riet K, Westerbeek JMM (1985) A new technique for the production of immobilized biocatalysts in large quantities. Biotech Bioeng 27:870-876.

Hunik JH, Tramper J (1993) Large-scale production of κ-carrageenan droplets for gel-bead production: theoretical and practical limitations of size and production rate. Biotech Progress 9:186-192.

Hunik JH, Tramper J, Wijffels RH (1993) A strategy to scale-up nitrification processes with immobilized cells of *Nitrosomonas europaea* and *Nitrobacter agilis*. Submitted for publication. (Chapter 7)

Kissel JC, McCarty PL, Street RL (1984) Numerical simulation of mixed-culture biofilm. J Environ Eng 110:393-411.

Klein J, Eng H (1979) The measurement of abrasion. In: Characterization of immobilized biocatalysts. Buchholz K (ed) Dechema monographs 84:292-299.

Klein J, Kressdorf B (1989) Polymers for the immobilization of whole cells and their application in biotechnology. Die Angewandte Makromolekulare Chemie 166/167:239-309.

Klein J, Vorlop K-D (1985) Immobilization techniques - cells. In: Comprehensive biotechnology, The principles of biotechnology: engineering considerations. Moo-Young M, Cooney CL, Humphrey AE (eds) Pergamon press, Oxford, UK, 2:203-224.

Klein J, Ziehr H (1990) Immobilization of microbial cells by adsorption. J Biotechnology 16:1-16.

Kokufuta E, Matsumoto W, Nakamura I (1982) Immobilization of *Nitrosomonas europaea* cells with polyelectrolyte complex. Biotechnol Bioeng 24:1591-1603.

Kokufuta E, Yukishige M, Nakamura I (1987) Coimmoblization of *Nitrosomonas europaea* and *Paracoccus denitrificans* cells using polyelectrolyte complex stabilized calcium alginate gel. J Ferment Technol 65:659-664.

Kokufuta E, Shimohashi M, Nakamura I (1988) Simultaneously occurring nitrification and denitrification under oxygen gradient by polyelectrolyte complex-coimmobilized *Nitrosomonas europaea* and *Paracoccus denitrificans* cells. Biotechn Bioeng 31:382-384.

Levenspiel O (1972) Chemical reactor engineering. 2nd ed. John Wiley, New York, USA

Lewandowski Z, Bakke R, Characklis WG (1987) Nitrification and autotrophic denitrification in calcium alginate beads. Wat Sci Tech 19:175-182.

Lewandowski Z, Walser G, Characklis WG (1991) Reaction kinetics in biofilms. Biotech Bioeng 38:877-882.

Lewandowski Z, Altobelli SA, Fukushima E (1993) NMR and microelectrode studies of hydrodynamics and kinetics in biofilms. Biotech Prog 9:40-45.

Lohmeier-Vogel EM, McIntyre DD, Vogel HJ (1991) Nuclear magnetic resonance spectroscopy as an analytical tool in biotechnology. In: Physiology of immobilized cells. Bont JAM de, Visser J, Mattiasson B, Tramper J (eds) Elsevier science publishers, Amsterdam, the Netherlands, 661-676.

Monbouquette HG, Sayles GD, Ollis DF (1990) Immobilized cell biocatalyst activation and pseudo-steady-state behaviour: model and experiment. Biotechnol Bioeng 35:609-629.

Moser A (1988) Bioprocess technology: kinetics and reactors, Spinger Verlag, New York, USA.

Müller W, Wehnert G, Scheper T (1988) Fluorescence monitoring of immobilized micro-organisms in cultures. Anal Chim Acta 213: 47-53

Myoga H, Asano H, Nomura Y, Yoshida H (1991) Effects of immobilization conditions on the nitrification treatability of entrapped cell reactors using the PVA freezing method. Wat Sci Tech 23:1117-1124.

Neerven ARW van, Wijffels RH, Zehnder AJB (1990) Scanning electron microscopy of immobilized bacteria in gel beads: a comparative study of fixation methods. J Microbiol Methods 11:157-168.

Ogbonna JC, Matsumura M, Yamagata T, Sakuma H, Kataoka H (1989) Production of micro-gel beads by a rotating disk atomizer. J Ferment Bioeng 68:40-48.

Ogbonna JC, Matsumura M, Kataoka H (1990) Effective oxygenation of immobilized cells through reduction in bead diameters: a review. Process Biochem 26:109-121.

Petersen SO, Henriksen K, Blackburn TH (1991) Coupled nitrification-denitrification associated with liquid manure in a gel-stabilized model system. Biol Fertil Soils 12:19-27.

Philips CR, Poon YC (1988) Immobilization of cells, Biotechnology monographs 5. Aiba S, Fan LT, Fiechter A, Klein J, Schrügerl K (eds), Spinger Verlag, Berlin, Germany.

Poncelet D, Neufeld RJ (1989) Shear breakage of nylon membrane microcapsules in a turbine reactor. Biotech Bioeng 33:95-103.

Reardon KF, Scheper T, Bailey JE (1986) In situ fluorescence monitoring of immobilized Clostridium acetobutylicum. Biotech lett 8:817-822.

Riet K van 't, Tramper J (1991) Basic bioreactor design. Marcel Dekker, New York, USA.

Rittmann BE, Manem JA (1992) Development and experimental evaluation of a steady-state, multispecies biofilm model. Biotechnol Bioeng 39:914-922.

Roels JA (1983) Energetics and kinetics in biotechnology. Elsevier biomedical press, Amsterdam, The Netherlands.

Santos VA, Tramper J, Wijffels RH (1992) Integrated nitrification and denitrification with immobilized microorganisms. In: Biofilms - Science and Technology. Melo LF, Bott TR, Fletcher M, Capedeville B (eds) Kluwer academic publishers, Dordrecht, The Netherlands. 449-453.

Schmidt J (1990) Untersuchung und modellierung der autotrophen trinkwasserdenitrification mit matriximmobilisierten Parracoccus denitrificans DSM 1403. PhD Thesis, University of Carolo-Wilhelmina, Braunschweig, Germany.

Schouten GH, Guit RP, Zieleman GJ, Luyben KChAM, Kossen NWF (1986) A comparative study of a fluidized bed reactor and a gas lift loop reactor for the IBE process: Part 1. Reactor design and scale-down approach. J Chem Tech Biotechnology 36:335-343.

Scott CD (1987) Immobilized cells: review of recent literature. Enzyme Microb Technol 9:66-73.

Sharma B, Ahler RC (1977) Nitrification and nitrogen control. Wat Res 11:897-925.

Sumino T, Nakamura H, Mori N, Kawaguchi Y, Tada M (1992) Immobilization of nitrifying bacteria in porous pellets of urethane gel for removal of ammonium nitrogen from waste-water. Appl Microbiol Biotechnol 36:556-560.

Sumino T, Nakamura H, Mori N, Kawaguchi Y (1992) Immobilization of nitrifying bacteria by polyethylene glycol prepolymer. J Ferment Bioeng 73:37-42.

Sweere APJ, Luyben KChAM, Kossen NWF (1987) Regime analysis and scale-down: tools to investigate the performance of bioreactors. Enzyme Microb Technol 9:386-398.

Tanaka H, Uzman S, Dunn IJ (1981) Kinetics of nitrification using a fluidized sand bed reactor with attached growth. Biotech Bioeng 23:1638-1702.

Tanaka H, Dunn IJ (1982) Kinetics of biofilm nitrification. Biotech Bioeng 24:669-689.

Tanaka K, Tada M, Kimata T, Harada S, Fujii Y, Mizuguchi T, Mori N, Emori H (1991) Development of new nitrogen removal systems using nitrifying bacteria immobilized in synthetic resin pellets. Wat Sci Tech 23:681-690.

Tramper J (1987) Nitrification and denitrification by immobilized viable cells. In: Enzyme Engineering 8, Laskin AI, Mosbach L, Thomas D, Wingard LB (eds) Ann N Y Acad Sci 501:362-366.

Tramper J (1984) Nitrification and denitrification by immobilized bacteria. In: Proc Third Eur Congr Biotechnol, VCH publishers, Weinheim, Germany, 4:363-368.

Tramper J, Man AWA de (1986) Characterization of *Nitrobacter agilis* immobilized in calcium alginate. Enzyme Microb Technol 8:472-476.

Tramper J, Grootjen DRJ (1986) Operating performance of *Nitrobacter agilis* immobilized in carrageenan. Enzyme Microb Technol 8:477-480.

Tramper J, Suwinska-Borowiec G, Klapwijk A (1985) Characterization of nitrifying bacteria immobilized in calcium alginate, Enzyme Microb Technol 7:155-160.

Tsai Y-L, Schlasner SM, Tuovinen OH (1986) Inhibitor evaluation with immobilized *Nitrobacter agilis* cells. Appl Environm Microb 52:1231-1235.

Venkatasubramanian K, Karkare SB, Vieth WR (1983) Chemical engineering analysis of immobilized-cell systems. Appl Biochemistry and Bioengineering 4:311-349.

Verlaan P (1987) Modelling and characterization of an airlift-loop reactor, PhD Thesis, Wageningen Agricultural University, The Netherlands.

21

Wanner O, Gujer W (1984) Competition in biofilms. Wat Sci Tech 17:27-44.

Wanner O, Gujer W (1986) A multispecies biofilm model. Biotechnol Bioeng 28:314-328.

Watson SW (1974) In: Bergey's Manual of determinative bacteriology, 8th edn, Buchanan RE, Gibbons NE (eds) Williams and Wilkins, Baltimore, USA.

Wildenauer FX, Menzel R, Vetter H, Vorlop K-D, Remmers P (1992) Process and equipment for the removal of ammonium, nitrite and nitrate from wastewater, European Patent 0475540A1.

Williamson K, McCarty PL (1976) Verification studies of the biofilm model for bacterial substrate utilization. J WPCF 48:281-296.

Wijffels RH, Gooijer CD de, Kortekaas S, Tramper J (1990) *Nitrobacter agilis* immobilized in carrageenan: oxygen consumption and biomass density. In: Physiology of immobilized cells. Bont JAM de, Visser J, Mattiasson B, Tramper J (eds) Elsevier science publishers, Amsterdam, the Netherlands, 475-480.

Wijffels RH, Gooyer CD de, Kortekaas S, Tramper J (1991) Growth and substrate consumption of *Nitrobacter agilis* cells immobilized in carrageenan. Part 2: Model evaluation, Biotech Bioeng 38:232-240.

Wijffels RH, Tramper J (1989) Performance of growing *Nitrosomonas europaea* cells immobilized in κ-carrageenan. Appl Microbiol Biotechnol 32:108-112.

Willke T, Vorlop KD (1990) Immobilization of especially cultivated nitrifying bacteria by adsorption or entrapment for application to environment and food. Dechema Biotechnology Conferences , VCH publishers.

Woodward J (1988) Methods of immobilization of microbial cells. J Microbiol Methods 8:91-102.

2 KINETICS OF *NITROSOMONAS EUROPAEA*

SUMMARY

N itrification of ammonia in concentrated waste streams is gaining a lot of attention nowadays. *Nitrosomonas europaea* is the predominant ammonia-oxidizing species in these environments. Prediction of the behaviour of a pure culture of *Nitrosomonas europaea* (ATCC 19718) under conditions prevailing in concentrated waste streams was the aim of this study. The initial oxygen consumption rate of a concentrated cell suspension was used as a rapid assay to measure the effects on *Nitrosomonas europaea* at various conditions. Several relations, based on Michaelis-Menten kinetics, were derived. They describe the behaviour of *Nitrosomonas europaea* at substrate (NH_4^+), product (NO_2^-) and K^+, Na^+, SO_4^{2-}, NO_3^-, Cl^- concentrations up to 500 M and a pHs ranging from 6.5 to 8.5. High concentrations of ions inhibited *Nitrosomonas europaea* but specific substrate inhibition was not observed. Product inhibition was strongly pH-dependent and severe inhibition at pH 6.5 was found.

INTRODUCTION

N itrogen removal by biological nitrification and denitrification is commonly used in sewage treatment plants, where ammonia concentrations are relatively low with maxima of 3.33 and 14.3 mM NH_4^+ reported by Wild et al. (1971) and Shieh & LaMotta (1979), respectively. Nitrification of waste streams, with high concentrations of ammonia, is gaining more attention due to problems in the treatment of manure (St-Arnaud et al. 1991; Loynachan et al. 1976; Bortone & Piccinini 1991; Osada et al. 1991), leachate of landfills (Knox 1985) and industrial waste waters. Concentrations up to 500 mM NH_4^+, together with high concentrations of other ions, can occur in these waste streams.

So far, kinetic studies with nitrifying bacteria have mainly been focused on the more-dilute waste streams. For example the total nitrogen concentrations in the kinetic experiments of Anthonisen et al. (1976), Laudelout et al. (1976) and Voets et al. (1975) are 71, 110, 94 mM, respectively. More recently Gee et al. (1990) estimated kinetic parameters for substrate inhibition in a mixed population of nitrifying bacteria, but the ammonia concentrations did not exceed 71 mM.

From the scarce literature available it became clear that there is a lack of kinetic studies with pure cultures of nitrifying bacteria under the conditions prevailing in the treatment of manure waste streams, leachate of landfills and industrial waste water. Only Loehr et al. (1973) reported nitrification of animal wastes with ammonia concentrations up to 500 mM NH_4^+, they qualitatively observed inhibition with increasing ammonia concentrations. In a study on the influence of copper on *Nitrosomonas europaea* by Sato et al. (1988), where ammonia concentrations up to 264 mM NH_4^+ are used as a control, substrate inhibition was only observed at the highest concentration of 264 mM NH_4^+.

Gaining a better understanding of the nitrification process is complicated due to the different behaviour of the two major bacterial genera, i.e. *Nitrosomonas* and *Nitrobacter*, under extreme conditions. An improved knowledge of the pertinent bacteria

24

is necessary for the design of treatment plants for concentrated waste streams. The oxidation of ammonium to nitrite is the first step in nitrification, and the predominant ammonium-oxidizing species isolated by Soriano & Walker(1973) in soil with a high ammonia concentration is *Nitrosomonas europaea*. Recently (St-Arnaud et al. 1991), *N. europaea* was successfully used as inoculum to enhance nitrification in swine manure. Therefore, we determined the behaviour of this species at ammonium, nitrite and nitrate concentrations ranging from 0 to 500 mM. In addition the influence of pH and high salt concentrations (up to 500 mM) was investigated.

Gradients of pH, substrate and product are observed (Szwerinski et al. 1986; Beer 1990) in nitrifying biofilms. Equations describing conversion of NH_4^+ and NO_2^- as a function of pH, substrate, product and salt concentration are thus useful for modelling the nitrification process in biofilms. Parameters for substrate affinity, product inhibition and salt inhibition at a wide range of concentrations were derived based on Michaelis-Menten kinetics for enzymes. The effects of pH, ranging from 6.5 to 8.5, on these parameters were also investigated. Substrate inhibition was not observed in contrast to product inhibition which strongly depends on the pH of the medium.

MATERIALS AND METHODS

Media. All media and solutions ware made up in demineralized water. The chemicals used were Analytical Grade and were obtained from Merck.

Chemostat. The *N. europaea* (ATCC 19718) cells were maintained in a 2.5 dm^3 sterile chemostat with a dilution rate of 0.0125 h^{-1}. The culture was kept at 30°C. The medium contained per dm^3 of demineralized water: 2.51 g $(NH_4)_2SO_4$; 0.25 g $MgSO_4.7H_2O$; 0.78 g $NaH_2PO_4.2H_2O$; 0.89 g $Na_2HPO_4.2H_2O$; 0.74 mg $CaCl_2.2H_2O$; 2.5 mg $FeSO_4.7H_2O$; 0.08 mg $CuSO_4$. The pH was kept at 7.4 with a $NaHCO_3$

(80 g.dm^{-3}) solution. Cells were withdrawn from the chemostat by collecting the effluent for 32 h in a sterile vessel, which was kept at 4 °C.

Cell harvesting and concentration. The cells collected from the chemostat were washed and concentrated before they were used in the activity assay. Approximately 1 dm^3 effluent of the chemostat was collected and first centrifuged at 16300 g for 30 min at a temperature of 4 °C. The pellet was resuspended in 0.1 dm^3 of a 1 mM phosphate buffer (pH 7.5) and centrifuged for the second time. The cells were resuspended in 25 cm^3 of a 1 mM phosphate buffer and stored on ice until they were used in the activity assay. The concentration and harvesting procedure was repeated for each measuring day.

Buffer. Phosphate and Tris/HCl have been used to determine the optimal pH of *N. europaea*. In the present study the activity was assayed in the pH range of 6.5 to 8.0 with phosphate buffer and 7.5 to 8.5 with Tris/HCl buffer. Also a combination of both buffers was tested over this pH range. This was done to avoid the fall in activity at the change of buffer at a pH of 7.5 such as observed by Ginkel et al. (1983). The pertinent pK_a for the pH range of the phosphate buffer is 7.2 and of Tris/HCl 8.1 at 30°C.

Trace elements and CO_2. With the concentration procedure the growth medium of the cells is replaced by a 1 mM phosphate buffer solution. For the activity assay, buffer and substrate were added, but for experimental convenience no trace elements nor bicarbonate were added. To study if experimental errors due to the absence of trace elements and bicarbonate could be introduced, Mg^{2+}, Ca^{2+}, Fe^{2+} and Cu^{2+} concentrations were tested in a range from 0 to 5 times the growth medium concentration and a concentration range of 0 to 10 mM for HCO_3^-. An additional washing step, similar to the second step in the concentration procedure with the concentrated cells suspension, was made to be sure that all trace elements from the medium were removed. Standard conditions (pH 7.5 and 25 mM NH_4^+) were used in these activity assays.

Activity assay. The oxygen consumption rate of a concentrated cell suspension was used as a rapid assay to screen and quantify the effects of the extreme conditions in

26

concentrated waste streams. The oxygen consumption rate was measured with a Biological Oxygen Monitor (Yellow Springs Instrument, Ohio, USA). In an 8 cm³ vessel, 0.5 cm³ of the concentrated cell suspension was added together with buffer and an appropriate concentrated solution of ions or product (as specified in the Results and Discussion section). Demineralized water was added to make up to 4 cm³ and the suspension was aerated for 5 min. Then the vessel was sealed with the O_2 electrode (model 5331, Yellow Springs Instrument, Ohio, USA) such that no air bubbles remained in the liquid. Ammonia was added through the seal with an analytical syringe (0.1 cm³) to make up to the desired substrate concentration. For that a concentrated NH_4^+ solution (2 M) was used such that the liquid volume did not change significantly. The decrease in oxygen concentration (between 100-80 % air saturation) was then recorded as a function of time. All activity assays were done at 30°C. A different procedure was followed in the experiments with a substrate concentration above 100 mM NH_4^+; the desired substrate concentration was then made up directly in the at the beginning of the experiment in the volume of 4 dm³.

The activity (V) was defined as the initial oxygen consumption rate of the *N. europaea* cell suspension under the conditions applied in the vessel. This activity was expressed as μmolO_2 consumed.s^{-1}.m^{-3} bacterial suspension or expressed as a percentage of a standard assay. This standard was defined as the activity at pH 7.5 with 50 mM Tris/HCl and 50 mM phosphate buffer and a substrate concentration of 25 mM NH_4^+. The activity of the standard (100%) is given in the text or legend of the figures.

Fitting of data. Parameters of Michaelis-Menten based equations were fitted to the experimental data with the non-linear regression program of Zwietering et al. (1990) using a Marquardt algorithm.

RESULTS AND DISCUSSION

B **uffer**. A phosphate concentration of 40-50 mM is optimal for activity assays with *N. europaea* according to Droogenbroeck & Laudelout (1967). From the different buffer combinations tested the combined buffer with a concentration of 50 mM of both phosphate and Tris/HCl did not show the fall in activity observed by Ginkel et al. (1983), and was therefore used in the activity assays.

Trace elements and CO_2. No influence of the trace elements nor bicarbonate concentration on the activity of *N. europaea* cell suspension was observed in the ranges measured. Therefore, the absence of trace elements or HCO_3^- in the activity assays could be neglected.

Activity assay. The initial O_2 consumption rate was used as activity assay to analyse the influence of different environmental conditions. In these assays NH_4^+ was the rate limiting substrate. The NH_4^+ concentration was assumed to be constant during the assay, which is justified as the change due to conversion by the cells was relatively small (less than 0.1%). The decrease in oxygen concentration as result of the conversion, was measured between air saturation and 80% air saturation. The O_2 concentration was never rate limiting, as the affinity constant (K_S) measured for O_2 is 0.005 mM, which is very small compared to 0.190 mM (80 % air saturation).

Also the biomass was assumed to be constant during the activity assay. It can be calculated from the maximum specific growth rate of *Nitrosomonas europaea* - in continuous culture between 0.039-0.064 h^{-1}, reported by Prosser (1989) - that the maximum change in biomass concentration during the activity assay will be less than 0.4 %. The assumption of a constant biomass during the 5 minutes of an activity assay is therefore valid.

Influence of pH and substrate on the activity. At five pH values, ranging from 6.5 to 8.5, the activity was measured at substrate concentrations between 0 and 100 mM

28

NH_4^+; higher substrate concentration were also studied but are discussed in combination with the influence of extreme ion concentrations. Figure 1 shows some of the results of these activity assays. For every pH the substrate affinity constant K_S and the maximum activity V_m from the Michaelis-Menten equation were estimated with the non-linear regression method. For each pH two or three identical runs were made and the estimated K_S and V_m are presented in Table I. The second column in Table I gives the estimated K_S values expressed as the total ammonia concentration (N_t), i.e. no distinction is made between NH_3 and NH_4^+.
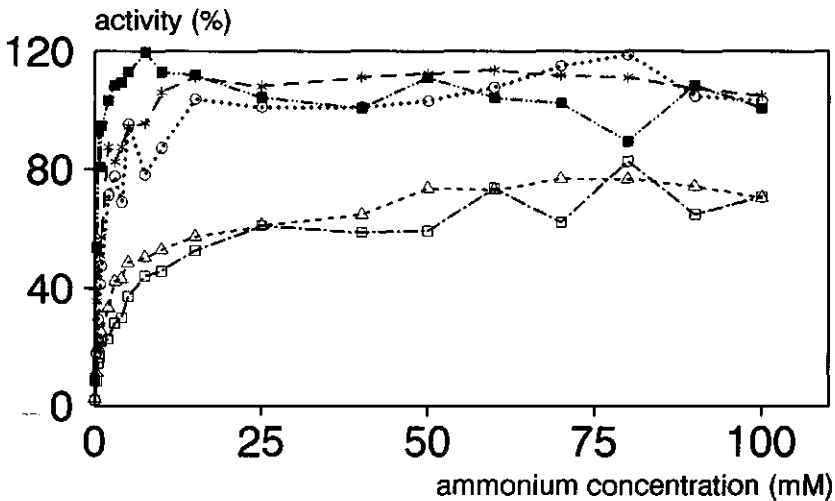

Figure 1   *The activity of N. europaea at different pH values as a function of the substrate concentration. The 100% corresponds with 2780 (pH 6.5 (□), 7.5 (○)), 2520 (pH 7.0 (▲), 8.0 (*)) and 1820 (pH 8.5 (■)) $\mu molO_2$ consumed.$s^{-1}.m^{-3}$ bacterial suspension.*

Suzuki (1974) showed that the substrate for *Nitrosomonas europaea* is NH_3 and

the acid-base dissociation constant K_a with a value of $10^{-9.093}$ mol.dm^{-3} was used to calculate the NH_3 concentration from N_t. In the third column K_S is expressed as the NH_3 concentration. In the last column the estimated V_m values are presented. In Table I some trends in the relation between pH and K_S and the maximum activity can be observed. First of all, a decrease in the K_S values, expressed as N_t, clearly occurs with an increase in pH. This is in contrast with the increase of K_S, expressed as NH_3, with increasing pH up to 8.0. The maximum activity also shows an increasing tendency when the pH goes from 6.5 to 8.5.

Table I   *The influence of pH on the maximum activity (V_m) and substrate affinity (K_S) of* **Nitrosomonas europaea.**

pH	K_S		V_m
	N_t (mM)	NH_3 (mM)	(% of standard)
6.5	4.4	0.011	72
	2.9	0.007	69
	2.0	0.005	57
7.0	2.4	0.019	73
	2.9	0.023	84
7.5	1.3	0.032	108
	1.5	0.037	107
8.0	0.79	0.056	111
	0.46	0.034	122
	0.39	0.029	87
8.5	0.17	0.034	108
	0.17	0.035	118
	0.19	0.037	100

Laudelout et al. (1976) and Boon & Laudelout (1962) showed that relations between pH, K_S and V_m can be modelled using Michaelis-Menten kinetics for enzymes (Dixon & Webb 1979). This approach is used to analyze the relations between pH, K_S and V_m from the data of Table I.

Relation between pH and K_S. The estimated K_S values of Table I were used to fit the acid-base equilibrium of the microorganism (K_{mo}) and a true substrate affinity constant (K_S^o) in eq (1). Where K_S^o is the pH independent substrate affinity constant for NH_3 and K_{mo} a pure theoretical parameter

$$K_S \ = \ K_S^o \ \cdot \ \left[\frac{1}{1 + \dfrac{[H^+]}{K_{mo}}} \right] \tag{1}$$

In eq (1) K_S is expressed as mol.dm^{-3} NH_3. Eq (1) was fitted to the data of K_S and pH from Table I with the non-linear regression method. A value of $10^{-6.96}$ mol.dm^{-3} for K_{mo} and $4*10^{-5}$ mol.dm^{-3} for K_S^o was obtained from this fit. In Figure 2 the fitted line with a 95% reliability interval (grey shaded area) is given with the measured data. In eq (1) the concentration of K_S is in mM NH_3, but usually K_S is expressed as the total ammonia $(NH_4^+ + NH_3)$ concentration in mM N_t. Using eq (1) and the K_a value of the ammonia equilibrium with the fitted values gives

$$K_S \ - \ 4*10^{-5} \ \cdot \ \left[\frac{1}{1 + \dfrac{[H^+]}{10^{-6.96}}} \right] \ \cdot \ \left[1 \ + \ \frac{[H^+]}{10^{-9.093}} \right] \tag{2}$$
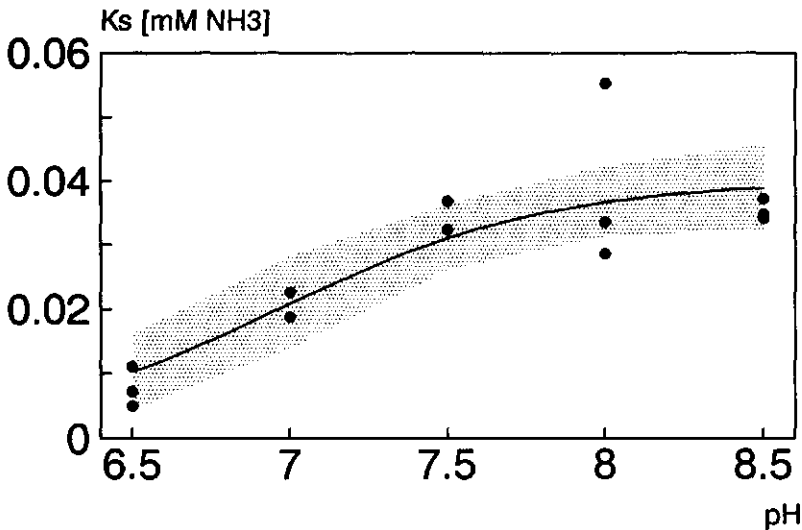
Figure 2   *The fitted value of K_S (line) with 95% reliability interval (grey area) as a function of pH. Measured values (Table I, 3rd column) are represented by dots.*

In Figure 3 literature values are compared with eq (2). The results of Knowles et al. (1965) and Gee et al. (1990) have been obtained with mixed cultures from waste-water treatment plants. They estimated a significant lower value of K_S. Keen & Prosser (1987) and Helder & de Vries (1983) determined a lower K_S also with pure cultures of *N. europaea*. The K_S values of Laudelout et al. (1976) and Suzuki et al. (1974) are in better agreement with our results.

Relation between pH and maximum activity. In enzyme kinetics the pH dependence of the maximum activity is explained with an acid-base equilibrium of a protonated group in the substrate-enzyme complex.
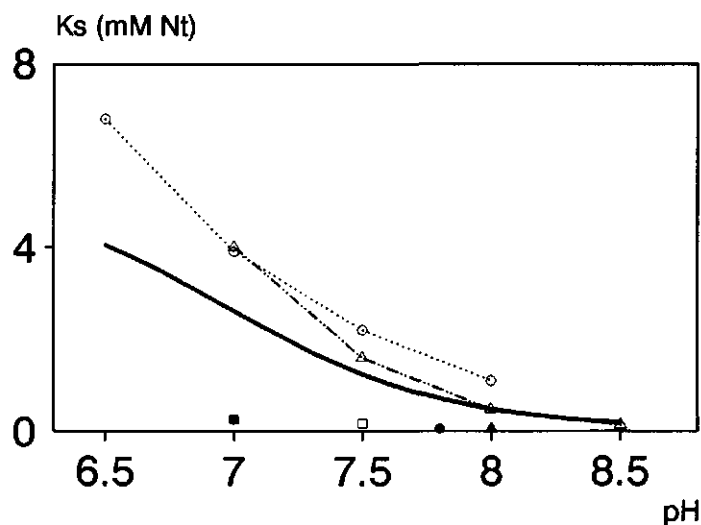
Ks (mM Nt)

Figure 3 *Comparison of literature values of K_S with measured values. The solid line represents eq (2), Keen & Prosser(1987) (■), Laudelout et al. (1976) (○), Knowles et al.(1965) (□), Gee et al.(1990) (▴), Suzuki et al.(1974) (△), Helder & de Vries(1983) (●).*

For *N. europaea* we assumed an analogous relation between pH and maximum activity (V_m) with K_{ms} as dissociation constant of the substrate-enzyme complex and V_m^0 the 'true' maximum activity

$$V_m = \left[\frac{V_m^0}{1 + \dfrac{[H^+]}{K_{ms}}} \right] \qquad (3)$$

33

Eq (3) was fitted to the data of Table I using the non-linear regression method. In Figure 4 the result is presented with the 95% reliability interval of the measured data. A value of 109.3% ± 9% for the V_m^0 and a K_{ms} of $10^{-6.37}$ mM, with $10^{-6.71}$ and $10^{-6.18}$ as upper and lower value for the reliability interval for K_{ms} were estimated.
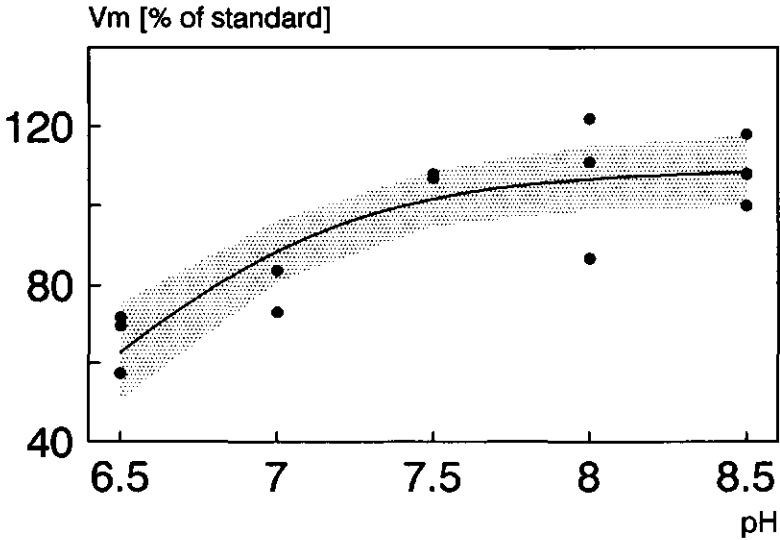

Figure 4 *The fitted values of V_m (line) with 95% reliability interval (grey area) as a function of pH. Measured values from Table I, 2nd column, are represented by dots.*

The relation between V_m and pH can thus be described by

$$V_m = \left[\frac{V_m^0}{1 + \dfrac{[H^+]}{10^{-6.37}}} \right] \quad (4)$$

The value of V_m^0 is more than 100% and this means that the optimal pH is not 7.5, which we used as standard, but above this pH. The parameter K_{ms} is a valuable tool to describe the relation between pH and maximum activity, but it is somewhat premature to draw any conclusions from this result about mechanisms of substrate conversion by these bacteria.

High concentrations of substrate, product and ions. The inhibitory effect of high substrate concentrations was, to a limited extent, reported by Laudelout et al. (1976), Anthonisen et al. (1976) and Prakasam & Loehr (1972). In Figure 5 the inhibitory effect of substrate (in duplo), and the influence of NaCl; KCl; $NaNO_3$ and $NaNO_2$ on the activity of *N. europaea* at pH 7.5 are presented. A severe inhibition of the activity was observed at increased concentrations. However no significant distinction between the different salts, substrate (NH_4^+) or product (NO_2^-) could be observed, thus an osmotic pressure effect due to the very high salt concentrations is more likely to explain the substrate inhibition. A linear regression analysis of all the data of Figure 5 results in eq (5)

$$\frac{V}{V_m} = 0.994 - 0.00187 * [salt \ concentration] \qquad (5)$$

For practical convenience the salt concentration is expressed in: [mmol/dm^3 (salt)]. The proportionality constant in eq (5) is estimated to be $-1.87 * 10^{-3}$ dm^3/mmol with and a 95% reliability interval of $-1.58 * 10^{-3}$ to $-2.16 * 10^{-3}$. It is not possible to avoid this type of inhibition of *N. europaea* under conditions prevailing in the treatment of concentrated waste streams and in practice this severe inhibition has to be taken into account.

High product concentration and pH. Together with high substrate concentrations also high product concentrations will also be reached. The product (NO_2^-) is a weak base and the unionized form is highly toxic to *Nitrobacter agilis* according to Boon & Laudelout (1962).
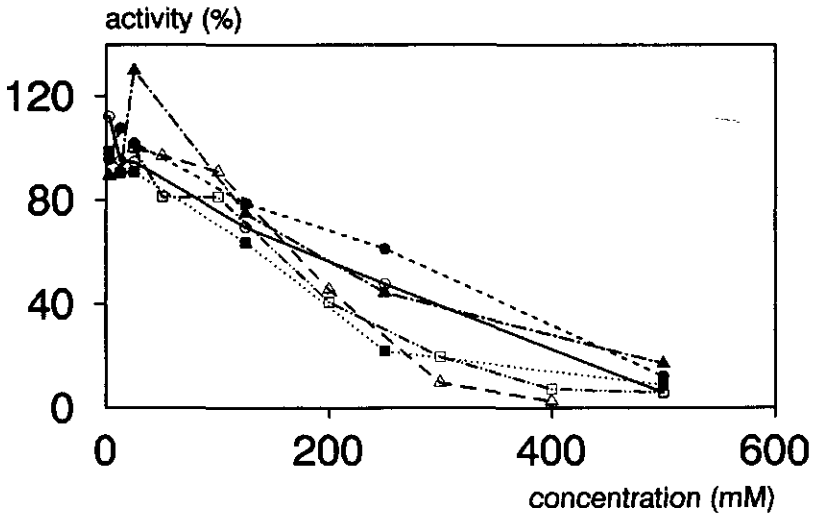
Figure 5   *The influence of the salt and substrate concentration (NH$_4$Cl (▲,□)), KCl (●), NaCl (○), NaNO$_2$ (■), NaNO$_3$ (▲)) on the activity of N. europaea. 100% is 3250 µmolO$_2$ consumed.s^{-1}.m^{-3} bacterial suspension.*

This effect can also be important for *Nitrosomonas europaea* and the influence of the product concentration at three pH values (6.5, 7.5, 8.5) on *N. europaea* has been determined. The product concentration varied between 0 - 500 mM NO$_2^-$ and to compensate for the osmotic effect at these extreme concentrations, NaCl at the same concentration as NaNO$_2$ was used as a reference. The results of these activity assays are shown in Figure 6: NO$_2^-$ is clearly inhibitory for *N. europaea*, particularly at a lower pH. This supports the suggestion that the unionized form (HNO$_2$) is responsible for this toxic effect. This product inhibition effect can thus be avoided in practise by raising the pH.
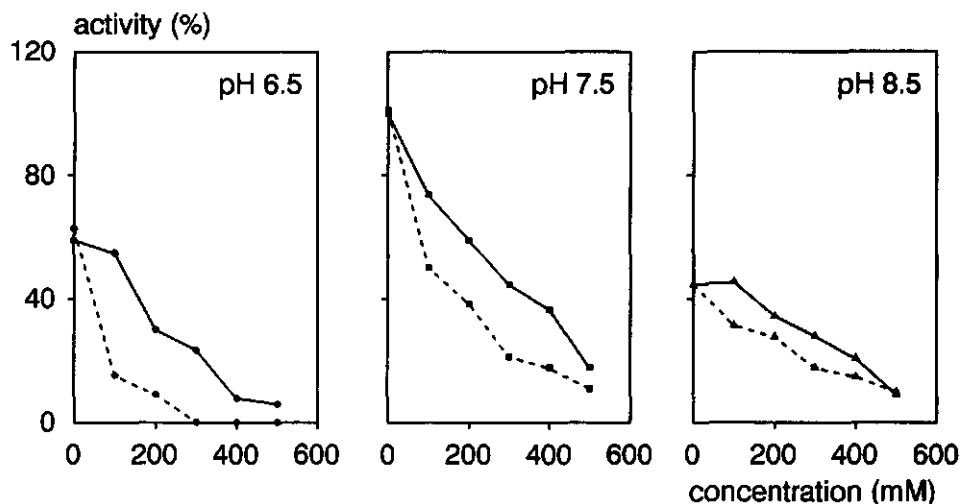
36

Figure 6 *The influence of high product concentration and pH on N. europaea. 100% is 3412 $\mu molO_2$ consumed.$s^{-1}.m^{-3}$ bacterial suspension. With dotted lines (---) for $NaNO_2$ and solid lines (———) for NaCl.*

CONCLUSIONS

T he influence of several extreme conditions prevailing in concentrated waste streams, on *N. europaea* was quantified. By using a combined phosphate and Tris/HCl buffer it was possible to estimate kinetic parameters over a wide pH range. The influence of pH on K_S and V_m is quantified and eqs (2) and (5) can be used for modelling nitrification processes. Particularly in biofilm models with non-steady-state conditions these equations can be a useful tool. Optimal conditions for ammonia conversion at wastewater treatment plants with nitrification problems can be determined. Adjustment of pH is a possibility to improve the ammonia conversion.

Substrate inhibition does not play an important role for *N. europaea*, but osmotic pressure in concentrated waste streams can severely inhibit this bacterium. Product inhibition is only observed at low pH and must not be confused with the influence of the osmotic pressure.

REFERENCES

Anthonisen AC; Loehr RC; Prakasam TBS; Srinath EG (1976) Inhibition of nitrification by ammonia and nitrous acid. Journal WPCF 48:835-852.

Boon B; Laudelout H (1962) Kinetics of nitrite oxidation by *Nitrobacter winogradskyi*. Biochem J 85:440-447.

Bortone G; Piccinini S (1991) Nitrification and denitrification in activated-sludge plants for pig slurry and waste water from cheese diaries. Biosource Technology 37:243-252

De Beer (1990) Microelectrode studies in biofilms and sediments. Thesis, University of Amsterdam, The Netherlands.

Dixon M; Webb EC (1979) Enzymes, 3rd edn. Longman group, London, Great Britain

Droogenbroeck R van; Laudelout H (1967) Phosphate requirements of the nitrifying bacteria. Antonie van Leeuwenhoek 33:287-296.

Gee CS; Suidan MT; Pfeffer JT (1990) Modeling of nitrification under substrate-inhibiting conditions. J Environmental Engineering 116:18-31.

Ginkel CG van; Tramper J; Luyben KChAM; Klapwijk A (1983) Characterization of *Nitrosomonas europaea* immobilized in calcium alginate. Enzyme Microb Technol 5:297-303.

Helder W; Vries RTP de (1983) Estuarine nitrite maxima and nitrifying bacteria (Ems-Dollard estuary). Netherlands Journal of Sea Research (English) 17:1-18.

Knowles G; Downing AL; Barrett MJ (1965) Determination of kinetic constants for nitrifying bacteria in mixed culture, with the aid of an electronic computer. J Gen Microbiol 38:263-278.

Keen GA; Prosser JI (1987) Steady state and transient growth of autotrophic nitrifying bacteria. Arch Microbiol 147:73-79.

Knox K (1985) Leachate treatment with nitrification of ammonia. Water Res 19:895-904.

Laudelout H; Lambert R; Pham ML (1976) Influence du pH et la pression partielle d'oxygène sur la nitrification. Ann Microbiol (Inst Pasteur) 127A:367-382.

Loehr RC; Prakasam TBS; Srinath EG; Joo YD (1973) Development and demonstration of nutrient removal from animal waste. Environmental Protection Technology Series, R2-73-095, Washington DC, USA.

Loynachan TE; Bartolomew WV; Wollum AG (1976) Nitrogen transformations in aerated swine manure slurries. J Environ Qual 5:293-297.

Osada T; Haga K; Harada Y (1991) Removal of nitrogen and phosphorus from swine wastewater by the activated sludge units with the intermittent aeration process. Wat Res 25:1377-1388.

Prakasam TBS; Loehr RC (1972) Microbial nitrification and denitrification in concentrated wastes. Wat Res 6:859-869.

Prosser JI (1989) Autotrophic nitrification in bacteria. Advances in Microbial Physiology 30:125-181.

Sato C; Leung SW; Schnoor JL (1988) Toxic response of Nitrosomonas europaea to copper in inorganic medium and wastewater. Wat Res 22:1117-1127.

Shieh WK; LaMotta EJ (1979) Effect of initial substrate concentration on the rate of nitrification in a batch experiment. Biotech Bioeng 21:201-211.

Soriano S; Walker N (1973) The nitrifying bacteria in soils from Rothamsted classical fields and elsewhere. J Appl Bact 36:523-529.

St-Arnaud S; Bisaillon J -G; Beaudet R (1991) Microbiological aspects of ammonia oxidation of swine waste. Can J Microbiol 37:918-923.

Suzuki I; Dular U; Kwok SC (1974) Ammonia or ammonium ion as substrate for oxidation by *Nitrosomonas europaea* cells and extracts. J Bacteriology 120:556-558.

Szwerinski H; Arvin E; Harremoës P (1986) pH-decrease in nitrifying biofilms. Wat. Res. 20:971-976.

Voets JP; Vanstaen H; Verstraete W (1975) Removal of nitrogen from highly nitrogenous wastewaters. J WPCF 47:394-398.

Wild HE; Sawyer CN; McMahan TC (1971) Factors affecting nitrification kinetics. J WPCF 43:1845-1854.

Zwietering MH; Jongenburger I; Rombouts FM; Riet K van 't (1990) Modeling of the bacterial growth curve. Appl Environ Microbiol 56:1875-1881.

3 KINETICS OF *NITROBACTER AGILIS*

SUMMARY

Measurement and description of the effects of extreme conditions on biological nitrite oxidation was the aim of this study, using *Nitrobacter agilis* (ATCC 14123) as model nitrifying bacterium. The initial oxygen consumption rate of a concentrated cell suspension was used as a rapid assay to measure the effects. Several relations, based on Michaelis-Menten kinetics, were derived. These relations describe the behaviour of *N. agilis* with respect to substrate inhibition, product inhibition and various salt concentrations up to 500 mM with the pH ranging from 6.5 to 8.5. Substrate and product inhibition were pH dependent and the subtrate inhibition could be related to the undissociated nitrite. In contrast with previous reports on nitrite oxidizing microorganisms, we did not observe severe inhibition by NH_4^+.

INTRODUCTION

N itrification of waste streams, with high concentrations of ammonia, from industry, agriculture or landfills, is gaining more attention (St-Arnaud et al.1991, Loynachan et al. 1976, Bortone & Piccinini 1991, Osada et al. 1991, Knox 1985). Concentrations up to 500 mM ammonia can occur in these waste streams. Kinetic studies about the nitrification process are mainly focused on mixed cultures at a relatively low nitrogen concentration (Knowles et al. 1965, Anthonisen et al. 1976). An improved knowledge of nitrifying bacteria under extreme environmental conditions is necessary for a better understanding of the nitrification process in concentrated waste streams. Gradients of substrate, product and pH are playing an important role in nitrifying biofilms (Swerinski et al. 1986). Therefore, the influence of pH on the kinetics of the microorganisms involved has also to be taken into account.

The predominant nitrifying bacteria in soil and water are *Nitrosomonas spp.* and *Nitrobacter spp.*. The effect of extreme conditions on the ammonia-oxidizing species *Nitrosomonas europaea* is described by Hunik et al. (1992). The situation with respect to the predominant nitrite-oxidizing species is somewhat complicated. In the 8th edition of *Bergey's Manual* (Watson, 1974) the previously known *Nitrobacter agilis* and *Nitrobacter winogradskyi* species were combined as two strains of the species *Nitrobacter winogradskyi*. This combination was supported by Pan (1971) who found no morphological or physiological differences between the two strains. Fliermans et al. (1974) however, clearly showed a difference in serotype using a fluorescent-antibody technique. They isolated a *N. agilis* strain from a freshwater environment with increased nitrate levels (for example: oxidation ditch), but only isolated *N. winogradskyi* from different types of soil with a relatively low concentration of nitrate. Furthermore, Fliermans & Schmidt (1975) described a difference in growth behaviour and activity between the two strains in a mixed culture. Based on these results we expected *N. agilis* to be the predominant strain

in nitrite oxidation of concentrated waste streams and have chosen this strain as a model.

The kinetics of *N. winogradskyi* at moderate conditions have been determined by Boon & Laudelout (1962) and their results are compared with ours, obtained with *N. agilis* (ATCC 14123) at more extreme conditions. Another important aspect of nitrification under extreme conditions is the presence of ammonia. Severe inhibition by ammonium of the NO_2^- conversion in waste-water treatment plants is reported by Anthonisen et al. (1976), Aleem & Alexander (1960), Alleman (1984), Gee et al.(1990), Prakasam & Loehr (1972) and Stojanovic & Alexander (1958). Determination of the kinetics of *N. agilis* at extreme concentrations of substrate (NO_2^-), product (NO_3^-) and salts at various pH values were the aim of the present study.

Parameters for substrate affinity, product inhibition and salt inhibition combined with pH effects are derived based on Michaelis-Menten kinetics for enzymes. A pH-dependent substrate(NO_2^-) and product (NO_3^-) inhibition was observed. In contrast to previous reports, *N.agilis* was not severely inhibited by ammonium. Compared to *Nitrosomonas europaea* (Hunik et al. 1992), *N. agilis* is less senstive to osmotic pressure at high salt concentrations. The derived kinetic parameters are useful for modelling biofilm processes.

MATERIAL & METHODS

M edia. All media and solutions ware made up in demineralized water. The chemicals used were Analytical Grade and obtained from Merck.

Chemostat . The *Nitrobacter agilis* (ATCC 14123) cells were maintained in a 2.5 dm^3 sterile chemostat with a dilution rate of $3.5 * 10^{-6}$ s^{-1}. The culture was kept at 30°C. The medium contained per dm^3 of demineralized water: 1.0 g $NaNO_2$; 0.17 g $NaHCO_3$; 0.052 g $MgSO_4$; 0.16 g $NaH_2PO_4.2H_2O$; 1.6 g $Na_2HPO_4.2H_2O$; 0.74 mg $CaCl_2.2H_2O$; 0.036 mg $FeSO_4.7H_2O$; 0.026 mg $CuSO_4$; 0.24 mg $Na_2MoO_4.2H_2O$; 4.3 mg $ZnSO_4.7H_2O$.

Cell harvesting and concentration. To obtain a sample of cells, effluent from the chemostat was collected for 48 hours in a sterile vessel at room temperature. The collected cells were washed and concentrated as follows before they were used in the activity assay. The approximately 1 dm^3 collected effluent was first centrifuged at 16300 g for 30 min at a temperature of 10 °C. The pellet was resuspended in 0.1 dm^3 of a 1 mM phosphate buffer (pH 7.5) and centrifuged for the second time. The cells were resuspended in 25 cm^3 of a 1 mM phosphate buffer and stored on ice until they were used in the activity assay. The concentration and harvesting procedure was repeated for each measuring day.

Trace elements and CO_2. For the activity assay, buffer and substrate were added, but for experimental convenience no trace elements nor bicarbonate was added. To study if experimental errors due to the absence of trace elements and bicarbonate could be introduced, MoO_4^{2-}, Zn^{2+}, Ca^{2+}, Fe^{2+} and Cu^{2+} concentrations were tested in a range from 0 to 5 times the growth medium concentration and a concentration range of 0 to 10 mM for HCO_3^-. An additional washing step, similar to the second step in the concentration procedure with the concentrated cells suspension, was made to be sure that all trace elements from the medium were removed. Standard conditions (pH 7.5 and 10 mM NO_2^-) were used in these activity assays.

Activity assay. The oxygen consumption rate of a concentrated cell suspension was used as a rapid assay to screen and quantify the effects of the extreme conditions in concentrated waste streams. The oxygen consumption rate was measured with a Biological Oxygen Monitor (Yellow Springs Instrument, Ohio, USA). In an 8 cm^3 vessel, 0.5 cm^3 of the concentrated cell suspension was added together with buffer and an appropriate concentrated solution of ions or product (as specified in the Results and Discussion section). Demineralized water was added to make up to 4 cm^3 and the suspension was aerated for 5 min. Then the vessel was sealed with the oxygen electrode (model 5331, Yellow Springs Instrument, Ohio, USA) such that no air bubbles remained

in the liquid. Nitrite was added through the seal with an analytical syringe (0.02 cm^3) to make up to the desired substrate concentration. For that a concentrated NO_2^- solution (2 M) was used such that the liquid volume did not significantly change. The decrease in oxygen concentration (between 100-80 % air saturation) was then recorded as a function of time. All activity assays were done at 30°C. A phosphate concentration of 50 mM is optimal for *Nitrobacter* according to Droogenbroeck & Laudelout (1967). To avoid a lack of phosphate at a pH above 7.5, where commonly Tris/HCl is used, and a change in activity when the buffer composition is changed, we used combined buffer of 50 mM of both Tris/HCl and phosphate over the whole pH range tested.

The activity was defined as the initial oxygen consumption rate of the *Nitrobacter agilis* cell suspension under the conditions applied in the vessel. This activity was expressed as $\mu molO_2$ consumed.$s^{-1}.m^{-3}$ bacterial suspension or expressed as a percentage of a standard assay. This internal standard for each experimental series was defined as the activity at pH 7.5 with 50 mM Tris/HCl and 50 mM phosphate buffer and a substrate concentration of 10 mM NO_2^-. The activity of the standard (100%) is given in the text or legend of the figures.

Parameters of Michaelis-Menten based equations were fitted to the experimental data with the non-linear regression method using a Marquardt algorithm (Zwietering et al. 1990).

RESULTS AND DISCUSSION

Trace elements and CO_2. No influence of the trace elements nor bicarbonate concentration on the activity of *Nitrobacter agilis* cell suspension was observed in the ranges measured. Therefore, the absence of trace elements and HCO_3^- in the activity assays could be neglected. This behaviour is similar to the results obtained with *N. europaea* (Hunik et al., 1992).

45

Activity assay. The initial oxygen consumption rate was used as activity assay to analyze the influence of different environmental conditions. In these assays NO_2^- was the rate limiting substrate. The NO_2^- concentration was assumed to be constant during the assay, which is justified as the change due to conversion by the cells was relatively small (less than 0.05%). The decrease in oxygen concentration as result of the conversion, was measured between air saturation and 80% air saturation. The O_2 concentration was never rate limiting, as the affinity constant (K_S) measured for O_2 is 0.02 mM, which is small compared to 0.190 mM (80 % air saturation).
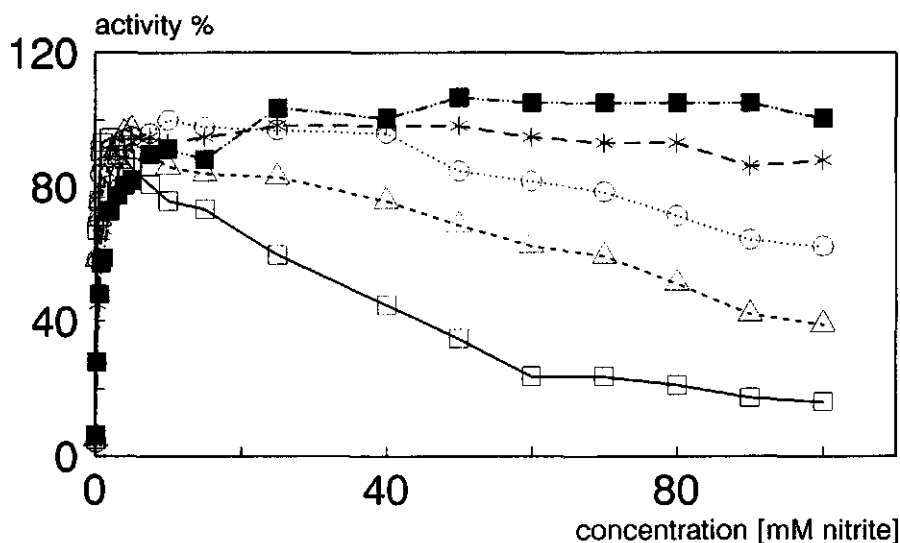
Figure 1   *The activity of **N. agilis** at different pH values as a function of the substrate concentrations. The 100% value corresponds with 845 (□, pH 6.5), 1026 (△,pH 7.0), 1029 (○, pH 7.5), 609 (*, pH 8.0), 679 (■, pH 8.5) μmol O_2 consumed.s^{-1}.m^{-3} bacterial suspension.*

Also the biomass was assumed to be constant during the activity assay. It can be calculated from the maximum specific growth rate of *N. agilis* - in continuous culture

between 0.018-0.043 h^{-1}, reported by Prosser (1989) - that the maximum change in biomass concentration during the activity assay will be less than 0.3 %. The assumption of a constant biomass during the 5 minutes of an activity assay is therefore valid.

Influence of pH and substrate concentration. The relation between substrate concentration, pH and activity was measured with 13 separate experiments at substrate concentrations between 0 and 100 mM NO_2^-. For five different pH values, two or three identical activity versus substrate concentration series were made. Figure 1 shows a representative example of five of these activity assays. The decrease in activity at lower pH and increased substrate concentrations, shown in Figure 1, was due to substrate inhibition. Two forms of nitrite can be distinguished in the pH range used: non-dissociated HNO_2 and the NO_2^- ion, which is the actual substrate (Cobley 1976, Kumar & Nicholas 1981).

To describe this, a similar approach, using Michaelis-Menten kinetics, was followed as in our previous kinetic study of *N. europaea* (Hunik et al., 1992). The effect of substrate inhibition is due to the non-competitive inhibition by HNO_2 (Boon & Laudelout 1962) and a non-competitive inhibition term was added to the Michaelis-Menten equation to obtain eq (1)

$$V = V_m \cdot \left[\frac{S}{K_S + S} \right] \cdot \left[\frac{1}{1 + \dfrac{S}{K_i}} \right] \tag{1}$$

The substrate affinity constant (K_S), maximum activity (V_m), and substrate inhibition constant (K_i) were estimated from a fit of the activity (V) versus substrate concentration (S) to eq (1). From the 13 data sets we estimated the K_S, V_m and K_i values with the non-linear regression method (Table I). The K_S is expressed as mM NO_2^- in Table I. Substrate inhibition is due to the non-competitive inhibition of HNO_2 and the inhibition constant K_i is thus expressed as μM HNO_2 in Table I. An acid-base dissociation constant

of $3.98 * 10^{-4}$ mol.dm^{-3} was used to calculate the HNO$_2$ concentration from the total nitrite concentration.

Table I   *The influence of pH on the maximum activity (V_m), the substrate affinity constant (K_S) and the substrate inhibition constant (K_i) of **N. agilis***

pH	V_m	K_S	K_i
	% activity	mM NO$_2^-$	μM HNO$_2$
6.5	111	0.17	17.9
	129	0.217	12.8
7.0	103	0.226	21.1
	129	0.536	9.96
	117	0.482	13.5
7.5	105	0.22	15.1
	118	0.429	6.6
	97	0.541	15.2
8	99	0.375	-
	121	0.50	-
	114	0.379	-
8.5	102	0.729	-
	114	1.38	-

In Figure 1 we can see that the effect of substrate inhibition was absent above pH 8.0. From the value of the HNO$_2$ dissociation constant it is clear that the HNO$_2$ concentrations are very low at higher pH's and the estimated values for K_i above pH 7.5 are unreliable and omitted for that reason.

From Table I some trends in the relationship between pH and V_m, K_S and K_i values can be observed. First of all the estimated V_m values are rather constant over the

pH range used in our experiments. Second, the estimated K_i values, expressed as μM HNO_2, in Table I, are also roughly constant at the lower pH range. This observation supports the non-competitive inhibition by HNO_2 of *N.agilis* and an average K_i value of 14.0 μM HNO_2 with a 95% reliability interval of 10.0 to 18.0 was obtained. This is about twice the value of 8.2 μM HNO_2 found by Boon & Laudelout (1962) for *N. winogradskyi*. The third observation is that the substrate affinity values (K_i) in Table I slightly increase when the pH changes from 6.5 to 8.5.
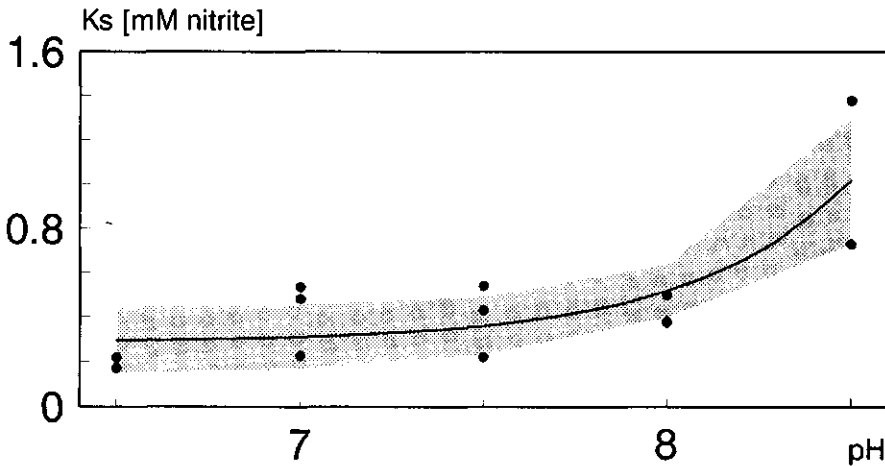

Figure 2   *The fitted value of the substrate affinity constant (K_S line) with a 95% reliability interval (grey area) as function of pH. Measured values are represented by dots.*

Relationships between pH and K_S can be modelled using Michaelis-Menten kinetics for enzymes (Dixon & Webb 1979, Boon & Laudelout 1962). This approach was used to analyze the relationship between pH and K_S from the data of Table I.

With the estimated K_S values of Table I the acid-base equilibrium of the microorganism

49

(K_{mo}) and the "true" substrate affinity constant K_s^0 of eq (2) were estimated. The K_s^0 value is the pH-independent substrate affinity constant for NO_2^- and K_{mo} a pure theoretical parameter.

$$K_S = K_S^0 \cdot \left[1 + \frac{K_{mo}}{[H^+]} \right] \tag{2}$$

Eq (2) was fitted to the data of K_S and pH from Table I with the non-linear regression method. For the pH-independent substrate affinity constant K_S^0 a value of 0.287 mM NO_2^- was obtained and a value of $8.04 * 10^{-9}$ mol/dm^3 for K_{mo}. In Figure 2 the fitted line with a 95% reliability interval (grey shaded area) for the measured data is shown.

The combined effect of pH and substrate concentration is expressed in eq (3). All concentrations in eq (3) are in mol/dm^3.

$$\frac{V}{V_m} = \frac{S}{2.78 * 10^{-4} * \left[1 + \frac{8.04 * 10^{-9}}{[H^+]} \right] * S}$$

$$* \frac{1}{1 + \left[\frac{S * [H^+]}{(3.98 * 10^{-4}) * (14.0 * 10^{-6})} \right]} \tag{3}$$

In Table II literature values are compared with values obtained with the kinetic parameters of eq (3). Only Boon & Laudelout (1962) present K_S values over a broad pH range, but their values are considerable higher than ours. From these results a significant difference in K_S values between *N.agilis* and *N.winogradskyi* seems a valid conclusion. This is not supported by the K_S values reported by Tsai & Tuovinen (1985), who found a higher K_S value for *N.agilis* compared to the K_S value for *N.winogradskyi*. The K_S values of Tsai & Tuovinen (1985) are both comparable with the values we found for *N.agilis*.

Very low values for K_S are reported by Gee et al. (1990) and Yosioka et al. (1982), but both *Nitrobacter* strains were not further characterized and the values they found can not easily be compared to the other K_S values of Table Ⅱ.

Table Ⅱ   *Literature values of K_S*

author(s)	*Nitrobacter* sp.	pH	K_s mM NO_2^-	origin
Boon & Laudelout (1962)	*winogradskyi*	6.5	1.62	soil
		7.0	1.68	
		7.5	1.85	
		8.0	2.4	
		8.5	4.14	
Keen & Prosser (1987)	sp.	8.0	0.2	soil
Gay & Corman (1984)	sp.	7.8	0.11	soil
	sp.	7.8	0.54	
Gee et al. (1990)	sp.	8	0.07	unknown
Tsai & Tuovinen (1985)	*agilis*	7.5	0.66	unknown
	winogradskyi	7.5	0.31	unknown
Helder & Vries (1983)	sp.	7.8	0.27	seawater
Yoshioka et al.(1982)	sp.	7.7	0.03	freshwater
Knowles et al. (1965)	spp.	7.7	0.12	waste water
equation 2	*agilis*	6.5	0.29	unknown
		7.0	0.31	
		7.5	0.36	
		8.0	0.54	
		8.5	1.11	
Remacle & De Leval (1978)	sp.	7.5	0.23	fresh water

Also the results of Keen & Prosser (1987), Gay & Corman (1984), Helder & Vries (1983) and Knowles et al. (1965) were obtained with non-identified strains of *Nitrobacter* and although they are in the same range as our values for K_S it is difficult to compare these with the results from the well specified *Nitrobacter* strains. Very low K_S values for *N.agilis* are reported by Gould & Lees (1960) but there is no pH given.

High concentrations of ions. The effect of high concentrations of NH_4^+, Na^+, K^+, NO_3^-, Cl^-, SO_4^{2-} and acetate on the activity of *N.agilis* is demonstrated in Figure 3. There is a clear distinction between the activity with NO_3^- ions present and the activity with the other ions. The influence of Na^+, K^+, Cl^-, SO_4^{2-} and acetate is most likely the result of an osmotic-pressure effect. A linear regression analysis of the latter data results in eq (4)

$$\frac{V}{V_m} = 1.04 - 0.00088 . [salt \quad concentration] \quad (4)$$

For practical convenience the salt concentration is expressed in: [mmol salt.dm^{-3}]. The proportionality constant, estimated from a linear regression analysis of the data in Figure 3, is $8.8 * 10^{-4}$ dm^3.mmol^{-1} with a reliability interval of 0.00132 to 0.00043. This osmotic effect is considerable less compared to the salt effect on *Nitrosomonas europaea* with a proportionality constant of $1.87 * 10^{-3}$ dm^3.mmol^{-1} reported by Hunik et al. 1992. The influence of product and ammonium concentration together with the pH effect is treated below.

Effect of pH and high concentrations of ammonium and nitrate. The influence of ammonium and the difference between NH_3 and NH_4^+ inhibition can be made clear by measuring the effect of ammonium at various pH values. Nitrate will be present as dissociated ion at all pH values examined. To distinguish the effects of NH_3, NH_4^+ and NO_3^- from the osmotic effect shown in Figure 3 and described by eq (4), we used NaCl as a blank for these experiments.
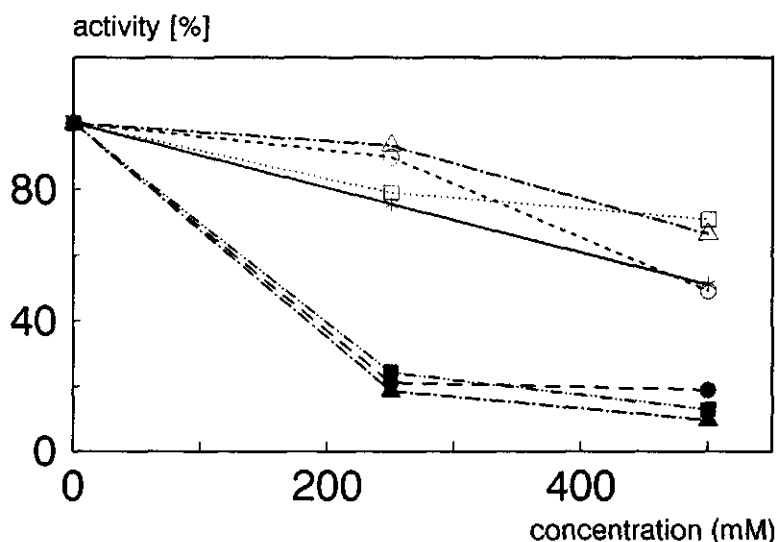
activity [%]

Figure 3 *The influence of the salt and substrate concentration on the activity of N.* ***agilis***; *100% is 600 μmolO$_2$ consumed.s^{-1}.m^{-3} bacterial suspension. KCl (▲),* *NaAc (□), NaCl (*), Na$_2$SO$_4$(○), KNO$_3$ (●), NaNO$_3$ (■), NH$_4$NO$_3$ (▲).*

Figure 4[a,b,c] present the results of the activity assays at pH 6.5, 7.5 and 8.5. The effect of increasing concentrations of NO$_3^-$, NaCl and ammonium in Figure 4[b] is comparable with the results of Figure 3. In Figure 4[a] at pH 6.5 both ammonium and nitrate show an increased inhibition of *N. agilis*. For pH 8.5, in Figure 4[c], the effects of the different salts on the activity is very small and negligible. The results with ammonium show considerably less inhibition compared to the results of other authors, who found a severe inhibition by ammonium at very low concentrations: 12 mM (50% inhibtion at pH 8.0, Gee et al. 1990), 17 mM (treshold value for inhibtion of nitrite oxidation at pH 7.7 in soil samples, Stojanovic & Alexander 1958), 0.01 mM (30% inhibition at pH 8.0, Alleem & Alexander 1960), 0.072 mM (50% inhibition at pH 7.4, Prakasam 1972). The presence of ammonia at pH 7.5 and 8.5 has little effect on the activity of *N. agilis* (Figure 4[b,c]). Only at pH 6.5 (Figure 4[a]) the inhibition of ammonium can be clearly distinguished
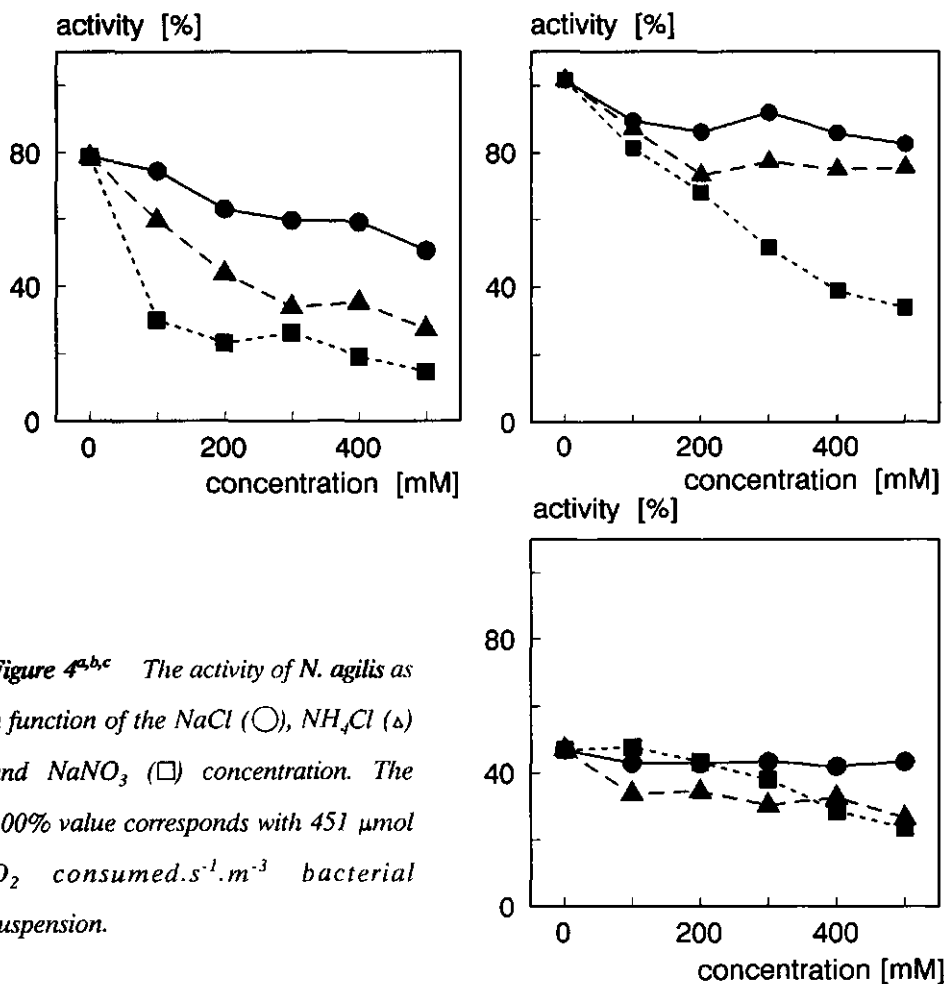
activity [%]

activity [%]

activity [%]

Figure 4[a,b,c]   The activity of N. agilis as a function of the NaCl (○), NH₄Cl (▵) and NaNO₃ (□) concentration. The 100% value corresponds with 451 µmol O_2 consumed.$s^{-1}.m^{-3}$ bacterial suspension.

from the inhibition by NaCl. At this pH the NH_3 concentration is a 100 times smaller than at pH 8.5 and inhibition of *N. agilis* by NH_3 is thus very unlikely. A relatively small effect of ammonium on *Nitrobacter* is also found by Cobley (1976) with cell-free extracts, who found no inhibition of the isolated electron-transport particles from *N. winogradskyi* by ammonium concentrations up to 12 mM.

The product (NO_3^-) inhibition at pH 6.5 was more severe than at pH 7.5 (Fig.4[a,b]). This increased effect of NO_3^- at decreasing pH is somewhat surprising because the nitrate

ion will be completely dissociated at all pH values tested. For a more quantitative determination of the inhibiting effect of NO_3^- on *N.agilis* a the experiment of Figure 4[b] was duplicated, but with much smaller intervals between the concentrations. Boon & Laudelout (1962) have shown that *N. agilis* is non-competitive inhibited by NO_3^- at pH 7.6. The data of the NO_3^- inhibition were therefore fitted to the following non-competitive inhibition equation

$$\frac{V}{V_m} = \left[\frac{1}{1 + \dfrac{[NO_3^-]}{K_P}} \right] \tag{5}$$

From the duplicate experiment a value of 188 mM NO_3^- for K_p in eq (5) was obtained.

Comparing *Nitrobacter agilis* with *Nitrosomonas europaea*. A comparison of the effects of substrate, product and intermediates on the nitrification process should incorporate *N. agilis* as well as *N. europaea*. The kinetics of *N.agilis* are therefore evaluated together with the results obtained with *N. europaea* (Hunik et al. 1992). Nitrification starts with the ammonia oxidation by *N. europaea*. The ammonia oxidation is more sensitive to high salt concentrations than the nitrite oxidation. The oxidation of nitrite is inhibited by the non-dissociated substrate (HNO_2). An effect of nitrite on *N. europaea* is also observed, where an increased inhibition by nitrite occurs at decreasing pH, which indicates that the non-dissociated HNO_2 inhibits the ammonia oxidation. The ammonia oxidation is not affected by the presence of nitrate. *N.agilis*, on the contrary, shows a severe product inhibition. This product inhibition is also pH dependent, even though nitrate is dissociated at the pH range from 6.5 to 8.5 used.

Consequences. The severe inhibition of *N. agilis* by NO_3^- will be a major drawback for the nitrification of concentrated waste streams. There is no way to avoid the high product concentrations in the nitrification of concentrated waste streams. Only a

combination with simultaneous denitrification seems a promising alternative. Such a method is proposed by Santos et al. (1992). Cells are immobilized in a double-layer bead with nitrifying microorganisms at the outside and denitrifying microorganisms on the inside.

Our results with the effect of ammonium on *N. agilis* show a minor inhibitory effect. Severe inhibition of *N. agilis* in the start-up phase due to high concentrations of NH_4^+ is thus not likely to happen. The osmotic pressure effect of high salt concentrations did also not severely inhibit *N. agilis*. Both *N. agilis* and *N. europaea* show a decrease in activity at pH 6.5. This effect is enhanced in the presence of NO_2^-, which is inhibitory for both microorganisms. In contrast to reports on the inhibition of *Nitrobacter spp.* by NH_4^+, we did not observe such effects. The derived equations for *N. agilis* offer the possibility to model growth of this microorganism at varying conditions and is a helpful tool for modelling nitrification in biofilm processes.

REFERENCES

Aleem MIH, Alexander M (1960) Nutrition and physiology of *Nitrobacter agilis*. Appl Microbiol 8:80-84.

Alleman JE (1984) Elevated nitrite occurrence in biological wastewater treatment systems. Wat Sci Tech 17:409-419.

Anthonisen AC, Loehr RC, Prakasam TBS, Srinath EG (1976) Inhibition of nitrification by ammonia and nitrous acid. Journal WPCF 48:835-852.

Boon B, Laudelout H (1962) Kinetics of nitrite oxidation by *Nitrobacter winogradskyi*. Biochem J 85:440-447.

Bortone G, Piccinini S (1991) Nitrification and denitrification in activated-sludge plants for pig slurry and waste water from cheese dairies. Bioresource Technology 37:243-252.

Cobley JG (1976) Energy-conserving reactions in phosphorylating electron-transport particles from *Nitrobacter winogradskyi*. Biochem J 156:481-491.

Dixon M, Webb EC (1979) Enzymes, 3rd edn. Longman group, London, Great Britain.

Droogenbroeck R van, Laudelout H (1967) Phosphate requirements of the nitrifying bacteria. Antonie van Leeuwenhoek 33:287-296.

Fliermans CB, Bohlool BB, Schmidt EL (1974) Autoecological study of the chemoautotroph *Nitrobacter* by immunofluorescence. Appl Microbiol 27:124-129.

Fliermans CB, Schimdt EL (1975) Autoradiography and immunofluorescence combined for autoecological study of single cell activity with *Nitrobacter* as a model system. Appl Microbiol 30:676-684.

Gay G, Corman A (1984) Comparative study of the growth of two strains of *Nitrobacter* in batch and continuous culture. Microb Ecol 10:99-105.

Gee CS, Suidan MT, Pfeffer JT (1990) Modeling of nitrification under substrate-inhibiting conditions. J Environmental Engineering 116:18-31.

Gould GW, Lees H (1960) The isolation and culture of the nitrifying organisms. Part 1 *Nitrobacter*. Can J Microbiol 6:299-307.

Helder W, Vries RTP de (1983) Estuarine nitrite maxima and nitrifying bacteria (Ems-Dollard estuary). Netherlands Journal of Sea Research (English) 17:1-18.

Hunik JH, Meijer HJG, Tramper J (1992) Kinetics of *Nitrosomonas europaea* at extreme subtrate, product and salt concentrations. Appl Microbiol Biotechnol 37:802-807.

Keen GA, Prosser JI (1987) Steady state and transient growth of autotrophic nitrifying bacteria. Arch Microbiol 147:73-79.

Knox K (1985) Leachate treatment with nitrification of ammonia. Water Res 19:895-904.

Knowles G, Downing AL, Barrett MJ (1965) Determination of kinetic constants for nitrifying bacteria in mixed culture, with the aid of an electronic computer. J Gen Microbiol 38:263-278.

Kumar S, Nicholas DJD (1981) Oxygen-dependent nitrite uptake and nitrate production by cells, spheroplasts and membrane vesicles of *Nitrobacter agilis*. FEMS Microbiology Letters 11:201-206.

Loynachan TE, Bartolomew WV, Wollum AG (1976) Nitrogen transformations in aerated swine manure slurries. J Environ Qual 5:293-297.

Osada T, Haga K, Harada Y (1991) Removal of nitrogen and phosphorus from swine wastewater by the activated sludge units with the intermittent aeration process. Wat Res 25:1377-1388.

Remacle J, De Leval J (1978) Approaches to nitrification in a river. In: Schlessinger (ed) Microbiology-1978, American Society for Microbiology Washington D.C. USA, p 352.

Pan PHC (1971) Lack of distinction between *Nitrobacter agilis* and *Nitrobacter winogradskyi*. J Bacteriol 108:1416-1418.

Prakasam TBS, Loehr RC (1972) Microbial nitrification and denitrification in concentrated wastes. Wat Res 6:859-869.

Prosser JI (1989) Autotrophic nitrification in bacteria. Advances in Microbial Physiology 30:125-181.

Santos VA, Wijffels RH, Tramper J (1992) Integrated nitrification and denitrification with immobilized microorganisms In: Melo LF, Bott TR, Fletcher M, Capdeville B (eds) Biofilms Science and Technology, Series E: Applied Sciences 223, 449-454. Kluwer, The Netherlands.

St-Arnaud S, Bisaillon J -G, Beaudet R (1991) Microbiological aspects of ammonia oxidation of swine waste. Can J Microbiol 37:918-923.

Stojanovic BJ, Alexander M (1958) Effect of inorganic nitrogen on nitrification. Soil Sci 86:208-215.

Szwerinski H, Arvin E, Harremoës P (1986) pH-decrease in nitrifying biofilms. Wat Res 20:971-976.

Tsai Y-L, Tuovinen OH (1985) Oxygen uptake by *Nitrobacter* spp. in the presence of metal ions and sulfooxanions. FEMS Microbiol Letters 28:11-14.

Watson SW (1974) In: Bergey's manual of determinative bacteriology, 8th edn, Buchanan RE and Gibbons NE (eds), Williams and Wilkins. Baltimore, USA.

Yoshioka T, Terai H, Saijo Y (1982) Growth kinetic studies of nitrifying bacteria by the immunofluorescent counting method. J Gen Appl Microbiol 28:169-180.

Zwietering MH, Jongenburger I, Rombouts FM, Riet K van 't (1990) Modeling of the bacterial growth curve. Appl Environ Microbiol 56:1875-1881.

4 IMMOBILIZATION

SUMMARY

I mmobilization of biocatalysts in κ-carrageenan gel beads is a widely used technique nowadays. Several methods are used to produce the gel beads. The gel-bead production rate is usually sufficient to make the relatively small quantities needed for bench-scale experiments. The droplet diameter can, within limits, be adjusted to the desired size, but is difficult to predict because of the non-Newtonian fluid behaviour of the κ-carrageenan solution. Here we present the further scale-up of the extrusion technique with the theory to predict the droplet diameters for non-Newtonian fluids. The emphasis is on the droplet formation, which is the rate limiting step in this extrusion technique. Uniform droplets were formed by breaking up a capillary jet with a sinusoid signal of a vibration exciter. At the maximum production rate of 27.6 $dm^3.h^{-1}$ uniform droplets with a diameter of 2.1 $\pm$ 0.12 $*10^{-3}$ m were obtained. This maximum flow rate was limited by the power transfer of the vibration exciter to the liquid flow. It was possible to get a good prediction of the droplet diameter by estimating the local viscosity from shear-rate calculations and an experimental relation between the shear rate and viscosity. In this way the theory of Newtonian fluids could be used for the non-Newtonian κ-carrageenan solution. The calculated optimal break-up frequencies and droplet sizes were in good agreement with those found in the experiments.

INTRODUCTION

I mmobilization of living cells is a common procedure in bioprocesses to increase biomass concentration or cell retention in bioreactors. Scott (1987) presented an extensive overview of immobilization methods and materials, and immobilized-cell bioreactors. Entrapment of cells in gel-forming materials such as alginate and κ-carrageenan, is the most commonly used immobilization method. In our nitrification studies we use, for example, viable nitrifying bacteria immobilized by entrapment in κ-carrageenan gel beads of 1-3 * 10^{-3} m (Tramper & Grootjen (1986) and Wijffels & Tramper (1989)). The entrapped cells are produced by first mixing a cell suspension with an aqueous κ-carrageenan solution. The suspension is extruded such that droplets are formed which are collected in a stirred potassium chloride solution for hardening. Then the produced beads are transferred to the medium with a usually lower potassium concentration and cell growth in the beads can start.

The dripping method is the easiest procedures for drop formation and still applied very often. The aqueous gel solution is pressed through a syringe with a low flow rate and droplets are formed at the tip of the needle. Droplets of a more uniform size will be obtained when an air flow arond the needle is applied. Liquid flows of 0.2 $dm^3.h^{-1}$ (Hulst et al. ,1985) and 0.43 $dm^3.h^{-1}$ (Schmidt, 1990) can be realized and scale up is done by using more syringes. Nevertheless, it takes 2-5 hours to produce enough gel beads for experiments in a bench-scale reactor of 4 dm^3 with a gel load of 25%(v/v). Experiments at a larger scale are hardly feasible with this method, and several procedures have been proposed to improve the gel-bead production rate. The rate limiting step of this method is the droplet formation.

Two main procedures for the production of gel beads are used to scale up the cell immobilization, i.e. extrusion techniques and dispersion of the gel solution in liquid or air. In the extrusion technique of Hulst et al. (1985) the aqueous gel solution is pressed

at such a high flow rate through a small orifice that a jet is formed. With a membrane, a sinusoidal vibration of a certain frequency is transferred to the liquid. This signal will cause the break-up of the jet in uniform droplets. A 100-fold increase in flow rate compared to the dripping method can thus be realized. The extrusion technique is also used for the production of ceramics and glasses with sol gel beads by Haas (1989). In the dispersion-in-air method of Ogbonna et al. (1991,1989[a]) a rotating-disk atomizer disperses an aqueous sodium-alginate solution in air. The droplets are collected in calcium-chloride solution for hardening. A production rate of 1.05 $dm^3.h^{-1}$ is reported for this method. The dispersion of an aqueous κ-carrageenan solution in a liquid is described by Audet & Lacroix (1989). The solution is dispersed in soy-bean oil and is hardened by lowering the temperature and by subsequently soaking the beads in potassium chloride. The procedure is shown to work batch wise in a 1.5 dm^3 vessel, and is amenable to scale up.

Immobilization methods for living cells require a high cell viability after immobilization. Hulst et al. (1985) do not observe a loss in cell viability after extrusion of the yeast *Saccharomyces cerevisieae* and plant cells of *Haplopappus gracilis*. Also Ogbonna et al. (1989[b]) and Lacroix et al. (1990) do not report a decrease in cell viability in their procedures for respectively *Corynebacterium glutamicum* and *Lactobacillus casei*. The dispersion methods are easy to scale up but the reproducibility of the droplet formation and the uniformity in size are considerable less than the extrusion technique of Hulst et al. (1985), according to Audet & Lacroix (1989) and Ogbonna et al. (1991), who use the dispersion method.

Compared to the conventional dripping method the extrusion technique of Hulst et al. (1985), with the advantage of the uniform droplets, inherently produces much larger quantities of immobilized cells. Also for this improved extrusion technique the formation of droplets is the rate-limiting step, and in this paper we will focus on this aspect. Problems with coalescence of the droplets at the surface of the gelling liquid can

61

be prevented by the use of a organic solvent layer on the gelling liquid (Buitelaar et al., 1988). The organic solvent will also retain the spherical shape of the gel beads. A theoretical background on the jet formation and break-up in uniform droplets is necessary for a further increase in capacity of the extrusion technique. Based on the theory, dimensions of the apparatus, and properties of the gel solution, the diameter of the droplets was predicted and compared with the experimental results. Theoretical relations for the minimum and maximum flow velocity were obtained on the basis on the diameter of the orifice and the liquid properties. The problem of a non-Newtonian fluid such as a κ-carrageenan solution was solved by estimating the local shear rate and the corresponding viscosity. The minimal flow for jet formation, droplet diameters and optimal frequencies thus predicted, were in good agreement with the experimental values. The maximum production was not limited by a theoretical maximum but by the maximum power transfer of the vibration exciter to the liquid.

THEORY

T he droplets formation in the extrusion technique begins with the formation of a capillary jet having a laminar-flow profile. Due to a disturbance of a certain frequency this capillary jet will break-up in droplets. Theoretical limits and optimal conditions for this process are evaluated here. The theory for the break-up of capillary jets is based on liquids with a Newtonian viscous behaviour. The κ-carrageenan solution, however, is a non-Newtonian fluid and the problem is approached with an estimation of the local viscosity. This viscosity depends on the local shear rate, which must thus be estimated first.

Jet formation. Different regimes of liquid flow emerging from a small outlet can be distinguished. Drops are formed at the orifice at very low flow rates. A capillary jet

with a laminar-flow profile will be formed at increasing flow rates. With a additional increase in flow rate a capillary jet with a turbulent- flow profile is formed. Eventually the liquid at the orifice will be atomized. We are interested in a jet with a laminar-flow regime. This flow regime is limited by a minimum flow rate at which the capillary jet with a laminar-flow profile changes to dripping and by a maximum flow rate where the jet becomes turbulent.

Greenwald (1980) derived a minimum-flow velocity (u_j) for a capillary jet from an energy balance, i.e. the kinetic energy of the liquid flow before the orifice is equal to the kinetic energy of the emerging jet and the energy of the new surface of the jet formed

$$u_j \ge 6 \sqrt{\frac{\sigma_l}{\rho_l \cdot d_j}} \tag{1}$$

The theoretical relation between d_j and d_t is given by Harmon (1955)

$$d_j = \frac{\sqrt{3}}{2} \cdot d_t \tag{2}$$

This relation is experimentally verified by Lindblad & Schneider(1965). Substitution of eq (2) in eq (1) provides the minimum flow velocity for a capillary jet from the liquid properties σ_l and ρ_l and the tube diameter d_t

$$u_j \ge 6.45 \sqrt{\frac{\sigma_l}{\rho_l \cdot d_t}} \tag{3}$$

63

The transition of a laminar-flow to a turbulent-flow profile in the jet occurs (Grant & Middleman, 1966) at a liqud velocity of

$$u_j \; > \; 325 \; . \; \left[\frac{\mu_l^{0.72} \; . \; \sigma_l^{0.14}}{\rho_l^{0.86} \; . \; d_t^{0.86}} \right] \tag{4}$$

The boundaries for the flow rate of a laminar capillary jet can thus be calculated with eqs (3,4).

In addition to this, a laminar-flow regime in the tube before the orifice is a prerequisite to obtain a laminar-flow profile in the capillary jet. This can be verified with the calculation of the *Re* number for the liquid flow in the tube, which must be below 2300 (Lefebvre, 1989) for laminiar flow or

$$u_j \; < \; 2300 \; . \; \left[\frac{\mu_l}{\rho_l \; . \; d_t} \right] \tag{5}$$

Break-up of viscous-liquid capillary jets in air. Lefebvre (1989) distinguished three situations for the influence of air viscosity on jet break-up: (A) The influence of the air viscosity on the break-up mechanism is negligible at low liquid flow rates, and break-up is entirely controlled by surface-tension forces. Disturbances in the liquid flow cause constrictions of the jet and eventually the break-up in uniform droplets. (B) At an increasing liquid flow rate aerodynamic forces become important in addition to the surface tension forces. The result of both forces is that a sinusoidal disturbance occurs, breaking up the jet in nonuniform droplets. (C) At very high liquid flow rates, merely aerodynamic forces control the break-up and atomization of the jet takes place immediately after emerging from the orifice.

For the formation of uniform droplets, the first break-up regime (A) is important.

According to Lefebvre (1989) the transition between the first (A) and second (B) regime occurs at

$$u_j \; > \; 22 \; \cdot \; \left[\frac{\mu_l^{0.28} \; \cdot \; \sigma_l^{0.36}}{\rho_l^{0.64} \; \cdot \; d_t^{0.64}} \right] \qquad (6)$$

Eqs (3-6) give the boundary conditions for a certain liquid and apparatus to form uniform droplets. For the maximum flow rate, the free-falling velocity of the droplets due to gravitation has also to be taken into account. This velocity must be faster than the flow rate of the jet to avoid the merging of the droplets in the jet after break-up. Practical limitations will be discussed in the Results and Discussion section.

Relation between droplet size and break-up frequency. The droplet size as a function of the applied frequency and flow rate can be predicted with a mass balance. When we assume that from each sinus wave one droplet originates, the following mass balance can be set up

$$Q \; = \; f \; \cdot \; \frac{1}{6} \; \pi \; d_p^3 \qquad (7)$$

Rearranging eq (7) gives

$$d_p \; = \; \left[\frac{Q \; \cdot \; 6}{f \; \cdot \; \pi} \right]^{\frac{1}{3}} \qquad (8)$$

Eq (8) can be applied for a wide range of experimental conditions

Optimal wavelength. The frequencies and corresponding wavelengths for breaking up the capillary jet must be within a certain interval. For wavelengths considerable shorter or longer than the jet diameter it is less probable that break-up of the jet will occur.

The optimal wavelength for breaking up the capillary jet (Weber 1931) is given by

$$\lambda_{opt} = 4.44 \cdot d_j \left[1 + \frac{3 \mu_l}{\sqrt{\rho_l \cdot \sigma_l \cdot d_j}} \right]^{0.5} \tag{9}$$

The frequency and wavelength are related by the jet velocity according to

$$f = \frac{u_j}{\lambda_j} \tag{10}$$

With eqs (9) and (10), both the optimal wavelength and optimal frequency can be calculated.

Viscosity estimation. The value for the viscosity (μ_l) is an important parameter in eqs (1), (3-6) and (10). For fluids with a Newtonian behaviour there is a shear-rate independent viscosity, but for non-Newtonian fluids the viscosity depends on the shear rate. Thus to estimate the appropriate viscosity of the κ-carrageenan solution local shear-rate values must be calculated. A viscosity versus shear-rate graph can be used to determine the local viscosity. There are two distinct places in the nozzle apparatus where the viscosity of the liquid jet is important. The first situation is in the tube where the average shear rate can be estimated using the Hagen-Poiseuille relation for a Newtonian fluid. From the Hagen-Poiseuille relation the average shear rate at half the distance between the wall and the centre of the tube can be calculated

$$\gamma = \left[\frac{2}{\pi \cdot (\frac{1}{2}d_t)^3} \right] \cdot Q \tag{11}$$

The other situation is treated with the determination of the optimal wavelength (see further in this section), where in eq (9) the dynamic viscosity of the liquid in the free-falling capillary jet is important. Weber (1931) pointed out that the velocity differences parallel to the jet direction are negligible. As a consequence the shear rate in the constricting jet is very small. The consequences for the non-Newtonian behaviour of the κ-carrageenan solution are discussed in the Result and Discussion section.

MATERIAL AND METHODS

C hemicals and preparation of the carrageen solution. The κ-carrageenan (Genugel 0909) powder was obtained from the Copenhagen Pectin Factory. The aqueous κ-carrageenan solution was prepared with tap water of 35 °C. κ-Carrageenan (2.6 % w/w) was dissolved with a Silverson Homogenizer and stored in a temperature-controlled vessel before using it in the vibration nozzle apparatus. All experiments were done at a temperature of 35 °C, at which temperature most cells will survive.

Vibration-nozzle apparatus. In Figure 1[a] the principle of the vibration nozzle apparatus is shown. The sinusoidal pulse for the vibration is generated by a Tandar TG 102 function generator. This signal is amplified by a Bruel & Kjaer, type 2706, amplifier with a maximum power consumption of 75 W. The amplified signal is transferred to a Bruel & Kjaer vibration exciter, type 4809, in which the signal is transferred to a vibration of the membrane in the six vibration chambers of the nozzle (Figure 1[b,c]). In the experiments orifices with a diameter of 0.6 mm or 0.8 mm were used. The frequency was varied between 50 and 600 s^{-1}. The produced droplets were visualized with a Griffin Xenon Stroboscope type 60.
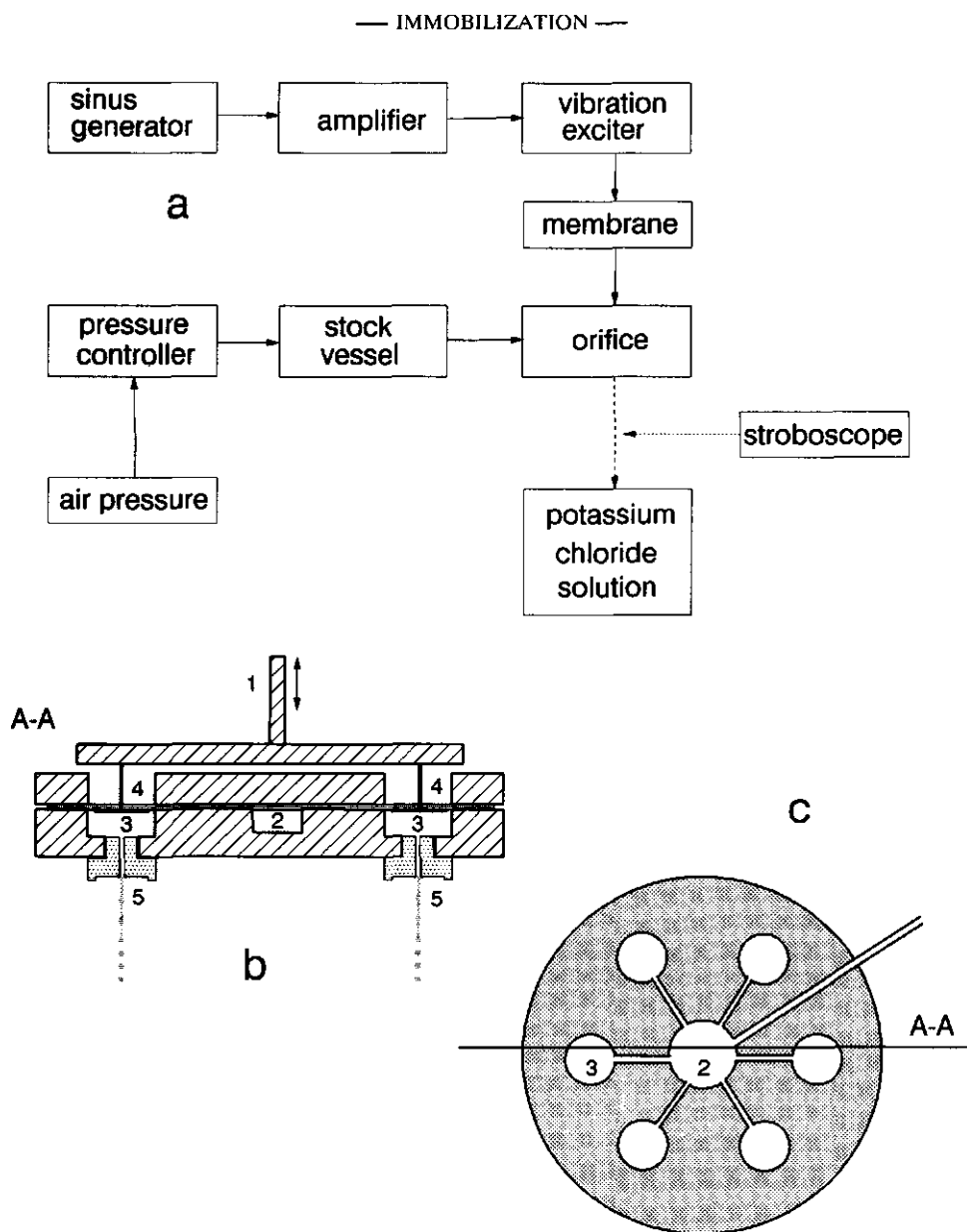
Figure 1 *a. Vibration nozzle setup.*

b,c. Vibration nozzle with connection to the vibration exciter (1) and membrane (4), the central chamber (2) where the liquid is divided over the six nozzle chambers (3), and the orifice (5) where the liquid is extruded.

Droplets-diameter measurement. Droplets were photographed at a flash time of 1/8000 s with a Nikon F3 camera equipped with a macro-lens, focus 100 mm, diaphragm f5.6 . A ruler at the same distance from the camera as the droplets was also included in every picture. Pictures were recorded on an Ilford PanF negative film and after developing projected on a large screen. The diameter of the droplets was directly measured from the projected negative exposures on the screen. The accuracy was 1%.

Shrinkage of droplets in the gelling solution. The density of the κ-carrageenan solution was determined with a conventional method. Approximately 200 κ-carrageenan gel beads were produced with the dripping method (Hulst et al. 1985). These droplets were collected in a 0.75 M KCl (Merck p.a.) solution for hardening. Volume of the collected droplets was determined by the increase in weight of the potassium chloride solution. The number and diameter of the gel beads was measured and the shrinkage could be calculated from these data.

Flow rate. The flow rate of the jet was measured by collecting droplets for 60 s.

Viscosity measurements. The viscosity of the κ-carrageenan solutions was measured with an Ostwald viscosity meter and a Haake Rotovisco RV 20 rotation viscosity meter at 35°C.

RESULTS AND DISCUSSION

Viscosity. Figure 2 shows the viscosity of the κ-carrageenan solution as a function of the shear rate. The κ-carrageenan solution shows the behaviour of a non-Newtonian fluid without a yield point for the range of shear rates tested.

Theoretical limitations of the extrusion technique. The maximum liquid flow velocity of a capillary jet breaking up in uniform droplets can be calculated with eqs (4-6). And the minimum velocity can be calculated with eq (3). The relative importance of eqs (4-6) is shown in Figure 3. The grey area shows the possible combinations between
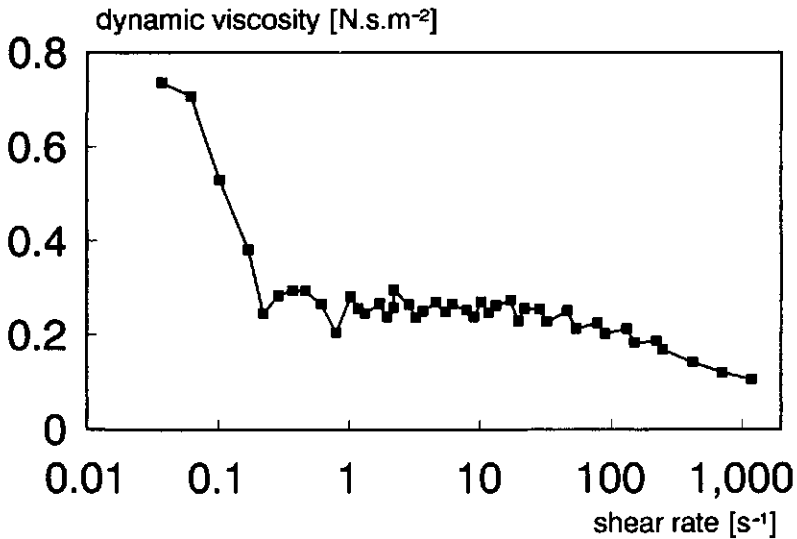
69

dynamic viscosity [N.s.m⁻²]

Figure 2 *Dynamic viscosity of 2.6 % (v/v) κ-carrageenan solution as a function of the shear rate.*

jet velocity and the dynamic viscosity, which will give uniform droplets. A measured value of 1008 kg.m^{-3} for ρ_1 and estimated value of 0.072 N.m^{-1} for σ_1 has been used in the calculations. This assumption is not only valid for the κ-carrageenan solution but also representative for other gel solutions, e.g., alginate, without surface active components. A dynamic viscosity ranging from 0.001 (water of 20°C) to 1 Pa.s (very viscous solution) has been taken for four different orifice diameters. The limit of the maximum jet velocity in all situations can be calculated with eq (6) and for the minimum jet velocity with eq (3). The eqs (4) and (5) are thus not important and the jet velocity for an extrusion technique is therefore limited on the low side by the capillary jet formation and on th high side by the transition between the uniform break-up regime (A) and the second (B) break-up regime for all the situations in Figure 3, which cover most of the gel-bead *formation conditions.*
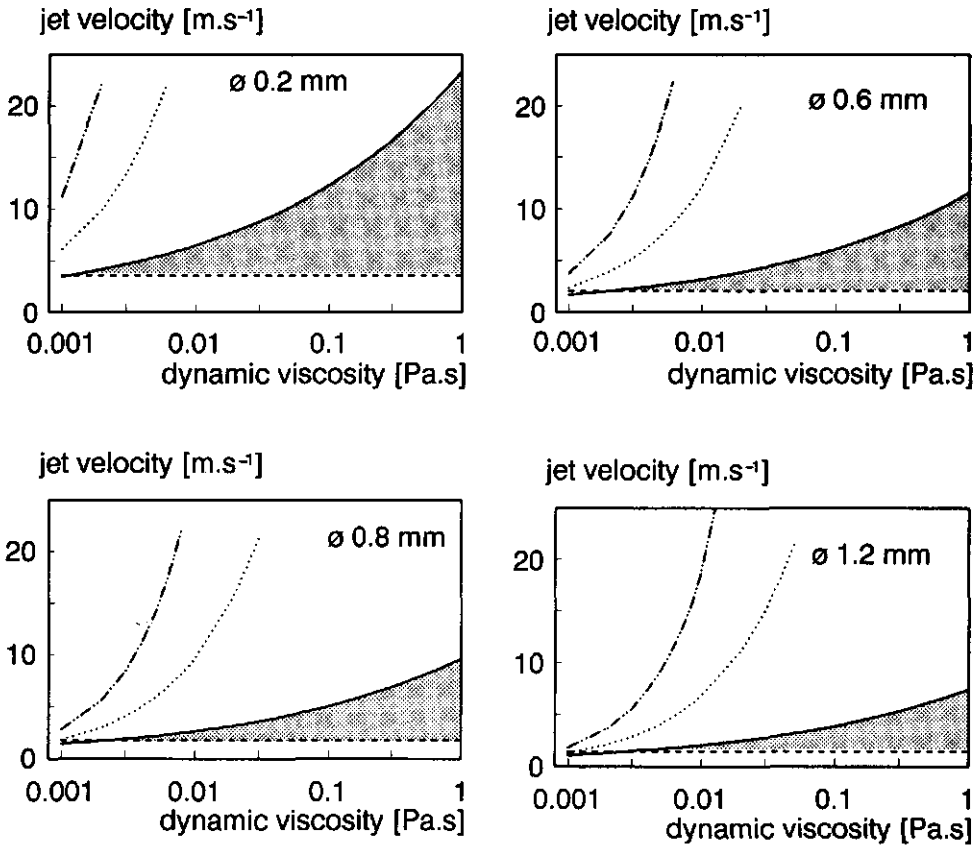
70

jet velocity [m.s⁻¹]

jet velocity [m.s⁻¹]

jet velocity [m.s⁻¹]

jet velocity [m.s⁻¹]

Figure 3   *The minimum (equation 3 ----) and maximum (equation 4 ... , 5 -··-, 6 ——)*
jet velocity (u_j) as a function of the dynamic viscosity (density of 1008 kg.m⁻³
and surface tension of 0.072 N.m⁻¹). The grey area indicates the conditions for
uniform droplet formation. Parameter: orifice diameter (Ø).

The theoretical minimum liquid velocity at least necessary to produce a capillary jet can thus be calculated from eq (3). For that the surface tension of water (0.072 N.m⁻¹) was taken as κ-carrageenan has no surface active properties. When the diameter of 0.8 mm and 0.6 mm of the orifice are used in eq (3) for d_j, a minimum liquid velocity of 1.92

and 2.22 m.s^{-1}, respectively, is calculated to obtain a capillary jet. In the experiments a stable capillary jet was formed above a flow rate of 1.89 and 2.42 m.s^{-1} for, respectively, the 0.8- and 0.6-mm nozzle. The flow rate at which a capillary jet was observed agree very well with the value calculated with eq (3).

The theoretical jet velocity for the transition between the first (A) and second (B) break-up regime is given by eq (6). For an almost negligible (Weber 1931) shear stress, a dynamic viscosity of 0.73 N.s.m^{-2} is measured (see Figure 2). Substituting this value in eq (6), we found a theoretical maximum velocity of the jet allowing uniform break-up of 8.97 and 10.7 m.s^{-1} for, respectively, the 0.8- and 0.6-mm orifices. The maximum velocity in our experiments was 2.97 and 4.11 m.s^{-1} for, respectively, the 0.8- and 0.6-mm orifices. At the maximum flow rates in our experiments this transition is thus not reached. At higher flow rates a sinusoidal disturbance (break-up regime B) will be formed and was indeed observed in experiments not described here, where a more diluted κ-carrageenan solution was used and higher velocities could be applied.

The maximum flow rate can also be limited by the free-falling velocity of the droplets. If the jet velocity exceeds the free-falling velocity, the droplets will merge and no break-up is visible. For droplets of 2 mm a free-falling velocity of 7.2 m.s^{-1} is calculated. This is above the maximum flow rate in all of our experiments. Merging of successive droplets was thus not likely to happen and indeed not observed.

The maximum flow rate in the experiments did not exceed the limits described above, but was in our experiments limited by the power transfer of the vibration exciter to the liquid. The power output of the apparatus at the highest flow rates was the maximum for the amplifier used. However, the other limiting factors must also be taken into account when other combinations of liquid, orifice and vibration exciter are used.

Droplet-formation experiments. For the two different orifice diameters several runs with various flow rates and vibration frequencies were performed. In Figure 4 a picture of the negative film is shown as an example how the droplet size was measured.

72

Visual observations of all experiments together with the average droplet diameter, standard deviation, and theoretical droplet diameter, based on eq (9), of the uniform droplets are shown in Table I[a,b]. During hardening in the 0.75 M KCl the κ-carrageenan solution shrank 6.9 vol %. The droplet sizes in Table 1[a,b] range between 1.3 and 2.75 mm which will be reduced to 1.27 and 2.68 mm, respectively, for gel beads obtained after hardening. The shrinkage of the gel beads will be influenced by the type of gelling solution and also the concentration of the gelling agent used.
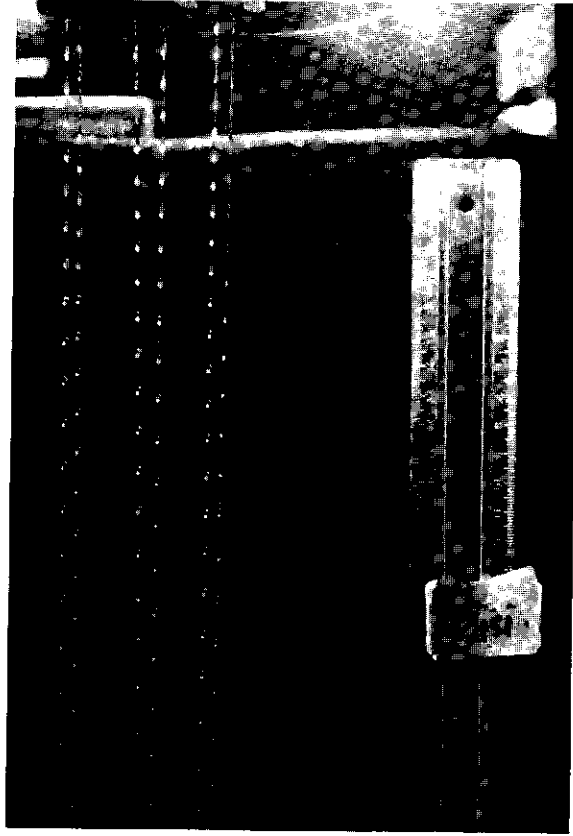

Figure 4   *A picture of up jet after break-up at a flow rate of 23.8 dm³.h⁻¹ with the 0.8 mm nozzle and a frequency of 151 s⁻¹.*

Table I[a]   *Visual observations of the liquid-jet break-up with the 0.8 mm orifice:*
-- = no break-up; - = no break-up and chain formation; + = break-up in
droplets of irregular shape; + + = break-up with satellite droplets.
Numerical values: Top, average diameter (mm); Middle, standard deviation
(mm); Bottom, theoretical diameter (eq.8)(mm).

flow rate		f_{opt} eq (9,10)	frequency [s⁻¹]					
dm³.h⁻¹	m.s⁻¹	s⁻¹	100	150	200	250	300	400
20.5	1.89	187		+	2.25 0.07 2.07	-	-	-
23.8	2.19	217	+ +	+	2.56 0.29 2.19	2.47 0.36 2.02	2.36 0.38 1.92	-
27.6	2.54	252		+	2.43 0.23 2.29	2.13 0.12 2.13	-	-
32.2	2.97	294	+ +	+	+	2.94 0.56 2.24		

Table I[b] *Visual observations of the liquid-jet break-up with the 0.6 mm orifice. Legend at Table I[a].*

flow rate		f_{opt} eq(9,10)	frequency [s⁻¹]						
dm³.h⁻¹	m.s⁻¹	s⁻¹	50	100	150	200	300	400	600
14.8	2.42	300	+ +	+	2.47 0.17 2.07	2.39 0.29 1.86	1.92 0.31 1.64	-	
17.0	2.78	344	+ +	+	2.30 0.18 2.17	1.97 0.11 1.96	1.71 0.12 1.71	1.30 0.53 1.55	
19.5	3.19	395	+ +	+	2.75 0.38 2.26	2.34 0.19 2.04	1.77 0.16 1.79	-	
25.1	4.11	508	+ +	+	+	2.38 0.32 2.23	2.02 0.37 1.95	1.75 0.25 1.77	-

The diameter range of gel beads obtained from the droplets in Table I[a,b] is suitable for application in different bioprocesses: among other, Schmidt (1990) uses 1.3-mm gel beads for denitrification; Tramper & Grootjen (1986) 3.2-mm gel beads for nitrification and Arnaud et al. (1992) 1.0-2.0-mm gel beads for the production of fermented diary products.

The visual observations showed that not all the jets were nicely broken up in uniform droplets. In Figure 5, for example, the formation of a chain of droplets

connected by thin threads of the liquid is shown. Tables I[a,b] show that formation of chains only occurs at relatively high frequencies. The formation of droplet chains is also observed by Goldin et al. (1969), who studied the stability of capillary jets for several viscoelastic fluids. They have no explanation for the stability of the thin threads formed between the droplets. These thin threads seem to be more stable than the jet itself. Besides chain formation also satellites are formed.

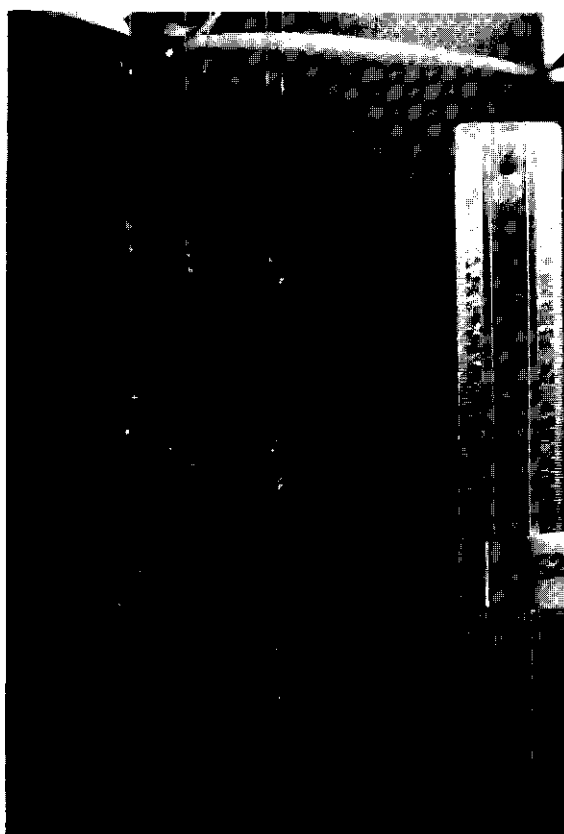**Figure 5** *A picture of a jet where a chain of droplets is formed connected by a thin thread. The flow rate was 25.1 $dm^3.h^{-1}$ with the 0.6 mm nozzle and a frequency of 52 s^{-1}.*

According to Rutland & Jameson (1970), satellites are always formed when a capillary jet breaks up in droplets. A minimum of satellites should be formed around the optimum frequency (f_{opt}), which agrees well with our results. The theoretical droplet diameters in Tables I[a,b] agree well or are slightly smaller compared to the measured droplet size, and the assumption of one droplet for each wavelength seems valid over a broad range of flow rates and frequencies (see numerical values for the diameter in

Table $I^{a,b}$). This is in contrast with the results of Hulst et al.(1985) where, on the basis on eq (9), we calculated that one droplet is formed for two wavelengths. We have no explanation of this deviation from the theory.

The optimal break-up frequency (f_{opt}) can be calculated with the assumed dynamic viscosity of the jet, 0.73 $N.s.m^{-2}$. The results are also presented in Table $I^{a,b}$. This optimal frequency agrees very well with the experimental results. The standard deviation of the bead diameter is the lowest around the optimal frequencies. The maximum production rate of 27.6 $dm^3.h^{-1}$ was reached, which is only slightly more compared to Hulst et al.(1985). The size of the beads produced by Hulst et al. (1985) at the maximum rate was 4-5 mm (personal communication). This is not a very practical gel bead size.

The uniformity of the beads in our experiments is considerable better compared to the two previously described dispersion techniques. Audet & Lacroix (1989) obtained beads with a diameter ranging from 0.09 to 6.0 mm and a median at 2.5 mm. The standard deviation is not given but 5 % (v/v) of the beads has a diameter below 0.4 mm; this percentage will be considerable more when based on the number of beads with a diameter below 0.4 mm. The experiments of Ogbonna et al. (1989) show a large difference in diameter. The median volumetric diameter is around 0.6 mm, but based on numbers, 50% of the beads has a diameter below 0.2 mm.

CONCLUSIONS

A considerable increase in production rate of uniform κ-carrageenan beads was obtained with the six-point vibration nozzle apparatus. The main aim of this study was the application of the available theory on the break-up of a capillary jet of a non-Newtonian fluid such as a κ-carrageenan solution. When this non-Newtonian behaviour is taken into account good predictions of droplet size and optimal break-up frequencies

were possible. This will provide the tools for a further scale-up of this technique. The maximum flow rate where uniform droplets were produced with the six-point vibration nozzle apparatus was 27.6 dm^3.h^{-1} with a bead diameter of 2.13 mm and a standard deviation of 0.12 mm. After hardening and shrinkage, gel beads with a diameter of 2.08 mm will be obtained. The flow rate in our experiments was limited by the power transfer of the vibration to the liquid and a new design for this technique must be optimized in this respect.

NOMENCLATURE

d	=	diameter	[m]
f	=	frequency	[s^{-1}]
Q	=	flow rate	[m^3.s^{-1}]
r	=	radius	[m]
Re	=	Reynolds number $(\rho.u.d)/\mu$	[-]
u	=	velocity	[m.s^{-1}]
λ	=	wavelength	[m]
μ	=	dynamic vicosity	[Pa.s]
ρ	=	density	[kg.m^{-3}]
σ	=	surface tension	[N.m^{-1}]
γ	=	shear rate	[s^{-1}]

subscripts

j	=	jet
l	=	liquid
p	=	droplet
t	=	orifice
opt	=	optimal

REFERENCES

Arnaud JP; Lacroix C; Choplin L (1992) Effect of agitation rate on cell release rate and metabolism during continuous fermentation with entrapped growing *Lactobacillus casei* subsp. *casei*. Biotechnol Techniques 6:265-270.

Audet P; Lacroix C (1989) Two-phase dispersion process for the production of biopolymer gel beads: effect of various parameters on bead size and their distribution. Proc Biochem 24:217-226.

Buitelaar RM; Hulst AC; Tramper J (1988) Immobilization of biocatalysts in thermogels using the resonance nozzle for rapid drop formation and an organic solvent for gelling. Biotechnol Techniques 2:109-114.

Goldin M; Yerushalmi J; Pfeffer R; Shinnar R (1969) Break-up of a laminar capillary jet of a viscoelastic fluid. J Fluid Mech 38:689-711.

Grant RP; Middleman S (1966) Newtonian jet stability. AICHE J 12:669-678.

Greenwald CG (1980) Particle morphology in spray drying of foods. PhD-thesis, University of California, Berkeley, USA.

Haas PA (1989) Gel processes for preparing ceramics and glasses. Chem Eng Progress 85:44-52.

Harmon DB (1955) Drop sizes from low-speed jets. J Franklin Inst 259:519-522.

Hulst AC; Tramper J; Riet K van 't; Westerbeek JMM (1985) A new technique for the production of immobilized biocatalyst in large quantities. Biotechnol Bioeng 27:870-876.

Lacroix C; Paquin C; Arnaud J-P (1990) Batch fermentation with entrapped growing cells of *Lactobacillus casei*. Appl Microbiol Biotechnol 32:403-408.

Lefebvre AH (1989) Atomization and sprays. Hemisphere Publishing Corporation, New York, USA.

Lindblad NR; Schneider JM (1965) Production of uniform-sized liquid droplets. J Sci Instum 42:635-638.

Ogbonna JC; Matsumura M; Kataoka H (1991) Effective oxygenation of immobilized cells through reduction in bead diameters: a review. Proc Biochem 26:109-121.

Ogbonna JC; Matsumura M; Yamagata T; Sakuma H; Kataoka H (1989[a]) Production of micro-gel beads by a rotating disk atomizer. J Ferment Bioeng 68:40-48.

Ogbonna JC; Pham CB; Matsumura M; Kataoka H (1989[b]) Evaluation of some gelling agents for immobilization of aerobic microbial cells in alginate and carrageenan gel beads. Biotechnol Techniques 3:421-424.

Rutland DF; Jameson GJ (1970) Theoretical prediction of the sizes of drops formed in the break-up of capillary jets. Chem Eng Sci 25:1689-1698.

Schmidt J (1990) Untersuchung und modellierung der autotrophen Trinkwasserdenitrification mit matriximmobilisierten *Paracoccus denitrificans* DSM 1403. PhD-Thesis, Technical University Carolo-Wilhelmina, Braunschweig, Germany.

Scott CD (1987) Immobilized cells: a review of recent literature. Enzyme Microb Technol 9:66-73.

Tramper J; Grootjen DRJ (1986) Operating performance of *Nitrobacter agilis* immobilized in carrageenan. Enzyme Microb Technol 8:477-480.

Weber C (1931) Zum zerfall eines flüssigkeitsstrahles. Ztschr fur angew Math und Mech 11:136-154.

Wijffels RH; Tramper J (1989) Performance of growing *Nitrosomonas europaea* immobilized in κ-carrageenan. Appl Microbiol Biotechnol 32:108-112.

80

5 BIOMASS PROFILES

A novel technique, combining labelling and stereological methods, for the determination of spatial distribution of two microorganisms in a biofilm is presented. Cells of *Nitrosomonas europaea* (ATCC 19718) and *Nitrobacter agilis* (ATCC 14123) were homogeneously distributed in a κ-carrageenan gel during immobilization and allowed to grow out to colonies. The gel beads were sliced in thin cross sections after fixation and embedding. A two-step labelling resulted in green fluorescent colonies of either *N.europaea* or *N.agilis* in the respective cross sections. The positions and surface areas of the colonies of each species were determined and from that a biomass volume distribution for *N.europaea* and *N.agilis* in κ-carrageenan gel beads was estimated. This technique will be useful for the validation of biofilm models, which predict such biomass distributions.

INTRODUCTION

I n natural environments submerged solid surfaces are readily colonized by microorganisms and as a result a biofilm will develop. The biofilm contains a wide variety of cells of different species, macromolecules and particulate material. The spatial distribution of the various microorganisms is an important aspect in understanding the development of such a biofilm. Modelling of biofilm processes is a helpful tool in gaining a better understanding of the structure and development of biofilms (Bryers & Banks, 1990; Wanner & Gujer, 1984). Cells artificially immobilized in κ-carrageenan gel beads of a fixed diameter provide a suitable model system for biofilm studies: For example, for the validation of a dynamic model for substrate conversion by growing *Nitrobacter agilis* cells can be grown immobilized in such gel beads (Gooijer et al. 1991; Wijffels et al. 1991). For measuring the spatial biomass distribution thin cross sections of the resin-embedded gel beads, aspecifically stained with toluidine blue are used.

In the field of biofilm research there is a need for accurate methods to determine biomass distributions in multispecies biofilms (Fruehn et al. 1991). Labour-intensive methods like radiolabelling are used (Bryers & Banks, 1990), but a discernment of only about 100 μm, which is not sufficient for aerobic biofilms since most of the cells are located in the outer 100-μm layer, has been achieved. Specific labelling by fluorescent-antibody (FA) techniques is a promising method for determining those biomass distributions.

The FA technique is widely used for counting specific microorganisms in waste water and soil (Fliermans & Schmidt, 1975; Hoff, 1988; Muyzer et al. 1987; Rennie & Schmidt, 1977; Völsch, 1990). For this method suspended cells are fixed on glass plates and stained by an FA-labelling technique. It was not possible to use the FA-labelling technique directly on activated sludge flocs obtained from waste water (Swerinski et al.1985). A **qualitative** spatial distribution of one artificial immobilized species has been

determined with an FA labelling technique (Al-Rubeai et al. 1990; Burrill et al. 1983; Kuhn et al. 1991; Monbouquette & Ollis, 1988; Monbouquette et al. 1990; Worden & Berry, 1992).

A **quantitative** determination of the spatial distribution of two microorganisms in a gel bead is the aim of this work. The cells of *Nitrosomonas europaea* and *Nitrobacter agilis* were homogeneously distributed in the κ-carrageenan gel during immobilization and allowed to grow out to colonies and then samples from the gel beads were used for immunolabelling. After fixation and embedding, semi-thin sections (2 μm) were used for specific labelling. Two adjacent cross sections of a gel bead were labelled, one with rabbit-anti-*Nitrosomonas europaea*, the other with rabbit-anti-*Nitrobacter agilis* antibodies, and then both with goat-anti-rabbit-FITC (fluorescein isothiocyanate) conjugate. This procedure results in green fluorescent colonies of either *N.europaea* or *N.agilis* in a cross section.

This method provides the tools for determining the biomass distribution of two microorganisms in one gel bead as a function of time. Validation of a dynamic two-microorganism biofilm model is thus feasible and also intrabiofilm relations between microorganisms can be studied in more detail.

MATERIALS AND METHODS

C ells. Cells of *Nitrosomonas europaea* (ATCC 19718) and *Nitrobacter agilis* (ATCC 14123) were cultivated according to the method previously described (Hunik et al. 1992; Wijffels et al. 1991).

Immobilization and Cultivation. After immobilization (Hulst et al. 1985; Wijffels et al. 1991), gel beads with an average diameter of 2.1 ± 0.1 mm were obtained. The immobilized cells in the gel beads were cultivated for 49 days in a continuously operated

air-lift loop reactor of 3.3 dm^3 at a temperature of 30°C. The liquid-phase dilution rate was 2.3 * 10^{-5} s^{-1} for a medium composed of the two chemostat media, in which sodium salts were replaced by potassium salts. The gel beads were kept in the reactor with a sieve screen. The pH was maintained at 7.4 with a K_2CO_3 solution (200 $g.dm^{-3}$) and a pH controller. Cell growth was monitored indirectly by measuring the NH_4^+, NO_2^- and NO_3^- concentrations in the effluent daily.

Sample preparation. Gel beads were harvested and stored in a 0.1 M KCl solution for one hour and then washed twice with a potassium phosphate buffer (PPB, 8.7 g of K_2HPO_4, 6.8 g of KH_2PO_4, 7.45 g of KCl per dm^3 and a pH of 7.4) for 10 minutes. The gel beads were fixed in paraformaldehyde (3% w/v in PPB) for two hours. The paraformaldehyde was removed by washing with PBB three times for 10 minutes followed by washing twice with 0.1 M KCl for 10 minutes. Gel beads were dehydrated in ethanol-KCl solutions (Van Neerven et al. 1990) starting with 10% ethanol- 0.09 M KCl and successively followed by 20% ethanol- 0.08 M KCl, 30% ethanol- 0.07 M KCl, 50% ethanol- 0.05 M KCl, 70% ethanol- 0.03 M KCl, 90% ethanol, 100% ethanol and finally ending with an additional 100% ethanol step. The gel beads were kept 20 minutes in each solution.

After dehydration, the 100% ethanol was replaced by Poly Ethylene Glycol (PEG) with an infiltration range at 55 °C. PEG was a 1:2 mixture of PEG 4000 (Merck 807490) and PEG 1500 (Merck 807489). The PEG/ethanol ratio changed successively from 1:10 to 1:4, 1:1, 4:1 and 10:1. The gel beads were kept for 30 minutes in each solution. Finally, the gel beads were kept in 100% PEG for 60 minutes. The PEG infiltrated gel beads were polymerized in a mould by cooling to room temperature. These PEG embedded gel beads could be used to slice 2 μm sections.

Fluorescent-antibody labelling. Sections 2 μm thick were obtained from the embedded beads with a Leitz rotary microtome equipped with a Kulzer knife (Figure 1).

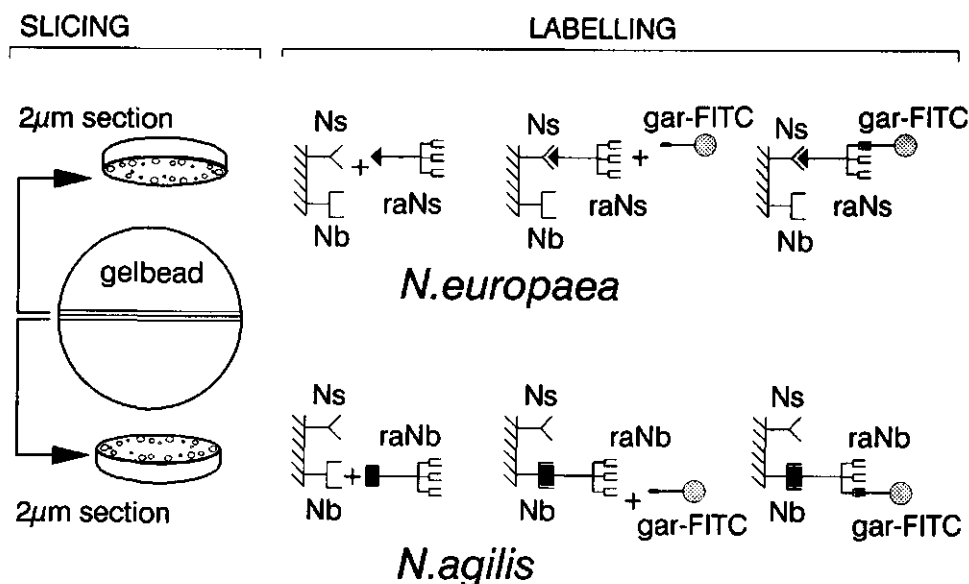SLICING   LABELLING

Figure 1   *Slicing and labelling of the gel beads.*

The sections were collected in a droplet of (40% w/v) PEG 6000 (Merck 807491) solution in phosphate buffered saline (PBS, pH 7.4) and attached to a poly-L-lysine coated glass slide. After the PEG was removed by rinsing with PBS the sections were ready for specific labelling according to the following protocol: washing with PBS, 10 min; aldehyde blocking with NH_4Cl (0.1M), 5 min; aldehyde blocking with $NaBH_4$ (0.5 $\mu g/dm^3$), 5 min; washing with PBS, 10 min; background blocking with 1% (w/v) bovine serum albumin (BSA) fraction V (Merck 12018)in PBS, 60 min; washing with 0.1 % (w/v) BSA in PBS, twice for 30 min each; labelling with rabbit-anti-*N.europaea* or rabbit-anti-*N.agilis*(diluted 1:300 in PBS), 45 min; washing with 0.1% (w/v) BSA in PBS, four times 5 min each; labelling with goat-anti-rabbit FITC conjugate (Sigma F6005, diluted 1:40 in PBS), 45 min; washing with PBS, 7 times for 6 min each.

Rabbit-anti-N.*europaea* (Verhagen & Laanbroek, 1991) and rabbit-anti-N.*agilis* (Laanbroek & Gerards, 1991) were generously provided by the Netherlands Institute for

Ecology - Centre for Terrestial Ecology, Heteren, The Netherlands. All steps were done at room temperature and high air humidity (above 60%). When FITC-conjugates were used, all steps were done in the dark. Finally the labelled sections were mounted in a Citifluor in glycerol solution (AF2, van Loenen Instruments, The Netherlands). Autofluorescence of the colonies was tested with a control in which the labelling with the goat-anti-rabbit FITC conjugate was omitted from the staining protocol. Also the non-specific binding of the goat-anti-rabbit-FITC was tested. For this the labelling with rabbit-anti-*N.europaea* or rabbit-anti-*N.agilis* was omitted from the protocol. Both rabbit-anti-*Nitrosomonas europaea* and rabbit-anti-*Nitrobacter agilis* antibodies were tested with cells from the pure cultures. They specifically stained the respective microorganisms and showed no cross reaction.

Microscopy. The FA-labelled samples were examined with a Microphot Nikon FXA microscope. A fluor pan Nikon objective (10x/0.5 NA) was used. The FITC fluorescence was observed with a DM500 dichroic mirror, B470-490 excitation filter and BA 520-560 emission filter. Photomicrographs were recorded on Kodak Ektachrome P800/1600 film (5020 EES at 800 ASA). The colony distribution was determined with a Hitachi camera unit attached to the microscope.

Quantitative analyses of spatial biomass distribution. The volumetric biomass fraction as function of the gel bead radius can be derived from the positions and surface areas of the colonies in the labelled sections. According to the principle of Delesse (Weibel, 1979) the volumetric density of the biomass in a gel bead is equal to the areal density of the cross-sectioned colonies in a section of that gel bead. Thus, the colony surface distribution in a thin section of a gel bead is directly related to the volumetric biomass density distribution in the gel beads. The colony surface distribution can be obtained from the microscopy data with the principle of Rosiwal (Weibel, 1979). For that determination, test lines are drawn (Figure 2) in the cross sections of the gel beads. The colony surface distribution in the cross section is equal to the fractional length of the test

86

line which intersects the colonies. Colonies were assumed to be spherical. The colony density in the core of the gel bead was very low, and an average colony density was therefore determined for that area between the centre and half the radius of the gel beads. For each distribution profile of one species two sections and two different areas in each cross section were examined.
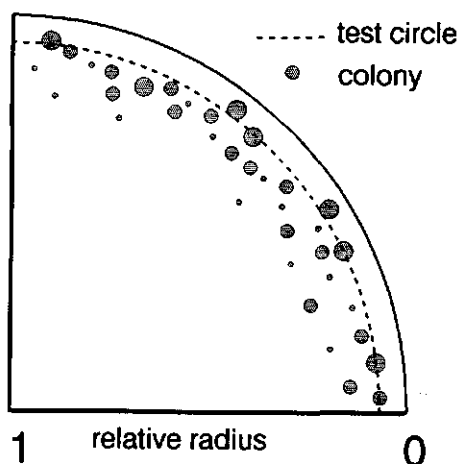

Figure 2   *Principle of the test circle for the determination of the volumetric colony distribution as function of the relative distance from the edge of the gel bead.*

RESULTS AND DISCUSSION

Cell cultivation. After 49 days of cultivation, the experiment was ended, since more than 98% of the influent ammonia was converted to nitrate, and therefore, colonies of both *N. europaea* and *N. agilis* cells were expected in the gel beads. For the determination of a biomass distribution, gel beads from day 49 are used as an example.
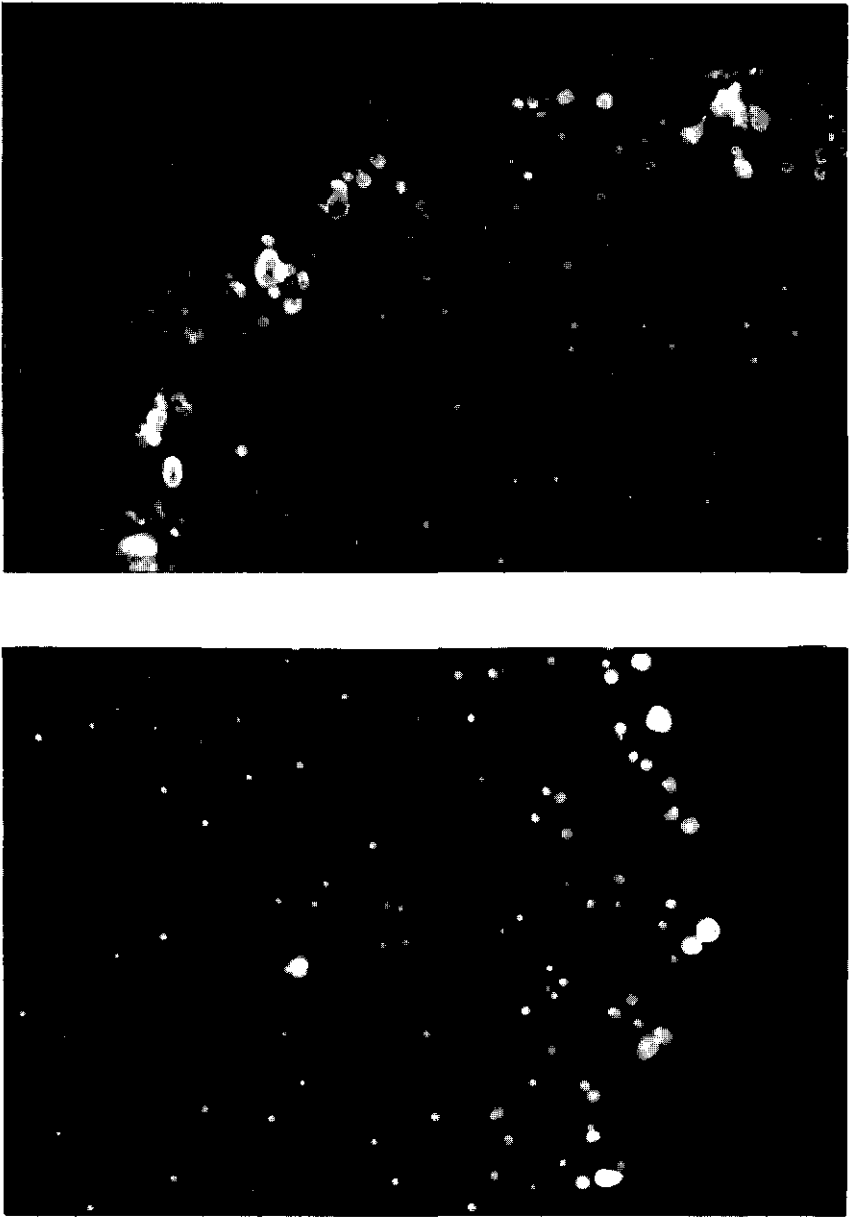
Figure 3   *Microphotographs N. europaea (top) and N. agilis (bottom) of a part of a labelled cross section. Gel beads after shrinking were 1.4 mm.*

Sample preparation. During dehydration the gel beads shrank 35% in diameter. The fixation with paraformaldehyde seemed to work very well, because no artifacts were observed in the gel itself or the microorganism colonies.

Fluorescent-antibody labelling. When the protocol for the FA labelling was developed, autofluorescence of the aging colonies was a serious problem. For the suppression of this autofluorescence, blocking with NH_4Cl, $NaBH_4$ and BSA was introduced into the labelling protocol. In Figure 3, photomicrographs with labelled colonies of *N. europaea* and *N. agilis* in a cross section of a gel bead after 49 days of cultivation are shown. A random distribution of colonies, in contrast with a profile in biomass distribution can be seen. Colonies which are closer to the edge are larger than the colonies more at the centre of the gel bead. Besides the labelled and bright fluorescent colonies in the samples, there are some colonies which are faintly visible due to autofluorescence of the nonlabelled microorganisms.

Spatial biomass distribution . The volumetric biomass distribution shown in Figure 4 was based on data from gel beads at the end of the experiment. In Figure 4 a region with an increased biomass volume fraction in the outer region of the gel bead is indicated. This effect originates from the substrate concentration profile developed in the gel bead, which results in a relatively high biomass concentration in the outer region and a low concentration in the centre of the gel bead (Gooijer et al. 1991). The sharp drop in volume fraction at the edge of the gel bead described in Figure 4 originates from the assumption of spherical colonies (Fig.2). This assumption does not allow for colony centres at the edges of the gel beads.

Infinitely thin sections are assumed, which means that only the surface of the cross-sectioned colony is labelled. This seems a valid assumption because diffusion of antibodies in κ-carrageenan gel 3% w/v is negligible (Chevalier et al. 1987). Diffusion of the antibody in a shrunk and fixed gel is even more unlikely.
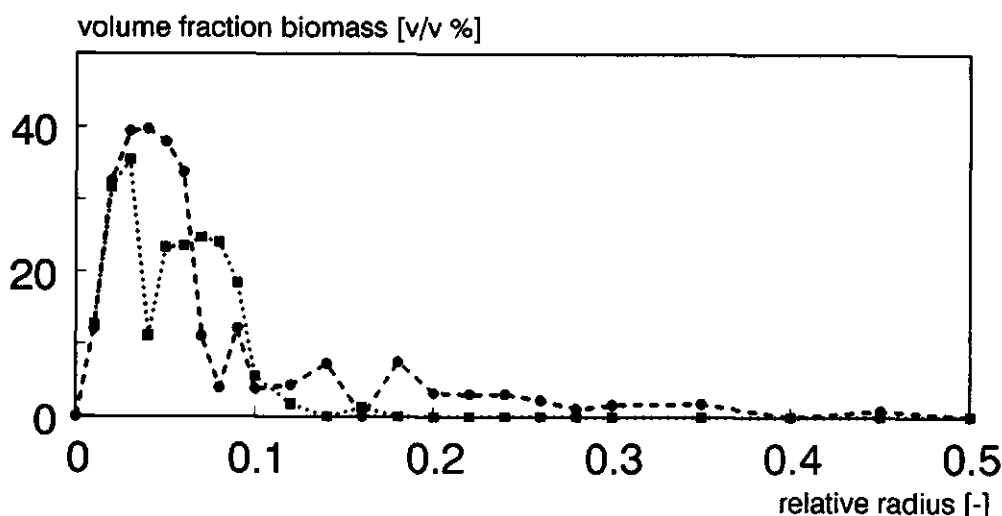
89

volume fraction biomass [v/v %]

Figure 4   Biomass distribution of **Nitrosomonas europaea** (---●---) and **Nitrobacter agilis**
(···■···) *after 49 days of cultivation. Volume fraction of biomass as
function of the gelbead radius (0 = edge of the bead).*

The effect of shrinkage on colony radius and position is minimized by using distances
relative to the size of the observed section of the gel bead.

In conclusion, the labelling technique described in this paper made it possible to
measure a biomass volume distribution of two immobilized species. This novel method,
a combination of labelling technique and stereological methods, provides a **quantitative**
spatial distribution measure of the biomass in the gel bead. The quantitative results are
a useful tool for the comparison with model predictions for the biomass concentration.
Experiments in which this labelling technique is used to validate a dynamic model for
the growth of *Nitrosomonas europaea* and *Nitrobacter agilis* are at present being carried
out in our laboratory.

90

REFERENCES

Al-Rubeai MA, S. C. Musgrave SC, Lambe CA, Walker AG, Evans NH, Spier RE (1990) Methods for the estimation of the number and quality of animal cells immobilized in carbohydrate gels. Enzyme Microb Technol 12:459-463.

Bryers JD, Banks MK (1990) Assessment of biofilm ecodynamics. In: De Bont J.A.M. (Eds.), Physiology of immobilized cells. Elsevier, Amsterdam, The Netherlands, 49-61.

Burrill HN, Bell LE, Greenfield Pf, Do DD (1983) Analysis of distributed growth of *Saccharomyces cerevisiae* cells immobilized in polyacrylamide gel. Appl Environ Microbiol 46:716-721.

Chevalier P, Cosentino GP, de la Noüe J, Rakhit S (1987) Comparative study on the diffusion of an IgG from various hydrogel beads. Biotechnol Techniques 1:201-206.

Fliermans CB, Schmidt EL (1975) Autoradiography and immunofluorescence combined for autoecological study of single cell activity with *Nitrobacter* as a model system. Appl Microbiol 30:676-684.

Fruhen M, Christan E, Gujer W, Wanner O (1991) Significance of spatial distribution of microbial species in mixed culture biofilms. Wat Sci Tech 23:1365-1374.

Gooijer CD de, Wijffels RH, Tramper J (1991) Growth and substrate consumption of *Nitrobacter agilis* cells immobilized in carrageenan: Part 1. Dynamic modeling. Biotech Bioeng 38:224-231.

Hoff KA (1988) Rapid and simple method for double staining of bacteria with 4',6-diamidino-2-phenylindole and fluorescein isothiocyanate-labeled antibodies. Appl Environ Microbiol 54:2949-2952.

Hulst AC, Tramper J, Van't Riet K, Westerbeek JMM (1985) A new technique for the production of immobilized biocatalyst in large quantities. Biotech Bioeng 27:870-876.

Hunik JH, Meijer HJG, Tramper J (1992) Kinetics of *Nitrosomonas europaea* at extreme substrate, product and salt concentrations. Appl Microbiol Biotechnol 37:802-807.

Kuhn RH, Peretti SW, Ollis DF (1991) Microfluorimetric analysis of spatial and temporal patterns of immobilized cell growth. Biotech Bioeng 38:340-352.

Laanbroek HJ, Gerards S (1991) Effects of organic manure on nitrification in arable soils. Biol Fertil Soils 12:147-153.

Monbouquette HG, Ollis DF (1988) Scanning microfluorimetry of Ca-alginate immobilized *Zymomonas mobilis*. BioTechnol 6:1076-1079.

Monbouquette HG, Sayles GD, Ollis DF (1990) Immobilized cell biocatalyst activation and pseudo-steady-state behaviour: Model and experiment. Biotech Bioeng 35:609-629.

Muyzer G, De Bruyn AC, Schmedding DJM, Bos P, Westbroek P, Kuenen GJ (1987) A combined immunofluorescence-DNA-fluorescence staining technique for enumeration of *Thiobacillus ferrooxidans* in a population of acidophilic bacteria. Appl Environ Microbiol 53:660-664.

Neerven ARW van, Wijffels RH, Zehnder AJB (1990) Scanning electron microscopy of immobilized bacteria in gel beads: a comparative study of fixation methods. J Microbiol Methods 11:157-168.

Rennie RJ, Schmidt EL (1977) Immunufluorescence studies of *Nitrobacter* populations in soils. Can J Microbiol 23:1011-1017.

Szwerinski H, Gaiser S, Bardtke D (1985) Immunofluorescence for the quantitative determination of nitrifying bacteria: interference of the test in biofilm reactors. Appl Microbiol Biotechnol 21:125-128.

Verhagen FJM, Laanbroek HJ (1991) Competition for ammonium between nitrifying and heterotrophic bacteria in dual energy-limited chemostats. Appl Environ Microbiol 57:3255-3263.

Völsch A, Nader WF, Geiss HK, Nebe G, Birr C (1990) Detection and analysis of two serotypes of ammonia-oxidizing bacteria in sewage plants by flow cytometry. Appl Environ Microbiol 56:2430-2435.

Wanner O, Gujer W (1984) Competition in Biofilms. Wat Sci Tech 17:27-44.

Weibel ER (1979) Stereological methods, 1. Practical methods for biological morphometry. Academic press. London. Great Britain.

Wijffels RH, Gooijer CD de, Kortekaas S, Tramper J (1991) Growth and substrate consumption of *Nitrobacter agilis* cells immobilized in carrageenan: Part 2. Model evaluation. Biotech Bioeng 38:232-240.

Worden RM, Berry LG (1992) The one-dimensional biocatalyst. A research tool for *In situ* analysis of immobilized-cell biocatalysts. Appl Biochem Biotechnol 34/35:487-498.

6 MODEL VALIDATION

SUMMARY

A dynamic model for two microbial species immobilized in a gel matrix is presented and validated with experiments. It characterizes the nitrification of ammonia with cells of *Nitrosomonas europaea* and *Nitrobacter agilis* co-immobilized in κ-carrageenan gel beads. The model consists of kinetic parameters for the microorganisms and mass transfer equations for the substrates and products in and outside the gel beads. The model predicts reactor bulk concentrations together with the substrate consumption rate, product formation, and biomass growth inside the gel beads as a function of time. A 50 day experiment with immobilized cells in a 3.3 dm^3 air-lift loop reactor was carried out to validate the model. The parameters values for the model were obtained from literature and separate experiments. The experimentally determined reactor bulk concentrations and the biomass distribution of the two microorganisms in the gel beads were well predicted by the model. A sensitivity analysis of the model for the given initial values indicated the most relevant parameters to be the maximum specific growth rate of the microorganisms, the diffusion coefficient of oxygen and the radius of the beads. The dynamic model provides a useful tool for further study and possible control of the nitrification process.

INTRODUCTION

Wash-out of nitrifying microorganisms from wastewater treatment plants can be overcome by biomass retention as applied in biofilm reactors. The heterogeneous and complex nature of biofilms makes description and control of the process difficult. This has been the driving force to develop various models aiming at a better description and understanding of biofilm processes, ultimately resulting in a better control. Steady-state biofilm models are used to describe fluidized bed reactors (Rittman & Manem, 1992), rotating biological contactors (Chen et al., 1990) and trickling filters (Siegrist & Gujer, 1987). For transient states, such as the start-up phase of the biofilm and a change in influent concentration, the steady-state model is not suitable. Therefore, dynamic models are developed to describe the transient behaviour of biofilms.

Several dynamic biofilm models with a heterogeneous population of microorganisms including nitrifying bacteria are developed. For example, Denac et al. (1983) developed a dynamic model for a nitrifying trickling filter, but without taking into account external diffusion limitation. Also Bryers (1988) and Sayles & Ollis (1989) neglect external diffusion resistance in their dynamic model. Kissel et al. (1984), on the contrary, present a dynamic model for a completely mixed fixed-film reactor with external diffusion limitation. Similarly, Wanner & Gujer (1986) have developed a multi-species biofilm model including external mass-transfer limitation. The above-mentioned models are not validated with experiments, only simulations are presented. An important problem with validation of these models is the structure and biomass distribution in the biofilm.

Only a few dynamic models for biofilms are validated experimentally, but they all deal with a single-species biofilm. For example, the dynamic model of Monbouquette et al. (1990) for *Zymomonas mobilis* is qualitatively validated with experiments. Their model includes external mass transfer resistance and a diffusion coefficient dependent

on the biomass density. Also the model developed in our laboratory (Wijffels et al. 1991, Gooijer et al. 1991) includes external mass transfer and a biomass-dependent diffusion coefficient. A large decrease in computation time is achieved in the latter model by separation of biomass growth and substrate conversion. The model is validated with biomass concentration profiles in the gel beads and oxygen fluxes to the gel beads, under the condition of one limiting substrate, oxygen, with a constant value in the bulk phase.

The model presented in this paper is a dynamic model for a two-species biofilm including external mass-transfer limitation. The two species are strictly autotrophic microorganisms, i.e. CO_2 is the sole carbon source, and ammonia is converted according to the following reaction equations

Nitrosomonas europaea:
$$NH_4^+ \; + \; 1.5 \; O_2 \; \Rightarrow \; NO_2^- \; + \; 2 \; H^+ \; + \; H_2O$$

Nitrobacter agilis:
$$NO_2^- \; + \; 0.5 \; O_2 \; \Rightarrow \; NO_3^-$$
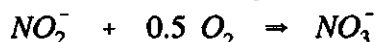
Every substrate, i.e. NH_4^+, NO_2^- and O_2, can be growth limiting and influent concentrations of the reactor can be varied. The model is validated with respect to the biomass concentration profiles in the beads and the reactor bulk concentrations. Input parameters are intrinsic kinetic parameters of the microorganisms, internal diffusion coefficients and mass transfer coefficients obtained from literature or separate experiments. The value of such a mechanistic model is the possibility to use it, with care, for predictions beyond the experimental boundaries where it is validated (Beck 1991). To identify the most important parameters of the model a sensitivity analysis is done, in which the influence of all input parameters on the model output is tested.

Three identical reactors were operated and weekly samples of gel beads analyzed for the spatial distribution of the individual microorganisms as described by Hunik et al.

(1993). The biomass distributions in the gel beads were predicted rather well. Reactor bulk concentrations of the nitrogenous compounds were analyzed daily. Predicted and measured bulk concentrations were in good agreement with each other. The dynamic model with the intrinsic biological and transport parameters obtained from literature was thus validated experimentally.

MODEL DEVELOPMENT

General considerations. In the model the gel bead is divided in 250 equally spaced spherical shells and uniform conditions within each shell are assumed. In the absence of a tangential gradient in biomass and substrate concentration, the problem is one-dimensional normal to the surface of the gel bead. The effective diffusion coefficient in the gel bead is assumed to be constant, which is in contrast to the model of Gooijer et al. (1991). The influence of the biomass on the effective diffusion coefficient in their model is 1% and therefore, we omitted this biomass-dependent diffusion coefficient. This negligible effect of biomass on the diffusion coefficient is also found by Westrin (1991). The limiting substrate for *Nitrosomonas europaea* is NH_4^+ or O_2. For *Nitrobacter agilis* NO_2^- or O_2 can be limiting. Within each shell in the gel bead the most limiting substrate for each microorganism is determined according to the criteria and equations given in Table I. It is assumed that kinetics of the immobilized cells are similar to those for suspended cells. The maintenance or decay rate of biomass is taken into account with the method proposed by Beeftink et al. (1990) and used by Gooijer et al. (1991) in their model. The biomass is assumed to be homogeneously distributed at the start of the experiment and there is no transport of biomass within the gel bead. The biomass concentration is limited by a maximum derived from the experimentally determined biomass concentration in the gel beads. Sayles & Ollis (1989), Gooijer et al. (1991) and Monbouquette et al.(1990) use a maximum biomass concentration derived from

literature. When in the model the maximum biomass concentration in a shell is reached the excess biomass produced is assumed to disappear from the reactor immediately. The actual situation in the experiments is obviously different and the consequences are discussed in the Results & Discussion section.

Table I   *The rate-limiting substrate (i) for the microorganism (m) determines the consumption rate equations $q^{i,m}$ (right-side Table) in eq (1). The selection criterium for the "most-limiting" substrate is given at the bottom.*

Nitrosomonas europaea	Nitrobacter agilis	rate controling equations $q^{i,m}$
limiting substrate		
NH_4^+	NO_2^-	$q^{NH4+,Ns}$ and $q^{NO2-,Nb}$
NH_4^+	O_2	$q^{NH4+,Ns}$ and $q^{O2,Nb}$
O_2	NO_2^-	$q^{O2,Ns}$ and $q^{NO2-,Nb}$
O_2	O_2	$q^{O2,Ns} + q^{O2,Nb}$

criteria for limiting substrate		
minimum of	minimum of	

$$\frac{S^{NH_4^+}}{K_S^{NH_4^+,Ns} + S^{NH_4^+}}$$ $$\frac{S^{NO_2^-}}{K_S^{NO_2^-,Nb} + S^{NO_2^-}}$$

and   and

$$\frac{S^{O_2}}{K_S^{O_2,Ns} + S^{O_2}}$$ $$\frac{S^{O_2}}{K_S^{O_2,Nb} + S^{O_2}}$$

The model uses a constant oxygen concentration in the bulk liquid, but all other parameters such as substrate concentration in the influent, dilution rate or mass transfer parameters can be varied as function of time within the model.

Equations. The biological part of the model is described by equations for substrate consumption and biomass production. When the "most" limiting substrate (i) for a microorganism (m) is determined, the consumption rate ($q^{i,m}$) for that substrate is given by

$$q^{i,m} = \frac{\mu^m \cdot X^m}{Y^m} + m_s^m \cdot X^m \cdot \left[\frac{S^i}{(K_S^{i,m} + S^i) \cdot K_I} \right] \quad (1)$$

The four different situations of limiting substrate are presented in the Table I. The criteria in Table I implicitly contain the assumption of a non-interactive model for substrate utilization. When oxygen is the limiting substrate for both microorganisms the oxygen consumption rate is a summation of $q^{O2,Ns}$ and $q^{O2,Nb}$. Conversion of the non-limiting substrate is derived by the stoichiometry of the reaction equations. This seems a valid approach because the yield coefficients for both nitrogen and oxygen of these microorganisms are very low.

For *Nitrosomonas europaea* the inhibition constant (K_I) is assumed to be 1 (Hunik et al. 1992). The K_I for *Nitrobacter agilis* is determined by by the inhibition concstants for NO_2^- and NO_3^- as follows

$$K_I = \left[1 + \frac{S^{NO_2}}{I_{NO_2}} \right] \cdot \left[1 + \frac{S^{NO_3}}{I_{NO_3}} \right] \quad (2)$$

The biomass production rate for microorganism (m) is defined as

$$\frac{dX^m}{dt} \;=\; \mu^m . X^m \;-\;$$

$$m_s^m . Y^m . X^m . \left[1 \;-\; \left[\frac{S^i}{(K_S^{i,m} \;+\; S^i) . K_I} \right] \right] \tag{3}$$

where the specific growth rate (μ^m) of microorganism (m) is given by

$$\mu^m \;=\; \mu_{max}^m . \left[\frac{S^i}{(K_S^{i,m} \;+\; S^i) . K_I} \right] \tag{4}$$

At very low substrate concentrations a net decrease in biomass, or biomass decay, is possible according to eq (3). At more elevated substrate concentrations, maintenance requirements are fulfilled with an additional substrate consumption as can be seen in eq (1) (Beeftink et al. 1991). For *Nitrobacter agilis* this situation is more complicated due to the substrate and product inhibition, K_I becomes smaller as 1. Nevertheless the maintenance requirements of *N. agilis* are treated in a similar fashion as for *N. europaea* up to moderate (50mM NO_2^-) substrate concentrations. At high substrate concentration, where substrate inhibition of NO_2^- becomes important, the substrate consumption rate will decrease and a net decrease in biomass will occur according to eq (3).

The transport phenomena are described with equations for the diffusion in the gel bead, external mass transfer resistance between bulk and gel bead and the reactor configuration.

The subtrate concentration in the gel bead as function of time and radial position is given by

$$\frac{\partial S^i}{\partial t} = I\!D^i_{gel} \cdot \left[\frac{\partial^2 S^i}{\partial r^2} + \frac{2}{r} \cdot \frac{\partial S^i}{\partial r} \right] - q^i \qquad (5)$$

with boundary conditions:

$$for \quad r = 0 \quad -I\!D \cdot \frac{\partial S}{\partial r} = 0$$

$$for \quad r = R \quad -I\!D \cdot \frac{\partial S}{\partial r} = \phi^i$$

The flow of substrate (ϕ^i) from bulk to gel bead is

$$\phi^i = k_l^i \cdot A \cdot (S^i_{bulk} - S^i_{sur}) \qquad (6)$$

where k_l^i is estimated according to the method described by Wijffels et al. (1991).

The model is based on a completely mixed reactor and the mass balance of the substrate is given by

$$\frac{d S^i_{bulk}}{d t} = D \cdot (S^i_{in} - S^i_{bulk}) - \phi^i \qquad (7)$$

Solutions. The ordinary differential eq (3) for the biomass growth in the gel beads was solved numerically with a second-order Runge-Kutta algorithm. The substrate concentrations (eqs 6,7) in the bulk phase could be solved adequately with an algorithm based on the trapezoidal rule, which required less computation time compared with the Runge-Kutta algorithm. The substrate concentration profiles in the gel beads could be solved when eq (1) was substituted in eq (5). The resulting equation was solved with a

100

Backwards in Time and Centred in Space algorithm (BTCS)(Press et al. 1988) for partial differential equations. This finite difference method was used for several reasons. First it allowed changes in limiting substrate at any place in the gel bead. This means that in each shell a choice based on the selection criteria for the appropriate rate controlling equations $q^{i,m}$ from Table I can be made. Second, the BTCS method uses a fully implicit differential scheme, which is in general unconditional stable[34]. The accuracy of the method strongly depends on the time-step size[34]. This time-step size was therefore varied over a wide range to derive the longest time step possible. Time steps of maximally 50 s give a sufficiently accurate solution. The last argumentation for using a finite differences method is the simple implementation in the algorithm of the non-linear term from the substitution of eq (1) in eq (5). Eq (1) is such a non-linear equation with respect to S and the BTCS algorithm has to be adapted to handle this term. For this the "Monod"-like part (e.g. kinetic relation in eq (1) for $K_I = 1$) of the eq (1) is split in a zero or first-order equivalent depending on the substrate concentrations in that particular shell. The criterium for this was the substrate concentration: first order for $S < 2 * K_S$ and zero order for $S \geq 2 * K_S$. The model runs on a IBM-compatible computer with 80486 processor. A run of the model for 50 days takes about 5 hours CPU time.

For the model input the NH_4^+-influent concentration, dilution rate, bulk oxygen concentration, gel bead loading and initial biomass concentration are necessary. The model parameters are given in Table II with their actual values (see input parameter section). The model output consists of the bulk concentrations, biomass and respective nitrogen and oxygen concentration profiles in the gel beads.

INPUT PARAMETERS

Diffusion coefficients. Diffusion coefficients of O_2, NH_4^+, NO_2^- and NO_3^- in the bulk liquid and in the gel beads are input parameters for the model. Wise & Houghton

(1966) determined the diffusion coefficients of several gases in water at different temperatures. From these data we calculated a value of $2.83 * 10^{-9}$ m^2.s^{-1} for D_w^{O2}. For the D_{gel}^{O2} several values exist in the literature. Hulst et al. (1989) give a value of $1.58 * 10^{-9}$ m^2.s^{-1} for the diffusion coefficient of O_2 in κ-carrageenan-gel beads. Kurosawa et al.(1989) determined a D_{gel}^{O2} of $2.3 * 10^{-9}$ m^2.s^{-1} in Ca-alginate beads at different cell densities and did not observe a decrease in the diffusion coefficient with an increase in cell concentrations. The reported values were not measured under similar conditions and they differ too much to take an average diffusion coefficient. From the results of Furusaki (1989) a decrease in diffusion coefficient to 70 % compared with the diffusion coefficient in water can be expected. In particular since the value of Hulst et al. (1989) is considerably lower than the value of Kurosawa et al. (1989) we determined the diffusion coefficient of O_2 in 2.6% (w/w) κ-carrageenan gel beads at 30°C in our laboratory. A value of $2.05 * 10^{-9}$ m^2.s^{-1} for D_{gel}^{O2} was found by Wijffels et al. (1993), which is 72% of the value for O_2 in water from Wise & Houghton (1966). This value was used as input in the present model.

For the diffusion coefficients of the ions NH_4^+, NO_2^- and NO_3^- a first approach is the diffusion coefficient at infinite dilution based on the molar ionic conductivity (λ^i) and Nernst-Einstein relation given by Newman (1973)

$$D_w^i \;-\; 2.663 \times 10^{-7} \;.\; \lambda^i \qquad (8)$$

In this form, eq (8) is only valid for mono-charged ions. Values for λ^i (molar ionic conductivity) of the different ions are given by Newman (1973) and Vanýsek (1992). Using these values for λ^i we obtained $1.95 * 10^{-9}$, $1.91 * 10^{-9}$ and $1.90 * 10^{-9}$ m^2.s^{-1} for respectively D_w^{NH4}, D_w^{NO2} and D_w^{NO3} at 25°C. At more realistic values for the concentration of the ions the influence of the counter ion becomes important (Robinson & Stokes, 1970). The main positively charged counter ion for NO_2^- and NO_3^- will be K^+ and the negatively charged counter ion for NH_4^+ will be Cl$^-$. Robinson & Stokes (1970)

give the overall diffusion coefficients for "concentrated" aqueous solutions up to 1 M for NH_4Cl and 0.01 M KNO_3. The diffusion coefficients at these concentrations deviate less than 5% from the infinite dilution diffusion coefficients.

Values for diffusion coefficients of ions in gel beads D_{gel}^{i} are very rare. Some have been obtained by fitting from experiments where substrate fluxes in biofilms were measured (Arvin & Kristensen 1982 and La Cour Jansen & Harremoës 1984). These are not reliable because of the large number of fitted parameters. Only three sets of experiments which were really set-up to measure diffusion coefficients - in agar and biofilm - are reported. Onuma & Omura (1982) report a D_{gel}^{NH4} of 1.3 * 10^{-9} $m^2.s^{-1}$ at 20°C in inactivated biofilm. Lemoine et al.(1991) report a D_{gel}^{NO2} value of 1.42 * 10^{-9} $m^2.s^{-1}$ and a value of 1.19 * 10^{-9} $m^2.s^{-1}$ for D_{gel}^{NO3} in agar at 25°C. Williamson & McCarthy (1976) report values of 1.49 * 10^{-9}, 1.45 * 10^{-9} and 1.56 * 10^{-9} $m^2.s^{-1}$ for respectively D_{gel}^{NH4}, D_{gel}^{NO2} and D_{gel}^{NO3} at 20°C. We used the average values of these data, because values for the diffusion coefficients with the appropriate counter ion were not available. All above mentioned diffusion coefficients were corrected for the temperature with an equation derived from the Nernst-Einstein relation (Newman ,1973)

$$\frac{D^{i} \cdot \eta}{T} = constant \qquad (9)$$

A value of 1.002 and 0.9 mPa.s for the dynamic viscosity (η) at respectively 30° and 25°C was used in eq (9). The temperature corrected diffusion coefficients of the bulk liquid and gel beads used as model input are listed in Table II.

Mass transfer coefficients. A single value of 2.65 * 10^{-5} $m.s^{-1}$ for the liquid-solid mass-transfer coefficients of both k_l^{NH4}, k_l^{NO2} and k_l^{NO3} was calculated as described by Wijffels et al. (1991). For oxygen a value of 3.13 * 10^{-5} $m.s^{-1}$ for k_l^{O2} was obtained. For the density of water and gel bead we used 996 $kg.m^{-3}$ and 1008 $kg.m^{-3}$, respectively.

Maximum specific growth rate. For the maximum specific growth rate (μ_{max}^{Nb}) of *Nitrobacter agilis* we used 1 * 10^{-5} s^{-1} (Wijffels et al. 1991). Literature data for the

maximum specific growth rate of *Nitrosomonas europaea* differ widely: $6.13 * 10^{-6}$ s^{-1} (Belser 1984), $1.55 * 10^{-5}$ s^{-1} (Belser & Schmidt 1980), $1.75 * 10^{-5}$ s^{-1} (Engel & Alexander 1958), $2.0 * 10^{-5}$ s^{-1} (Loveless & Painter 1968), $1.75 * 10^{-5}$ s^{-1} (Skinner & Walker 1961), $1.44 * 10^{-5}$ s^{-1} (Powell & Prosser 1985), $2.33 * 10^{-5}$ s^{-1} (Powell & Prosser 1986[a]) and $1.25 * 10^{-5}$ s^{-1} (Powell & Prosser 1986[b]). An average value of $1.59 * 10^{-5}$ s^{-1} for (μ_{max}^{Ns}) is used as input for the model.

Table II *Model parameters.*

parameter	value	dimension
μ_{max}^{Nb}, μ_{max}^{Ns}	$1.0 * 10^{-5}$; $1.59 * 10^{-5}$	s^{-1}
m_s^{Nb}, m_s^{Ns}	$2.2 * 10^{-3}$; $9.4 * 10^{-4}$	molN.(kg biomass)$^{-1}$.s^{-1}
Y^{Nb}, Y^{Ns}	$0.58 * 10^{-3}$; $1.66 * 10^{-3}$	(kg biomass). molN^{-1}
$K_s^{NH4,Ns}$	$1.25 * 10^{-3}$	mol.dm^{-3}
$K_s^{O2,Ns}$	$5.05 * 10^{-6}$	mol.dm^{-3}
$K_s^{NO2,Nb}$	$0.36 * 10^{-3}$	mol.dm^{-3}
$K_s^{O2,Nb}$	$17.0 * 10^{-6}$	mol.dm^{-3}
I_{NO2}^{Nb}, I_{NO3}^{Nb}	0.159; 0.188	mol.dm^{-3}
maximum X^{Nb}, X^{Ns}	6.5; 13	kg.(m gel)$^{-3}$
R	$1.08 * 10^{-3}$	m
k_l^{NH4}, k_l^{NO2}, k_l^{NO3}, k_l^{O2}	$2.65 * 10^{-5}$; $3.13 * 10^{-5}$	m.s^{-1}
D_w^{NH4}, D_w^{NO2}, D_w^{NO3}, D_{gel}^{NH4}, D_{gel}^{NO2}, D_{gel}^{NO3}	$2.2 * 10^{-9}$; $2.2 * 10^{-9}$; $2.2 * 10^{-9}$; $1.9 * 10^{-9}$; $1.9 * 10^{-9}$; $1.9 * 10^{-9}$	m^2.s^{-1}
D_w^{O2}, D_{gel}^{O2}	$2.83 * 10^{-9}$; $2.05 * 10^{-9}$	m^2.s^{-1}

Kinetic parameters for substrate affinity of O_2, NO_2^- and NH_4^+ . The substrate affinity constant ($K_s^{O2,Nb}$) of 17μM O_2 for *N. agilis* is obtained from Wijffels et al.(1991).

For the substrate affinity constant of O_2 ($K_s^{O2,Ns}$) for *N. europaea* two literature data were found: 9.3 μM (Loveless & Painter,1968) and 7.7 μM (Peeters et al.,1969). The value of 9.3 μM is measured at 20°C and for the value of 7.7 no temperature nor other conditions are given. Therefore we determined the $K_s^{O2,Ns}$ in a series of batch experiments in which the oxygen depletion of a cell suspension in a small volume was followed. We obtained and used in our model a value of 5.05 μM O_2 with a 95% reliability interval of 3.94-6.15 μM O_2. For the substrate affinity constant ($K_s^{NH4,Ns}$) of *N. europaea* we used 1.25 mM NH_4^+ (Hunik et al., 1992). The substrate affinity constant ($K_s^{NO2,Nb}$) of *N. agilis* is 0.36 mM NO_2^- (Hunik et al., 1993). In addition to this, a substrate inhibition constant (I_{NO2}) for *N. agilis* of 159 mM NO_2^- and a product inhibition constant (I_{NO3}) of 188 mM NO_3^- were used (Hunik et al., 1993).

Yield and maintenance coefficients. The yield and maintenance coefficients for *N. agilis* given by Wijffels et al. (1991) were converted from an O_2 to an N-based value with the stoichiometry of the reaction. A yield Y^{Nb} and maintenance m_s^{Nb} of 0.58 * 10^{-3} (kg biomass). $molN^{-1}$ and 2.2 * 10^{-3} molN.(kg biomass)$^{-1}$.s^{-1} respectively were derived. Literature yield coefficients for *N. europaea* are expressed as number of cells per mol ammonia consumed. To convert number of cells to kg biomass an average cell weight is needed. We found several cell weight values: 3.8 * 10^{-16} kg.cell^{-1} (Engel & Alexander, 1958); 1.2 * 10^{-16} kg.cell^{-1} (Skinner & Walker, 1961) and 3 * 10^{-16} kg.cell^{-1} (Keen & Prosser, 1987). An average of 2.7 * 10^{-16} kg.cell^{-1} was used to convert number of cells to biomass. With this conversion factor we calculated a Y^{Ns} of: 1.41 * 10^{-3} kg.molN^{-1} (Belser & Schmidt, 1980); 1.68 * 10^{-3} kg.molN^{-1} (Laudelout et al., 1974); 1.78 * 10^{-3} kg.molN^{-1} (Skinner & Walker, 1961); 0.62 * 10^{-3} kg.molN^{-1} (Engel & Alexander, 1958). A value of 2.33 * 10^{-3} kg.molN^{-1} is given by Keen & Prosser (1987). From a CO_2 uptake experiment of Belser (1984) and an average biomass composition (Roels, 1983) a yield of 2.12 * 10^{-3} kg.molN^{-1} was calculated. From these values an average Y^{Ns} of 1.66 * 10^{-3} kg.molN^{-1} was used as input parameter for the model. It must be emphasized that this yield value is

very much dependent of the mass of one *N. europaea* cell, which is a difficult parameter to measure and may change with nutrient conditions. In the literature several maintenance coefficients (m_s^{Ns}) for *N. europaea* can be found. After recalculating the results of Laudelout et al. (1968) a value of 8.07 * 10^{-4} molN.(kg biomass)$^{-1}$.s^{-1} is found under aerobic conditions 9.17 * 10^{-4} molN.(kg biomass)$^{-1}$.s^{-1} and under anaerobic conditions, both without ammonia. From the data presented by Keen & Prosser (1987) an m_s^{Ns} of 1.11 * 10^{-3} molN.(kg biomass)$^{-1}$.s^{-1} was calculated. An average value of 9.4 * 10^{-4} molN.(kg biomass)$^{-1}$.s^{-1} was taken as input for the model.

EXPERIMENTAL METHODS

A ll solutions are made with demineralized water and Merck analytical grade chemicals.

Strains and media. Cells of *N. europaea* ATCC 19718 and *N. agilis* ATCC 14123 were used for the experiments. The cells were cultivated at 30°C in separate chemostats, each with a dilution rate of 3.5 * 10^{-6} s^{-1} under sterile conditions. Media contained per dm^3: 2.5 g (NH_4)$_2SO_4$; 0.052 g $MgSO_4$; 0.78 g $NaH_2PO_4.2H_2O$; 0.89 g $Na_2HPO_4.2H_2O$; 0.74 mg $CaCl_2.2H_2O$; 2.5 mg $FeSO_4.7H_2O$; 0.08 mg $CuSO_4$ for *N. europaea* and 1.0 g $NaNO_2$; 0.052 g $MgSO_4$; 0.16 g $NaH_2PO_4.2H_2O$; 1.6 g $Na_2HPO_4.2H_2O$; 0.17 g $NaHCO_3$ (C-source); 0.74 mg $CaCl_2.2H_2O$; 0.036 mg $FeSO_4.7H_2O$; 0.026 mg $CuSO_4$; 0.24 mg $Na_2MoO_4.2H_2O$; 4.3 mg $ZnSO_4.7H_2O$ for *N. agilis*. The pH of the *N. europaea* culture was maintained at pH 7.4 with a $NaHCO_3$ solution (80 g.dm^{-3})(C-source) using a pH controller (LH Fermentation 500 series III).

Immobilization . The effluent of the two chemostats was collected and centrifuged at 16300 g for 30 min at 4°C. The pellets were resuspended in 1mM phosphate buffer (pH 7.5). These concentrated cell suspensions of *N. europaea* and *N. agilis* were co-

immobilized in a 2.6 % (w/w) κ-carrageenan solution (Genugel, X0828, A/s Kobenhavens Pektinfabrik, DK LilleSkenved) according to the method described by Hulst et al.(1985). After immobilization, beads with an average diameter of 2.1 ± 0.1 mm were obtained. The specific oxygen consumption rate of the two cell suspensions was measured before immobilization and from that initial biomass concentrations in the gel beads were estimated: $X^{Ns} = 4 * 10^{-3}$ kg.m^{-3} and $X^{Nb} = 2 * 10^{-4}$ kg.m^{-3}. A gel bead hold up of 25% (v/v) was used.

Reactor operation. The beads with the immobilized cells were cultivated for 49 days in a continuously operated air-lift loop reactor of 3.3 dm^3 at 30°C. The liquid-phase dilution rate was 2.3 * 10^{-5} s^{-1} with the following medium composition: 6.6 g (NH$_4$)$_2$SO$_4$ (50 mM); 0.87 g K$_2$HPO$_4$; 0.68 g KH$_2$PO$_4$; 0.052 g MgSO.7H$_2$O; 1.86 g KCl; 0.74 mg CaCl$_2$.2H$_2$O; 2.5 mg FeSO$_4$.7H$_2$O; 0.125 mg CuSO$_4$.5H$_2$O; 0.24 mg Na$_2$MoO$_4$.2H$_2$O; 4.3 mg ZnSO$_4$.7H$_2$O per dm^3. The gel beads were kept in the reactor with a sieve screen. The pH was maintained at 7.4 with a 200g K$_2$CO$_3$/dm^3 solution (also C-source) and a pH controller (L.H. Fermentation 500 series III). A controlled air flow was used to maintain 80% air saturation in the reactor.

Analyses. The NH$_4^+$, NO$_2^-$ and NO$_3^-$ concentration were measured daily with a Skalar autoanalyser. The NH$_4^+$ was chlorinated to monochloramine, which reacts with salicylate to 5-aminosalicylate. After oxidation and oxidative coupling, a green coloured indophenol-blue complex was formed, which was measured spectrophotometricly at 660 nm. The NO$_2^-$ reacts with a sulphanilamide, forming a diazonium salt, which was coupled to N-(1-naphthyl) ethylene diamine dichloride, the reddish-purple coloured complex was measured at 540 nm. The NO$_3^-$ was reduced to NO$_2^-$ in a copper coated cadmium column and further treated as the NO$_2^-$ ion. Appropriate standards were used to convert the extinctions to concentrations.

Biomass profiles . The biomass-volume distribution was determined according to the method described by Hunik et al. (1993). A total biomass volume of a gel bead was

107

obtained from a summation of these experimentally determined biomass volumes at the various radial positions. The volume distribution was converted to a biomass-concentration profile with a specific biomass density. This specific biomass density was obtained from a summation of the biomass volume of a gel bead and the maximum oxygen consumption rate of the gel beads., These values can be converted to a biomass concentration with Y^m.

Initial biomass concentration from colony counts. By assuming that each colony originated from one cell it was possible to obtain a value for the cell density at the beginning of the experiment. This is an alternative for the method based on the oxygen consumption rate described in the immobilization paragraph to estimate an initial biomass concentration of viable cells for both microorganisms. From the biomass volume distribution (G_v) and the colony counting of gel-bead slices (N_a), a colony density (N_v) in the gel-bead slices can be derived by (Weibel,1979)

$$N_v = \frac{N_a^{\frac{3}{2}}}{\beta * G_v^{\frac{1}{2}}} \tag{10}$$

For circles, like colonies, β has a value of 1.38 (Weibel,1979).

RESULTS AND DISCUSSION

E xperiments. Typical experimental results of one of the reactors are shown in Figure 1[abc]. Operation of the reactor was accidentally disturbed and the influent NH_4^+ concentration between day 2 and 5 was 38 mM instead of 50 mM. Furthermore, the dilution rate was unintentionally raised between day 15 and 21 from $2.3 * 10^{-5}$ to $3.89 * 10^{-5}$ s^{-1}. The advantage of a dynamic model is the possibility to account for such changes in the operating conditions as shown below.

In Figure 1[a] the NH_4^+ in the bulk is rapidly decreasing between day 0 and 10, accompanied by a corresponding increase in NO_2^-. Growth of *N. europaea* can be assumed there. Between day 23 and 28 the NO_2^- concentration rapidly decreases indicating growth of *N. agilis*. The biomass concentrations of the two microorganisms in the gel beads is shown in Figure 1[b,c] as projection of a 3-dimensional graph. In Figure 1[b,c] the start of the growth phases are less pronounced compared to the increase in NH_4^+ and NO_2^- consumption rates in Figure 1[a]. From a summation of the biomass volume distribution at the end of the experiment we obtained the total biomass volume in a gel bead. A biomass density of 28 and 33 (kg dry weight biomass).m^{-3} biomass in the gel for respectively *N. agilis* and *N. europaea* was calculated and used with the measured volume distribution to obtain a biomass-concentration profile of the microorganisms.
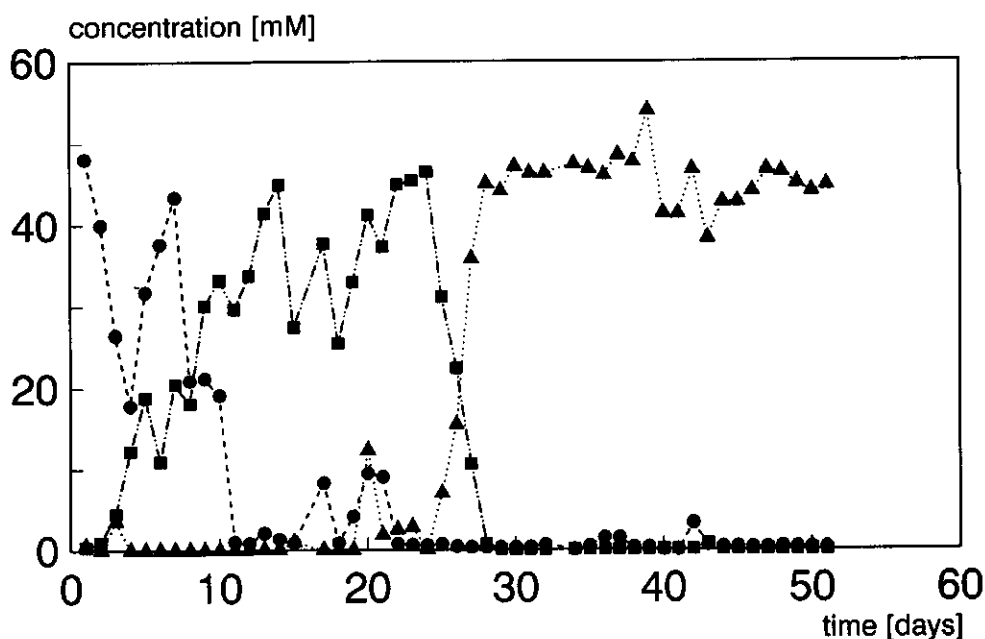

Figure 1[a]   Experimental results. Reactor bulk concentrations NH_4^+ (--●--), NO_2^- (-·-■-·-), NO_3^- (···▲···).

The average biomass concentration, for both microorganisms at the end of the experiment in the outer 50 μm of the bead, was used as an input parameter for the maximum biomass concentration in the model. These maximum biomass concentrations were 8.9 and 3.8 kg.m^{-3} gel respectively for *N. europaea* and *N. agilis*. Gujer & Boller (1989) predicted 40 and 14 kg.m^{-3} biofilm for the respective biomass densities in a biofilm. However, their values are based on a arbitrary fixed value of the total ammount of biological material in the biofilm of 80 kg.m^{-3}. Wijffels et al. (1991) measured 11 kg.m^{-3} gel for *N. agilis*.
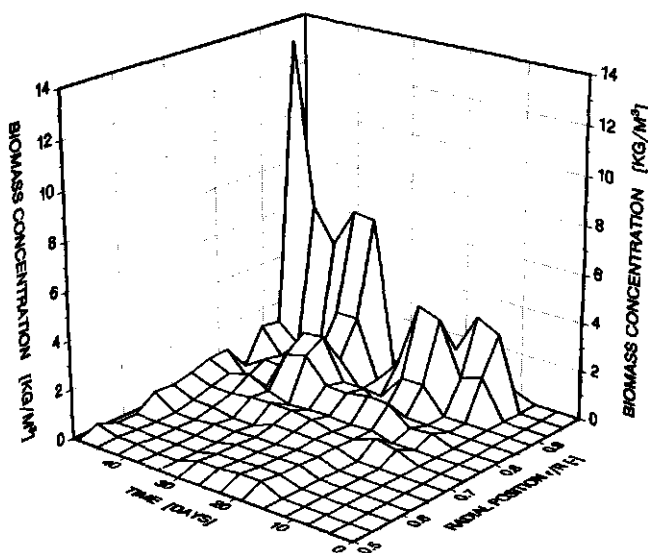

Figure 1[b]   *Experimental results: biomass distribution of Nitrosomonas europaea.*

The maximum biomass concentration values are similar to those reported by the other authors. Our maximum value for X^m is strongly dependent of the value for Y^m

which is difficult to estimate correctly. Nevertheless, the experimentally determined values in Figure 1[b,c] and the model simulations in Figure 2[b,c] are based on the same value of Y^m which makes comparison possible. The excess biomass in our experiment was released into the bulk phase and washed out of the reactor. We tried to measure the oxygen consumption rate of this biomass in the bulk phase of the reactor, but the concentration was too low. Therefore, the assumption in the model that excess biomass disappeared seems valid.
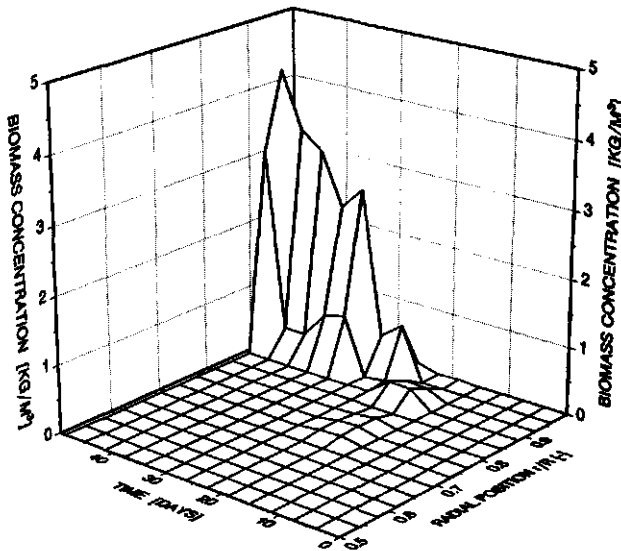
Figure 1[c]   *Experimental results: biomass distribution of* **Nitrobacter agilis.**

Model. In Figure 2 the model output is shown for the bulk concentrations (Fig.2[a]) and the biomass (Fig.2[b,c]) in the gel bead. The changes in concentration observed in Figure 2[a] are caused by the changes in influent concentration and dilution rate as

111

mentioned in the material and method section. The reactor bulk concentrations show a rapid consumption of NH_4^+ at day 5 and a similar pattern for NO_2^- conversion is seen around day 21. This change in bulk concentration corresponds with a rapid growth of *N. europaea* and *N. agilis* shown in Figure $2^{b,c}$. The development of a biofilm close to the surface of the gel beads is shown in Figure $2^{b,c}$. This biomass profile gets steeper towards the end of the experiment. Biomass in the centre of the beads decays, because of the low substrate concentrations.

Figure 2^a *Model predictions: reactor bulk conc. NH_4^+ (----), NO_2^- (———), NO_3^- (······).*

Figure 2^b   Model predictions: biomass profile **Nitrosomonas europaea.**
Figure 2^c   Model predictions: biomass profile **Nitrobacter agilis.**
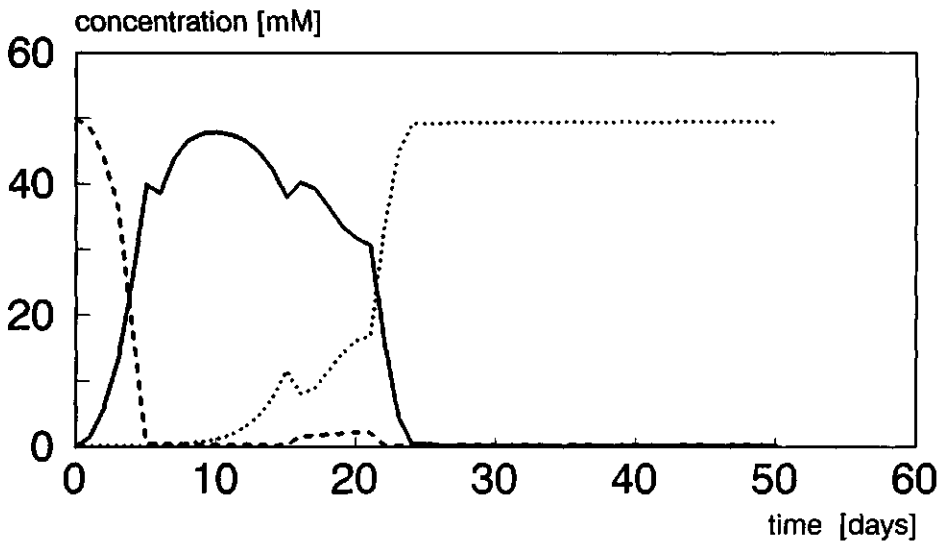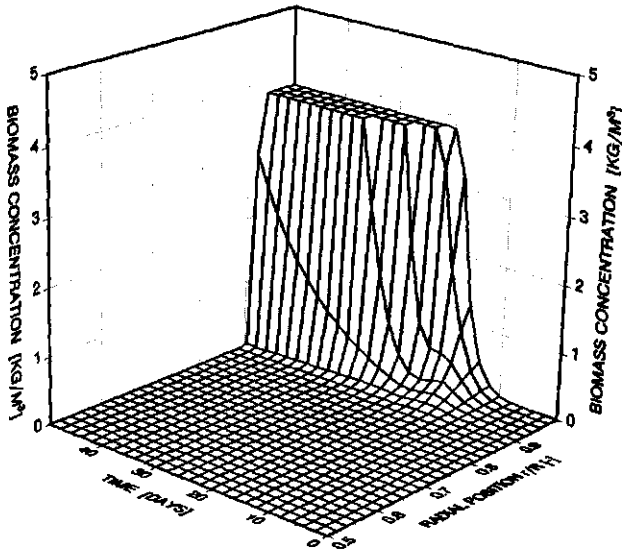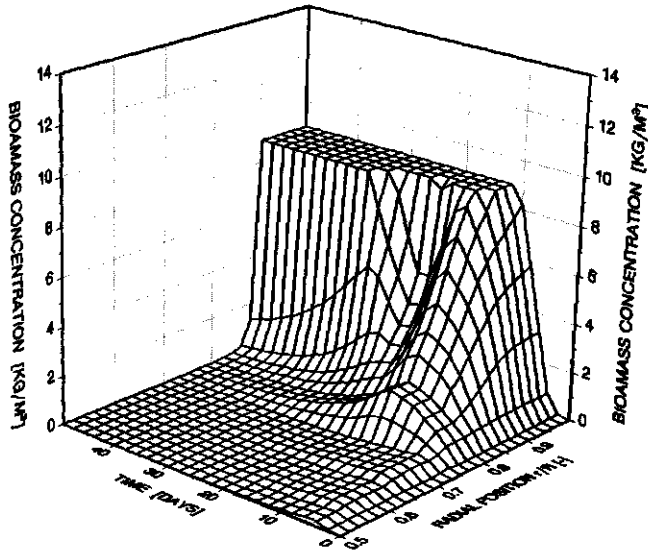
113

Validation. For the validation of the model, bulk concentrations and biomass profiles predicted by the model are compared with the experimental data. For the comparison of the bulk concentrations of Figures 1^a and 2^a, we introduce a time at which 50% of the NH_4^+ is consumed ($t_{1/2}^{NH4}$) and the time ($t_{1/2}^{NO2}$) at which 50% of the NH_4^+ is converted to NO_3^-. The latter definition is representative for the conversion rate of NO_2^- by *N. agilis* in the reactor. The values for $t_{1/2}^{NH4}$ and $t_{1/2}^{NO2}$ correspond with the start of the exponential growth phase of both microorganisms. The model predicted lower values for $t_{1/2}^{NH4}$ and $t_{1/2}^{NO2}$ than the experimental values found in from Figure 1^a. From the sensitivity analysis we know that this $t_{1/2}^{NH4}$ and $t_{1/2}^{NO2}$ values are highly influenced by the respective maximum specific growth rates (μ_{max}) of the microorganisms.

The reactor bulk concentrations in Figure 2^a are predicted rather well compared with the experimental data in Figure 1^a. The rapid decrease of NO_2^- in the experiment around day 25 occurs slightly later than predicted by the model, which could be explained by a small delay in growth or a low survival of the cells after the immobilization. This survival rate of the cells is estimated from the colony counts at the end of the experiment. From the gel-bead slices, a colony number per volume of $2 * 10^{13}$ and $0.6 * 10^{13}$ cells.m^{-3} gel were measured for respectively *N. europaea* and *N. agilis*. With a cell weight of $2.7 * 10^{-16}$ and $1 * 10^{-16}$ kg.cell^{-1} for respectively *N. europaea* and *N. agilis* and with eq (10) we obtained an initial X^{Ns} of $5.4 * 10^{-3}$ kg.m^{-3} gel and $6 * 10^{-4}$ kg.m^{-3} gel for the initial X^{Nb}. Only the viable cells will grow into colonies and comparing these values with the estimated values from the specific oxygen consumption rate of the cell suspension before immobilization, $4 * 10^{-3}$ and $2 * 10^{-4}$ kg.m^{-3} gel, for the initial X^{Ns} and X^{Nb} respectively, we can conclude that the cell survival rate is very high. The influence of the growth rate is dicussed in the sensitivity analysis.

The biomass concentration profiles used for the validation allowed a quantitative comparison between model and experiment, which is more accurate than the more qualitative comparison of Monbouquette et al.(1990). The well-defined species we used

114

are an advantage over the multi-species biofilm models of Wanner & Gujer (1986), which make the validation of their model very difficult. Further improvements of the model would include the colony-like growth of the biomass, which is assumed to be homogeneously distributed in the present model but actually is segregated in colonies. This effect can be seen at the edge of the beads when Figure 1[b,c] and 2[b,c] are compared. The model predicts a maximum biomass concentration up to the outer layer of the bead, but the experimental results show a sharp decrease. It can easily be seen that the centre of a colony can not be at the edge of a bead. Before such a situation can occur the colony will be disrupted and the cells are washed out of the reactor. With light microscopic photographs (not shown) of aging beads we observed regions in the outer layer where such a process had taken place. A drop in biomass concentration in the outer layer of the biofilm is also observed by Wijffels et al.(1991). Recently Gooijer et al. (1992) presented an extension of their model, which incorporated a set of equations to take the colony growth in the beads into account (Salmon, 1989).

With the explanation for the biomass decrease at the edge of the gel bead taken into account, the resemblance between the predicted (Fig. 2[b,c]) and measured biomass profile (Fig. 1[b,c]) is rather well. The thickness of the profile and the time at which the biomass is rapidly increasing are similar for the predicted and measured profiles. The influence of colonies in general on the model depends strongly on their distance and size. Diffusion limitation within the colonies will be important when the colonies get too large. Also the distance between the *N. europaea* and *N. agilis* colonies is important. Above a certain distance the diffusion between the colonies will be the rate-limiting step in the process and the nitrite concentration in the bulk will increase. Such an increase was not observed and this inter-colony mass-transfer resistance thus seemed to be no problem.

Sensitivity analysis. From the output values of the model we selected the criteria for the sensitivity analysis. In contrast to Gooijer et al. (1991) it was not possible to use merely the maximum attainable oxygen consumption rate. In our experiment this oxygen

consumption rate will be limited by the amount of NH_4^+ in the influent of the reactor. This influent concentration had a constant value and was completely converted to the product, so the oxygen consumption rate will be constant too. As an alternative we took 6 output values of the model for the sensitivity analysis: $t_{1/2}^{NH4}$, $t_{1/2}^{NO2}$, the substrate flux (NH_4^+, NO_2^-) to the gel beads at $t_{1/2}^{NH4}$ and $t_{1/2}^{NO2}$ and the total biomass concentration of both microorganisms at the end of the experiment.

The sensitivity of the model for step-wise variations in the input parameters was tested. For each input parameter the value of Table II was varied in five steps between 0.6 and 1.4 times its original value. The total number of parameters was 27 and some parameters were varied as a block (Table II).

The tested parameters together with the blocks in which they were changed are indicated in Table III. In Table III an overview of all the parameters and the effects of the step-wise variations on the output data is shown. Those parameters which had an effect larger than +5% or -5% on the 6 selected output data of the model are presented as a plus (+) in Table III. These parameters are also presented in Figure 3[abcdef].

From the data presented in Figure 3 we can conclude that the $t_{1/2}^{NH4}$ and $t_{1/2}^{NO2}$ values in Figure 1[a] were mainly influenced by the growth rate of the two microorganisms. The effect of the D_{gel}^{O2} is considerably smaller. The flux of substrate at $t_{1/2}^{NH4}$ and $t_{1/2}^{NO2}$ was determined by the radius (R) of the beads and to a lesser extent by the maximum growth rate (μ_{max}). Several parameters (r, m_s^m, D_{gel}^{O2}) had a minor effect on the total biomass concentration at the end of the experiment. This last observation is due to the maximum biomass concentration in the gel beads for the model. The total biomass can only increase when the biofilm depth increases, which is obviously not the case here.

Table III   *Overview of the relative sensitivity of the model parameters. A (+) indicates more than 5% change of output values compared to the initial value.*

parameter	$t_{1/2}^{NH4}$	flux $t_{1/2}^{NH4}$	$t_{1/2}^{NO2}$	flux $t_{1/2}^{NO2}$	X^{Ns}	X^{Nb}
X^{Ns} at time 0	+	-	-	-	-	-
X^{Nb} at time 0	-	-	-	-	-	-
$\mu_{max}^{Nb}, \mu_{max}^{Ns}$	+	+	+	+	+	+
m_s^{Nb}, m_s^{Ns}	-	-	-	-	+	+
Y_N^{Nb}, Y_N^{Ns}	+	-	+	-	+	+
$K_S^{NH4,Ns}$	-	-	-	-	-	-
$K_S^{O2,Ns}$	-	-	-	-	-	-
$K_S^{NO2,Nb}$	-	-	-	-	-	-
$K_S^{O2,Nb}$	-	-	+	-	-	-
$J_{NO2}^{Nb}, J_{NO3}^{Nb}$	-	-	+	-	-	-
maximum X^{Nb}, X^{Ns}	-	-	-	-	+	+
R	+	+	+	+	+	+
k_l	-	-	+	-	+	+
$D_w^{NH4}, D_w^{NO2}, D_w^{NO3}, D_{gel}^{NH4}, D_{gel}^{NO2}, D_{gel}^{NO3}$	-	-	-	-	-	-
D_w^{O2}, D_{gel}^{O2}	+	-	+	-	+	+

When the most influential parameters of the model output are determined with the sensitivity analysis, it is useful to estimate the error in those parameter values given in Table II. For example, the radius (R) was determined accurately and several times during the experiment. The error in this parameter is thus small and influence of errors in this parameter on the model output will be small too. For the maximum growth rate (μ_{max}) and oxygen diffusion coefficient in the gel bead (D_{gel}^{O2}) the estimated value was less accurate.

117
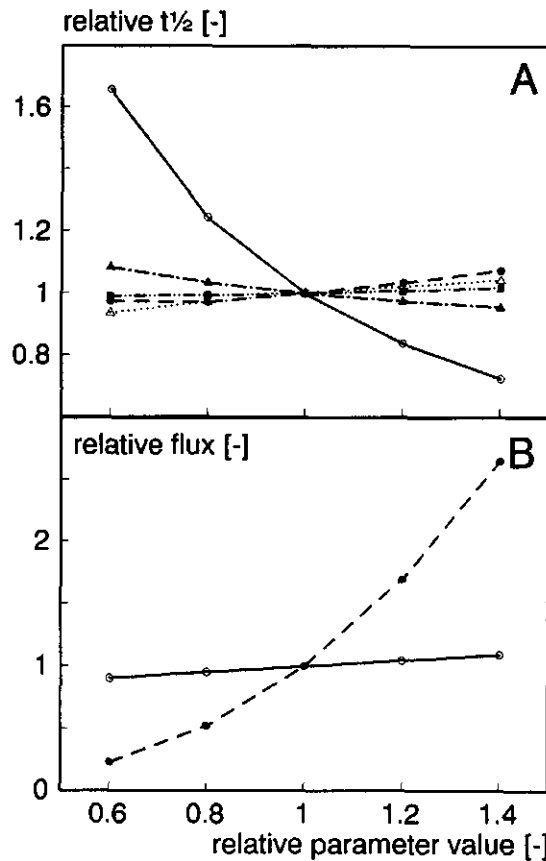
Figure 3 ^{a,b} *Most sensitive model parameters for NH_4^+ conversion(Table II). A: $t_{1/2}^{NH4}$, B: flux at $t_{1/2}^{NH4}$. With μ_{max}^{Ns} and μ_{max}^{Nb} ($\bigcirc$), m_s^{Ns} and m_s^{Nb} ($\square$), Y^{Ns} and Y^{Nb} ($\triangle$), R ($\bullet$), k_iO and k_iN ($\blacksquare$), D_w^{O2} and D_{gel}^{O2} ($\blacktriangle$).*

The growth rate is an average of several literature values of suspended cells and a standard deviation of $0.52 * 10^{-3}$ s^{-1} (33%) can be calculated from the literature values of *N. europaea* mentioned before. A similar standard deviation for *N. agilis* can be calculated from the data given by Wijffels et al. (1991).
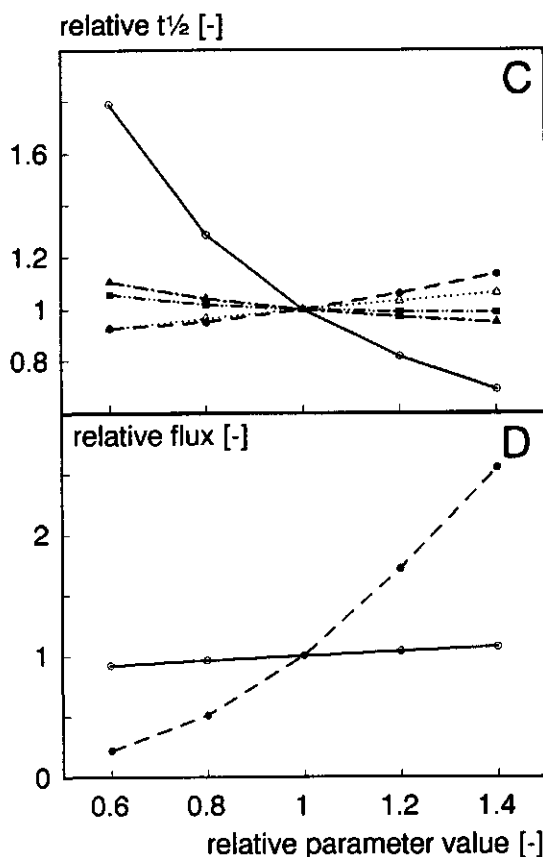
Figure 3 [c,d]   Model parameters for NO_2^- conversion. C: $t_{1/2}^{NO2}$, D: flux at $t_{1/2}^{NO2}$. Legend Fig 3[a,b].

The effect of a 33% change in μ_{max} can be seen in Figure 3[a,c]. Especially a lower growth rate increases the $t_{1/2}^{NH4}$ and $t_{1/2}^{NO2}$. The corresponding error in $t_{1/2}^{NO2}$ can explain the difference between predicted and experimental data in Figures 1[a] and 2[a]. A standard deviation of 10% is given for D_{gel}^{O2} by Wijffels et al. (1993). This is a diffusion coefficient for a gel without microorganisms.

relative biomass concentration [-]

relative parameter value [-]
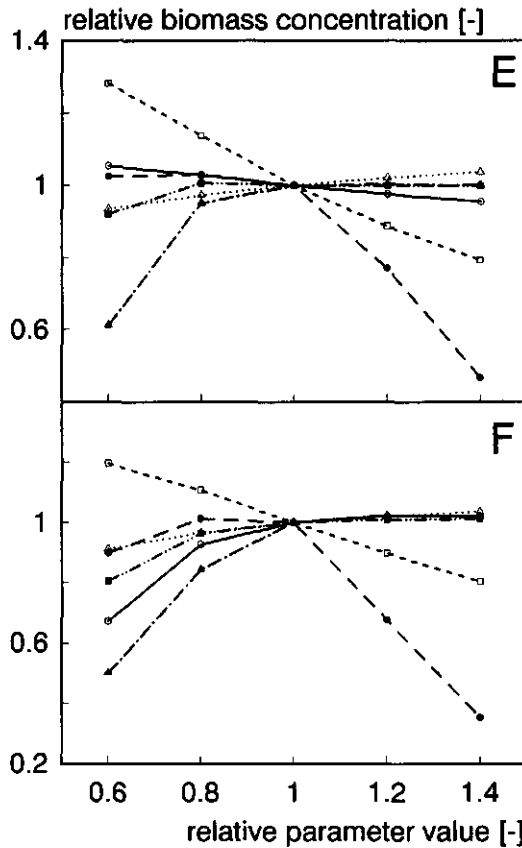
Figure 3 ^{e,f} *Most sensitive model parameters for biomass. Cummulative biomass at day 50. E: N.europaea, F: N.agilis. Legend Fig. 3*^{a,b}.

The effect of D_{gel}^{O2} on $t_{1/2}^{NH4}$ and $t_{1/2}^{NO2}$ was less dramatic compared to the maximum growth rate. The estimated values of the diffusion coefficients in Table II are, according to the sensitivity analysis, accurate enough as input parameter for the model. From the sensitivity analysis it can be concluded that the model output data are most sensitive with respect to the maximum growth rate of the microorganisms.

The outcome of the sensitivity analysis should be used carefully because the results are not only dependent on the model equations and parameter values. Also input values as, for example, influent concentrations or oxygen concentration in the bulk phase of the reactor determine the outcome of the sensitivity analysis. The relative importance of the model parameters are therefore limited to the situation with the given input values.

CONCLUSIONS

S imilar to previously developed one-species models by for example de Gooijer et al. (1991) and Monbouquette et al.(1990), a two-species dynamic biofilm model was developed and validated. Reactor bulk concentrations and biomass profiles in the gel beads were used to validate the model. The developed model was able to predict the experimental results very well. A sensitivity analysis was used to distinguish the relative importance of the parameters and it can be used for a better tuning of the model. The developed and validated model has a mechanistic background and is therefore useful to predict the dynamic behaviour of a nitrification process with immobilized cells at various conditions.

NOMENCLATURE

A	specific surface area of the gel beads	$[m^{-1}]$
D	dilution rate	$[s^{-1}]$
G_v	colony volume fraction	$[-]$
$D_{gel}{}^i$	diffusion coefficient of i in the gel bead	$[m^2.s^{-1}]$
$D_w{}^i$	diffusion coefficient of i in water	$[m^2.s^{-1}]$
$I^m{}_{NO2}$	constant of nitrite inhibition	$[mol.m^{-3}]$
$I^m{}_{NO3}$	constant of nitrate inhibition	$[mol.m^{-3}]$
K_I	combined inhibition constant	$[-]$
$k_l{}^i$	mass transfer coefficient liquid to solid phase	$[m.s^{-1}]$
$K_S{}^{i,m}$	affinity constant of m for i	$[mol.m^{-3}]$
$m_s{}^m$	maintenance coefficient for m	$[molN.(kg\ biomass)^{-1}.s^{-1}]$
N_a	number of colonies per surface unit	$[m^{-2}]$
N_v	number of colonies per gel bead volume	$[m^{-3}]$
q^i	consumption rate of i	$[mol.m^{-3}.s^{-1}]$
r	position in the bead from the edge	$[m]$
R	radius of the gel bead	$[m]$
$S_{bulk}{}^i$	concentration of i in bulk phase	$[mol.m^{-3}]$
$S_{in}{}^i$	concentration of i in influent	$[mol.m^{-3}]$
$S_{sur}{}^i$	concentration of i at surface of the gel bead	$[mol.m^{-3}]$
S^i	local concentration of i in gel bead	$[mol.m^{-3}]$
T	temperature	$[K]$
t	time	$[s]$
X^m	biomass concentration of m	$[kg.m^{-3}]$
Y^m	biomass yield for m on nitrogen	$[kg\ biomass.(mol\ N)^{-1}]$
β	geometry parameter (1.38 for spheres)	$[-]$
μ^m	growth rate of m	$[s^{-1}]$
$\mu_{max}{}^m$	maximum growth rate of m	$[s^{-1}]$
λ^i	molar ionic conductivity	$[m^2.S.(mol)^{-1}]$
η	dynamic viscosity of water	$[Pa.s]$
Φ^i	substrate flow of i to the gel bead	$[mol.m^{-3}.s^{-1}]$

supercripts
m Nb for *Nitrobacter agilis*, Ns for *Nitrosomonas europaea*
i $NH_4{}^+$, $NO_2{}^-$, $NO_2{}^-$ and O_2

REFERENCES

Arvin E, Kristensen GH (1982) Effect of denitrification on the pH of bioflims. Wat Sci Tech 14:833-848.

Beck MB (1991) Principles of modelling. Wat Sci Tech 24:1-8.

Beeftink HH, Heijden RTJM van der, Heijnen JJ (1990) Maintenance requirements: energy supply from simultaneous endogeneous respiration and substrate consumption. FEMS Microb Ecol 73:203-209.

Belser LW, Schmidt EL (1980) Growth and oxidation kinetics of three genera of ammmona oxidizing nitrifiers. FEMS Microbiol Lett 7:213-216.

Belser LW (1984) Bicarbonate uptake by nitrifiers: Effects of growth rate, pH, substrate concentration and metabolic inhibitors. Appl Environ Microbiol 48:1100-1104.

Bryers JD (1988) Modeling biofilm accumulation. In: Bazin MJ; Prosser JI (ed). Physiolological models in microbiology, vol 2. CRC Press, Boca Raton Fl, USA, 109-144.

Chen GH, Ozaki H, Terashima Y (1990) Modelling of the simultaneous removal of organic substances and nitrogen in a biofilm. Wat Sci Tech 21:791-804.

Denac M, Uzman S, Tanaka H, Dunn IJ (1983) Modeling of experiments on biofilm penetration effects in a fluidized bed nitrification reactor. Biotechnol Bioeng 25:1841-1861.

Engel MS, Alexander M (1958) Growth and autotophic metabolism of *Nitrosomonas europaea*. J Bacteriol 76:217-222.

Gooijer CD de, Wijffels RH, Tramper J (1991) Growth and substrate consumption of Nitrobacter agilis cells immobilized in carrageenan: part 1. dynamic modelling. Biotechnol Bioeng 38:224-231.

Gooijer CD de, Wijffels RH, Tramper J (1992) Dynamic modelling the growth of immobilized nitrifying bacteria: biofilm development. In: Melo LF et al. (ed). Biofilms - Science and technology. Kluwer academic publishers, the Netherlands. 291-296.

Gujer W, Boller M (1989) A mathematical model for rotating biological contactors. In: Proceedings of the technical advances in bioreactors conference, Nice, CFRP-AGHTM Paris. 69-89.

Furusaki S (1989) Intradiffusion effect on reactivity of immobilized microorganisms. In: A Fiechter, H Okada, RD Tanner (eds), Bioproducts and bioprocesses, Springer-Verlag, Berlin. 71-85.

Hulst AC, Tramper J, Riet K van 't, Westerbeek JMM (1985) A new technique for the production of immobilized biocatalyst in large quantities. Biotechnol Bioeng 27:870-876.

Hulst AC, Hens HJH, Buitelaar RM, Tramper J (1989) Determination of the effective diffusion coefficient of oxygen in gel materials in relation to concentration. Biotechnol Techniques 3:199-204.

Hunik JH, Meijer HJG, Tramper J (1992) Kinetics of *Nitrosomonas europaea* at extreme substrate, product and salt concentrations. Appl Microbiol Biotechnol 37:802-807.

Hunik JH, Meijer HJG, Tramper J (1993) Kinetics of *Nitrobacter agilis* at extreme substrate, product and salt concentrations. Accepted for publication in Appl Microbiol Biotechnol. (Chapter 3)

Hunik JH, Hoogen MP van den, Boer W de, Smit M, Tramper J (1993) Quantitative determination of a spatial biomass distribution of *Nitrosomonas europaea* and *Nitrobacter agilis* cells immobilized in κ-carrageenan beads using a specific fluorescent-antibody technique. Appl Environ Microbiol 59: 1951-1954. (Chapter 5)

Keen GA, Prosser JI (1987) Steady state and transient growth of autotrophic nitrifying bacteria. Arch Microbiol 147:73-79.

Kissel JC, McCarty PL, Street RL (1984) Numerical simulation of mixed-culture biofilm. J Environ Eng 110:393-411.

Kurosawa H, Matsumura M, Tanaka H (1989) Oxygen diffusivity in gel beads containing viable cells. Biotech Bioeng 34:926-932.

La Cour Jansen J, Harremoës P (1984) Removal of soluble substrates in fixed films. Wat Sci Tech 17:1-14.

Laudelout H, Lambert R, Fripat JL, Pham ML (1974) Effet de la température sur la vitesse d'oxidation de l'ammonium en nitrate par des cultures mixtes de nitrifiants (French). Ann Microbiol (Inst. Pasteur) 125 B:75-84.

Laudelout H, Simonart P-Ch, Droogenbroeck R van (1968) Calorimetric measurement of free energy utilization by *Nitrosomonas* and *Nitrobacter*. Arch Mikro 63:256-277.

Lemoine D, Jouenne T, Junter G-A (1991) Biological denitrification of water in a two-chambered immobilized-cell bioreactor. Appl Microbiol Biotechnol 36:257-264.

Loveless JE, Painter HA (1968) The influence of metal ion concentrations and pH value on the growth of a Nitrosomonas strain isolated from activated sludge. J Gen Microbiol 52:1-14.

Monbouquette HG, Sayles GD, Ollis DF (1990) Immobilized cell biocatalyst activation and pseudo-steady-state behavior: model and experiment. Biotechnol Bioeng 35:609-629.

Newman JS (1973) Electrochemical systems, Prentice-Hall, Englewood Cliffs, New Jersey.

Onuma M, Omura T (1982) Mass-transfer characteristics within microbial systems. Wat Sci Tech 14:553-568.

Peeters TL, Gool AP van, Laudelout H (1969) Kinetic study of oxygen-limited respiration in nitrifying bacteria. Bacteriol Proc Am Soc Microbiol 69:141.

Powell SJ, Prosser JI (1985) The effect of nitrapyrin and chloropicolinic acid on ammonium oxidation of *Nitrosomonas europaea*. FEMS Microbiol Lett 28:51-54.

Powell SJ, Prosser JI (1986[a]) Effect of copper on inhibition by nitrapyrin of growth of *Nitrosomonas europaea*. Current Microbiol 14:177-179.

Powell SJ, Prosser JI (1986[b]) Inhibition of ammonium oxidation by nitrapyrin in soil and liquid culture. Appl Environ Microbiol 52:782-787.

Press WH, Flannery BP, Teukolsky SA, Vetterling WT (1988) Numerical recipes: the art of scientific computing, Cambridge University Press, Cambridge, New York.

Roels JA (1983) Energetics and kinetics in Biotechnology. Elsevier Biomedical Press, Amsterdam, The Netherlands.

Rittmann BE, Manem JA (1992) Development and experimental evaluation of a steady-state, multispecies biofilm model. Biotechnol Bioeng 39:914-922.

Robinson RA, Stokes RH (1970) Electrolyte solutions. 2nd edition. Butterworth & Co, Bath, England.

Salmon PM (1989) Mass transport phenomena in reactors containing entrapped enzymes or bacterial cells. Ph.D. thesis, Stanford University, California, USA.

Sayles GD, Ollis DF (1989) Periodic operation of immobilized cell systems: analysis. Biotechnol Bioeng 34:160-170.

Siegrist H, Gujer W (1987) Demonstration of mass transfer and pH effects in a nitrifying biofilm. Wat Res 21:1481-1487.

Skinner FA, Walker N (1961) Growth of *Nitrosomonas europaea* in batch and continuous culture. Archiv Mikrobiol 38:339-349.

Vanýsek P (1992) Ionic conductivity and diffusion at infinite dilution. In: DR Lide (ed), CRC Handbook of chemistry and physics, 73rd, CRC Press, Boca Raton, Florida. 5:111-112.

Wanner O, Gujer W (1986) A multispecies biofilm model. Biotechnol Bioeng 28:314-328.

Weibel ER (1979) Stereological methods. vol 1. Practical methods for biological morphometry. Academic Press. London.

Westrin BA (1991) Diffusion measurements in gels. A methodological study. Ph.D. Thesis, Lund University, Lund, Sweden.

Wijffels RH, Gooijer CD de, Kortekaas S, Tramper J (1991) Growth and substrate consumption of Nitrobacter agilis cells immobilized in carrageenan: part 2. model evaluation. Biotechnol Bioeng 38:232-240.

Wijffels RH, Englund G, Hunik JH, Leenen ETJM, Bakketun Å, Günther A, Obón de Castro JM, Tramper J (1993) Effects of diffusion limitation on immobilized nitrifying organisms at low temperature. Submitted.

Williamson K, McCarthy PL (1976) Verification studies of the biofilm model for bacteria substrate utilization. J WPCF 48:281-296.

Wise DL, Houghton G (1966) The diffusion coefficients of ten slightly soluble gases in water at 10-60°C. Chem Eng Sci 21:999-1010.

7 SCALE-UP

SUMMARY

A scale-up strategy for a nitrification process with immobilized cells is presented. The complete description of such a process for a wide range of conditions is time consuming or even impossible. For a successful scale up of the process knowledge of the rate-limiting step is essential. To estimate the rate-limiting step a regime analysis was used. A new element in this regime analysis is a solid third phase in which cells grow non-homogeneously. Three different conditions of the nitrification process were considered: low temperature (7°C) with a low ammonia concentration (2 mM), and optimal temperature (30°C) with an ammonia concentration of 2 and 250 mM. The regime analysis proved to be a helpful tool for the understanding of the process and for establishing the rate-limiting step. A set of design rules for the different nitrification conditions was obtained from the results of this regime analysis.

INTRODUCTION

P roblems related to the discharge of nitrogen compounds into the environment are topical nowadays. Both diluted wastestreams such as sewage and more concentrated wastestreams like manure contribute to nitrogen-related environmental problems. For example, discharges of ammonia from various sources have a considerable effect on algal blooms in the North Sea (Zevenboom et al. 1990). The removal of ammonia with biological nitrification is a widely used process in wastewater treatment. The active-sludge process with biomass retention gives a considerable ammonia removal in diluted waste streams (2-5 mM NH_4^+) at moderate temperatures (15-25 °C). Nitrification in an active-sludge process is, however, limited by a slow growth of the two main bacterial species involved: *Nitrosomonas spp.* and *Nitrobacter spp.*. This growth-rate limitation is most severe at unfavourable conditions like, for example, lower temperatures (Randall & Buth 1984, Painter 1986, Laudelout et al. 1974) or concentrated wastestreams where inhibition of substrate and product are important (Bortone & Piccinini 1991).

Immobilization of nitrifying bacteria can be a successful strategy to handle biomass-retention problems (Okey & Albertson, 1989). Several immobilization methods are applied. For example, at low temperatures rotating biological contactors are used by Gullicks & Cleasby (1991) and by Murphy et al. (1977), and immobilization of pure cultures in κ-carrageenan gels by Leenen et al. (1992) and by Wijffels et al. (1990). Also for manure treatment rotating biological contactors are applied (St-Arnaud et al. 1991).

Most of the research on nitrification focuses on small-scale experiments and extensive modelling of immobilized nitrifying bacteria. Several dynamic models for immobilized nitrifying bacteria are presented and validated (Wijffels et al. 1991, Gooijer et al. 1991, Wanner & Gujer 1985, Gujer & Boller 1989, Hunik et al. 1993). Large-scale applications of this immobilized-cell process are limited to a few plants because this complicated process is difficult to scale up (Heijnen et al. 1991). A better understanding

of the rate-limiting factors, important for scaling up, can be obtained with a regime analysis (Sweere et al ,1987). From such a regime analysis a set of design directives for the different applications of immobilized nitrifying bacteria can be derived.

Air-lift loop reactors are most suitable for immobilized-cell processes. They lack mechanical stirring and are easy to scale up. Mechanical stirring can cause abrasion of the immobilization material and should therefore be avoided. Air-lift loop reactors are characterized, among others, by Verlaan (1987) and Chisti (1988) with respect to their liquid circulation, mixing properties and mass transfer.

The regime analysis presented here is based on an air-lift loop reactor design for a nitrification process with immobilized cells. The existing theory for regime analysis was extended with cells growing non-homogeneously in gel beads. Reactor performance and other information necessary for the regime analysis were simulated with a dynamic model (Hunik et al. 1993). The regime analysis was used to derive the rate-limiting step and design directives for three cases of the nitrification process with immobilized cells: low temperature (7°C) with low ammonia concentration (2 mM), and optimal temperature (30 °C) with an ammonia concentration of 2 mM and 250 mM.

THEORY

R egime analysis. A system with immobilized cells for nitrification has a complex behaviour. A complete description of the process for a wide range of conditions is time consuming or even impossible. This argument is valid for most biotechnological processes and a consistent approach to simplify these processes is regime analysis (Roels 1983, Moser 1988). In the regime analysis presented by Schouten et al (1986), with immobilized *Clostridium spp.* for isopropanol/butanol production, the effectiveness factor for the immobilized cells was estimated to be 1. They conclude that the

isopropanol/butanol production is not diffusion controlled and the immobilized cells behave as free cells. New for the regime analysis presented here is the addition of a solid third phase with immobilized cells growing in a diffusion-controlled situation.
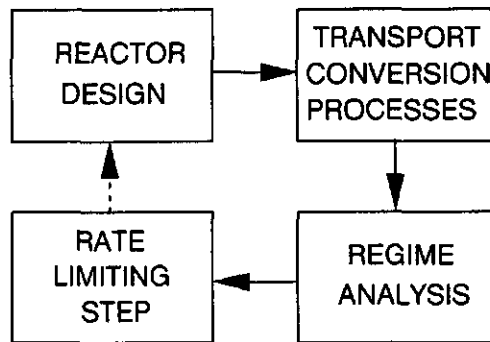
Figure 1   *Regime analysis.*

Regime analysis can either be used for the optimization of the reactor design or to reveal the rate-limiting step of a process, see Figure 1 (Sweere et al. 1987). Optimization of the reactor design requires several iterations until a previously defined optimum is obtained. Here we are interested in the rate-limiting step of the process and not in optimization of the reactor design. The regime analysis starts with an inventory of all transport and conversion mechanisms of the process. The characteristic time of each mechanism is then estimated; relatively slow mechanisms have a high characteristic time, while lower characteristic times apply to faster mechanisms. The comparison of characteristic times for conversion and transport mechanisms of a particular substrate can thus reveal the rate-limiting step.

130

For nitrification with cells non-homogeneously growing in a gel bead several transport mechanisms for the substrates (O_2 and NH_4^+), intermediate (NO_2^-) and product (NO_3^-) can be distinguished: mass transfer of oxygen from air bubbles to the liquid phase; mass transfer of oxygen and ammonia from the bulk phase to the gel beads; mass transfer of oxygen, ammonia and nitrite within the beads to the cells, and mass transfer of nitrite (intermediate) and nitrate (product) from the beads to the liquid. All these transport mechanisms are characterized with either a mass-transfer coefficient or a diffusion coefficient. The conversion is characterized by the substrate consumption rate. This chain of transport and conversion should be combined with the reactor characteristics in the actual regime analysis. Mixing, circulation, gas and liquid retention times should be compared with the characteristic times for transport and conversion to reveal if gradients in the reactor bulk phase can be expected.

Characteristic times. Examples of relations for characteristic times are found in the literature (Moser 1988, Sweere et al. 1987, Gooijer et al. 1991). In general these relations are obtained from the ratio between a capacity and a flow

$$\tau = \frac{capacity}{flow} \tag{1}$$

Capacity is defined as the available substrate for transport or conversion at process conditions. The flow is the rate of that particular transport or conversion. The characteristic time for mixing and circulation, which have already time as dimension, are directly used in the regime analysis.

When regime analysis is used for a three-phase system one phase must be used as a sort of "pivot" for the characteristic-time calculations. Most convenient is the continuous (liquid) phase, which is therefore, unless mentioned otherwise, used as "pivot" phase for the characteristic- time definitions given below.

The characteristic time (τ^O_{lg}) for the mass transfer of oxygen from the gas phase to the liquid phase is given by

$$\tau^O_{lg} = \frac{1}{k_{lg} * a_{lg}} \tag{2}$$

with k_{lg} as the gas-liquid mass-transfer coefficient [m. s^{-1}] and a_{lg} as the gas-surface area per unit of liquid volume [m^2. m^{-3}]. The latter is given by

$$a_{lg} = a_g \cdot \frac{\epsilon_g}{1 - \epsilon_g} \tag{3}$$

with ϵ_g as the gas hold up [m^3 gas. m^{-3} liquid] and a_g as the specific surface area of the gas phase per unit of gas volume [m^2. m^{-3}] based on d_b, the gas bubble diameter [m]:

$$a_g = \frac{6}{d_b} \tag{4}$$

Transport of oxygen from the gas bubble to the liquid phase depletes the gas bubbles of oxygen. The characteristic time for the gas-bubble oxygen exhaustion (τ^O_{ex}) is given by

$$\tau^O_{ex} = \frac{H}{k_{lg} * a_g} \tag{5}$$

with the H as the Henry coefficient [m^3 liquid. m^{-3} gas]. The τ^O_{ex} in eq (5) is based on the gas phase, because the depletion of this phase is considered here.

The characteristic time (τ_{ls}) for the mass transfer from the liquid to the solid phase is given by

$$\tau_{ls} = \frac{1}{k_{ls} * a_{ls}} \tag{6}$$

with k_{ls} as the liquid-solid mass transfer coefficient [m. s⁻¹] and a_{ls} as the solid-surface area per unit of liquid volume [m². m⁻³]. The latter is given by

$$a_{ls} = a_s \cdot \frac{\epsilon_s}{1 - \epsilon_s} \qquad (7)$$

with ϵ_s as the solid hold up [m³ solid. m⁻³ liquid] and a_s as the specific surface area of the solid phase per unit of solid volume [m². m⁻³] based on d_b the gel bead diameter [m]:

$$a_s = \frac{6}{d_p} \qquad (8)$$

Characteristic times for liquid circulation, mixing and gas-phase retention time in air-lift loop reactors are related to the size of the reactor. The mixing time (τ_{mix}) for an air-lift loop reactor is calculated from the circulation time (τ_{circ}) as shown by Verlaan (1987):

$$\tau_{mix} = (4 \ to \ 7) \cdot \tau_{circ} \qquad (9)$$

This value of τ_{circ} can be measured easily in an existing reactor or calculated for a given reactor design (Verlaan, 1987).

The maximum gas-phase-retention time (τ_{ret}^{gas}) in an air-lift loop reactor is calculated from the ratio of the reactor height and terminal rising velocity (approximately 0.25 m/s, Heijnen & Riet 1984) of the gas bubbles. The actual value for gas-phase retention time (τ_{ret}^{gas}) will be shorter when liquid circulation in the loop reactor is taken into account. The liquid-retention time (τ_{ret}^{liq}) is the reciprocal value of the dilution rate.

The characteristic time τ_{kin} for the substrate conversion by free cells is derived from the biomass concentration X [kg.m^{-3}], the substrate concentration S [mol.m^{-3}], and the kinetic parameters K_S [mol.m^{-3}], Y [kg.mol^{-1}], and μ_{max} [s^{-1}] of the relevant microorganism (Roels, 1983):

$$\tau_{kin} = \frac{S}{\left[\dfrac{\mu_{max} * X}{Y} \right] \cdot \left[\dfrac{S}{K_S + S} \right]} \tag{10}$$

When we consider solid gel beads with immobilized cells and if all the cells in these gel beads "feel" the substrate concentration at the surface (S_{sur}), eq (10) will reduce to

$$\tau_{kin} = \left[\frac{Y}{\mu_{max} * X} \right] \cdot (K_S + S_{sur}) \tag{11}$$

with X expressed as kg.m^{-3} gel.

The situation inside the gel beads is more complicated because substrate and biomass concentrations vary with the radius of the gel bead. It is not possible to define an overall characteristic time for transport or conversion in such a situation. To circumvent this problem we introduce the internal effectiveness factor which is defined as the ratio between the observed conversion rate (actual flow) and the conversion rate which would be observed if all the biomass would "feel" the substrate concentration at the surface of the gel beads (flow for S_{sur}; Riet & Tramper, 1991). In this effectiveness factor both transport and conversion are taken into account. For the calculation of the effectiveness factor it is important to realize that the observed conversion rate of the cells in the gel beads (actual flow) is equal to the flow of substrate from the bulk to the gel-bead surface. This liquid to solid mass-transfer rate is substituted in the definition for

the actual flow in the internal effectiveness factor (η), which yields

$$\eta = \frac{k_{ls} \cdot a_{ls} \cdot (S_{bulk} - S_{sur})}{\left[\dfrac{\mu_{max} \cdot X}{Y}\right] \cdot \left[\dfrac{S_{sur}}{K_S + S_{sur}}\right]} \qquad (12)$$

The value for the effectiveness factor approaches 0 for a strictly transport-controlled process and 1 for a completely kinetically controlled process. With η going from 1 to 0, the relative conversion rate decreases and the corresponding characteristic time increases. Therefore, τ_{kin} and the reciprocal value for η were combined in eq (13) to derive a characteristic time for substrate conversion by immobilized cells (τ_{conv}). This results in a ratio between capacity (S_{sur}) and actual flow of substrate to the gel beads (denominator of eq (13)), which is exactly the definition of a characteristic time (eq (1)) for the overall substrate conversion by the gel beads (τ_{conv}):

$$\tau_{conv} = \frac{S_{sur}}{k_{ls} \cdot a_{ls} \cdot (S_{bulk} - S_{sur})} \qquad (13)$$

The substrate concentration at the surface of the gel beads (S_{sur}) is the key value, which determines the relative importance of the liquid-solid mass transfer and the conversion by the immobilized cells. This can be illustrated by taken the ratio of eq (6) and eq (13) yielding a relation between the characteristic time for liquid-solid mass transfer and substrate conversion in the gel beads

$$\frac{\tau_{conv}}{\tau_{ls}} = \frac{S_{sur}}{S_{bulk} - S_{sur}} \qquad (14)$$

The effect of S_{sur} on the ratio of the characteristic time for substrate conversion (τ_{conv}) and solid-liquid mass transfer (τ_{ls}) is shown in Figure 2. This figure shows that with a surface concentration of half that of the bulk concentration, the characteristic times τ_{kin} and τ_{conv} are equal. Two extreme situations can be distinguished in Figure 2. First, when S_{sur} is 0 the conversion is completely controlled by liquid-solid mass transfer. Second, for S_{sur} is equal to S_{bulk}, the conversion is copletely kinetically controlled. The surface concentration (S_{sur}) of the biocatalyst is not easy to measure, but can be estimated from experimental results or model predictions.
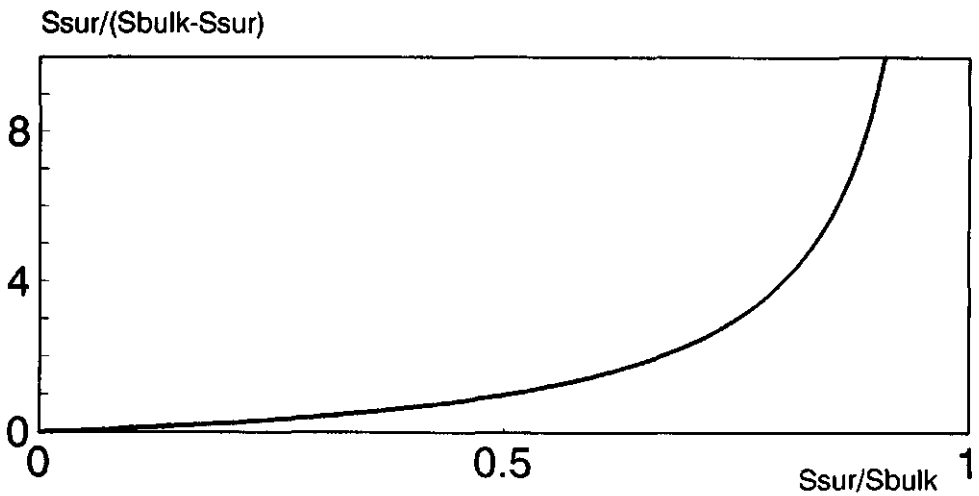

Figure 2   *Relation between S_{sur} and S_{bulk} with respect to solid/liquid mass transfer and conversion rate of the biocatalyst in eqs (6) and (13).*

PROCESS DESCRIPTION

T hree different cases for the nitrification process with immobilized cells were considered in the regime analysis: Nitrification at low temperature (7°C) with a low ammonia concentration of 2 mM (LTLA), nitrification in an extreme environment of ammonia (250 mM) and an optimal temperature of 30°C (OTEE), and nitrification at optimal temperature (30°C) and low ammonia concentration of 2 mM (OTLA). The latter was taken as the reference for the two other cases. A dynamic model (Hunik et al.1993) was used to simulate the nitrification process for these three cases. The original model uses parameter values based on a temperature of 30°C, but incorporation of the effects of lower temperatures on these model parameters are described here.

Model. The dynamic model consists of a set of transport and kinetic equations for the conversion of ammonia via nitrite to nitrate with immobilized *Nitrosomonas europaea* and *Nitrobacter agilis* cells in an air-lift loop reactor. The dynamic character of the model allows changes in reactor conditions. The growth of cells and the concentration of substrate, intermediate and product together with biomass concentrations for *N. europaea* and *N. agilis* are predicted as a function of the gel-bead radius. The model input consists of a set of parameters obtained from independent experiments together with the initial values for biomass concentrations, reactor set-up and experimental cases like temperature and influent concentrations. For the regime analysis the model was used to predict the conversion capacities and the S_{sur} value for the three nitrification cases considered. The parameters used for the model are shown in Table I. A more detailed description of the model is given by Hunik et al.(1993). The parameters for gas-liquid transport (H, d_b, k_{lg}) necessary for the regime analysis are obtained from Heijnen & Riet (1984) and also shown in Table I.

137

Table I   *Model parameters*

parameter	value at 30°C Hunik et al. (1993)	value at 7°C	dimension
CONVERSION			
μ_{max}^{Ns}; μ_{max}^{Nb}	1.59 *10⁻⁵; 1.0 *10⁻⁵	1.9 *10⁻⁶; 2.3 *10⁻⁶	s⁻¹
m_s^{Ns}; m_s^{Nb}	9.4 *10⁻⁴; 2.2 *10⁻³	2.6 *10⁻⁴; 6.4 *10⁻⁴	molN.(kg biomass)⁻¹.s⁻¹
Y^{Ns}; Y^{Nb}	1.66 *10⁻³; 0.58 *10⁻³	1.66 *10⁻³; 0.58 *10⁻³	(kg biomass). molN⁻¹
$K_s^{NH4,Ns}$	1.25 *10⁻³	1.16 *10⁻⁴	mol.dm⁻³
$K_s^{O2,Ns}$	5.05 *10⁻⁶	9.3 *10⁻⁷	mol.dm⁻³
$K_s^{NO2,Nb}$	3.6 *10⁻⁴	2.5 *10⁻⁵	mol.dm⁻³
$K_s^{O2,Nb}$	17.0 *10⁻⁶	3.1 *10⁻⁶	mol.dm⁻³
I_{NO2}^{Nb}, I_{NO3}^{Nb}	0.159; 0.188		mol.dm⁻³
TRANSPORT gas-liquid			
k_{lg} (O₂)	4.4 *10⁻⁴	2.7 *10⁻⁴	m.s⁻¹
H	39	25	m³.m⁻³
d_b	6 *10⁻³	6 *10⁻³	m
TRANSPORT liquid-solid			
k_{ls} N-comp; O₂	2.65 *10⁻⁵; 3.13 *10⁻⁵	1.41 *10⁻⁵; 1.75 *10⁻⁵	m.s⁻¹
d_p	2 *10⁻³		m
ε_s	0.25		[-]
ω	8.4 *10⁻⁴	1.66 *10⁻³	N.s.m⁻²
ID_w N-comp; O₂	2.2 *10⁻⁹; 2.83 *10⁻⁹	1.1 *10⁻⁹; 1.55 *10⁻⁹	m².s⁻¹
ID_{gel} N-comp; O₂	1.9 *10⁻⁹; 2.05 *10⁻⁹	1.0 *10⁻⁹; 1.2 *10⁻⁹	m².s⁻¹

Temperature *T* influence on parameters. The optimal temperature for nitrification is around 30°C and parameters used in the model of Hunik et al. (1993) are based on this temperature. Knowledge of the temperature influence on the model parameters is necessary for the simulations at 7°C. This temperature influence can be expressed with

an Arrhenius type of equation

$$Z^T = z^\infty \cdot e^{\left[\frac{-E_a}{R \cdot T}\right]}$$ (15)

with Z^T the parameter value at temperature T, z^∞ as a constant, E_a [J.mol^{-1}] as the activation energy and R [J.mol^{-1}.K^{-1}] as the gas constant.

Influence of T on the maximum specific growth rate. For the determination of the activation energy (E_a) for the growth rate of *Nitrosomonas europaea* and *Nitrobacter agilis* experimental data given in several literature sources (Helder & De Vries 1983, Knowles et al. 1965, Stratton & McCarty 1967) were used. In Figure 3[a,b] the μ_{max} values given in these sources for both microorganisms are plotted as function of temperature. In these figures the fits of eq (15) for the various sets are also drawn. The E_a values used in this study for the two microorganisms are averages of the values obtained from the 3 sets. These average E_a values are 65 and 45 kJ.mol^{-1} for *N. europaea* and *N. agilis*, respectively. The z^∞ values are obtained from substitution of the average E_a values and the values for μ_{max} at 30°C from Table I in eq (15). The resulting equation is used for calculating μ_{max} values at 7°C. With this procedure we obtained μ_{max} values of $1.9 * 10^{-6}$ and $2.3 * 10^{-6}$ s^{-1} for *N. europaea* and *N. agilis*, respectively, at 7°C.

Influence of T on the substrate-affinity constants. Little information about the effect of temperature on the affinity constants for O_2, NH_4^+ and NO_2^- is available in the literature. In fact three studies were found (Laudelout & van Tichelen 1960, Boon & Laudelout 1962, Knowles et al. 1965). The E_a values found in these three literature sources were used with the substrate affinity values of Table I at 30°C to substitute in eq (15) in order to obtain the values for z^∞.
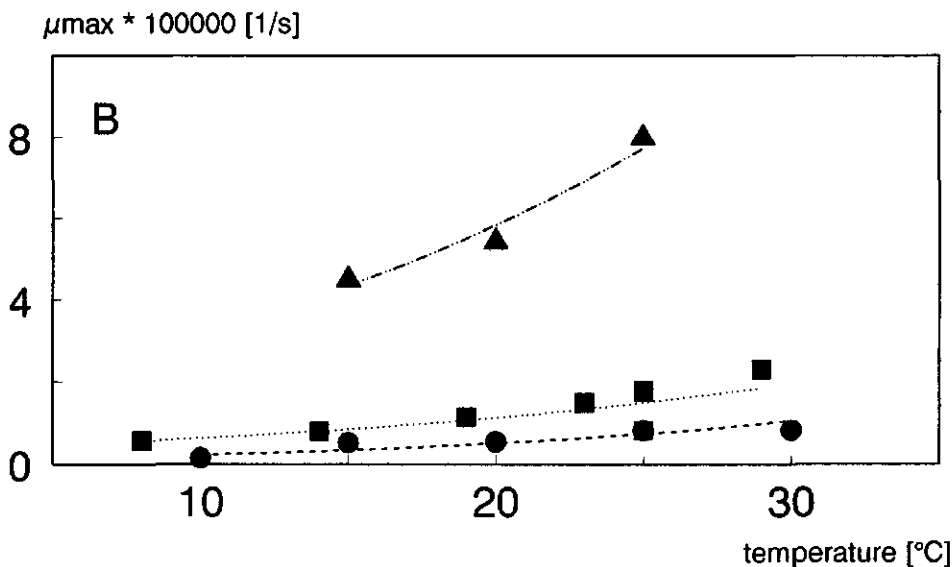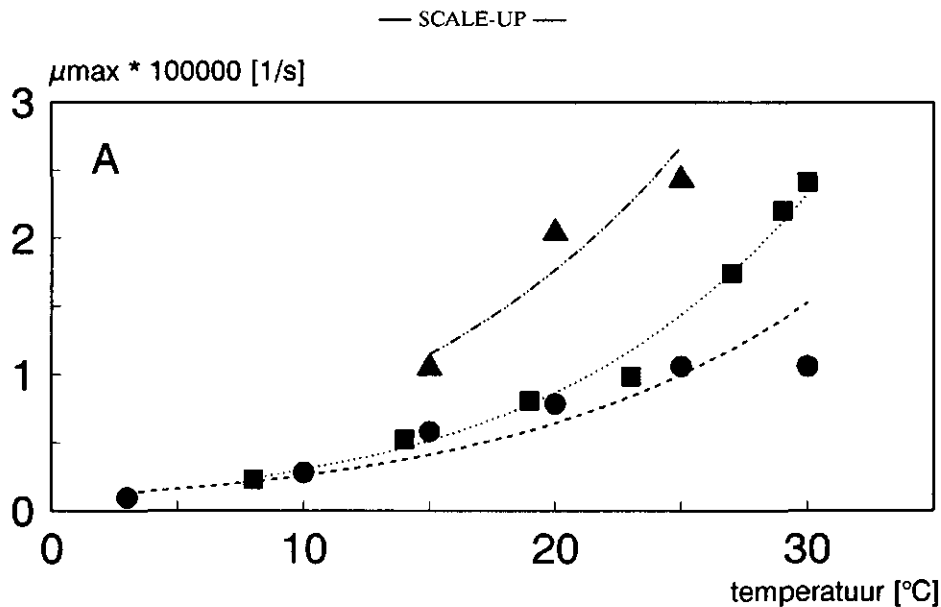
Figure 3[a,b]   The maximum growth rate of (A) Nitrosomonas spp. and (B) Nitrobacter spp.
at different temperature. Symbols are the measured values, lines are based on
eq (15) fitted to these values. With ---●--- (Helder & de Vries, 1983), ······■······
(Knowles et al. 1965), –··–▲–··– (Stratton & Mc Carty, 1967).

Boon and Laudelout (1962) measured an E_a of 52 kJ.mol^{-1} for the affinity constant of oxygen ($K_s^{O2,Nb}$) with *N. winogradskyi* (z^{∞}: 1.57 * 10^7 mol.m^{-3}). Laudelout & van Tichelen (1960) obtained an E_a value of 82 kJ.mol^{-1} for the affinity constant of NO$_2^-$ ($K_s^{NO2,Nb}$) also for *N. winogradskyi* (z^{∞}: 4.92 * 10^{13} mol.m^{-3}). From the data of Knowles et al. (1965) we obtained an E_a of 73 kJ.mol^{-1} for the NH$_4^+$ affinity constant ($K_s^{NH4,Ns}$) of a mixed culture (z^{∞}: 4.82 * 10^{12} mol.m^{-3}). For the missing E_a value of the affinity constant of oxygen for *N. europaea* ($K_s^{O2,Ns}$) we used 52 kJ.mol^{-1} which is the same value as the affinity constant of oxygen for *N. winogradskyi*. This latter value is also used by Laudelout et al. (1976) for *N. europaea*. (z^{∞}: 4.65 * 10^6 mol.m^{-3}). The substrate affinity constants at 7°C are estimated with this z^{∞} and E_a values.

Influence of T on maintenance and yield. The effect of temperature on the maintenance (m_s) of a large number of aerobic microorganisms is described by Heijnen & Roels (1981). They found an activation energy (E_a) of 38 kJ.mol^{-1} for the maintenance of all aerobic microorganisms. The m_s at 7°C calculated with this E_a and maintenance values at 30°C of Table I was 2.6 * 10^{-4} and 6.4 * 10^{-4} mol N.kg^{-1}.s^{-1} for *N. europaea* and *N. agilis*, respectively. Concerning biomass yield, in the literature survey of Heijnen and Roels (1981) it can be read that the biomass yield (Y) is independent of T.

Influence of T on the dynamic viscosity. Eq (15) was fitted to the data of the dynamic viscosity (ω) of water, given by Weast & Astle (1980). A value of 6.021 * 10^{-7} N.s.m^{-2} and 18.1 kJ.mol^{-1} was obtained for z^{∞} and E_a, respectively.

Influence of T on D of O$_2$ and nitrogen compounds. The influence of temperature on the diffusion coefficient of oxygen in water is given by Wise & Houghton (1966). A value of 4.2 * 10^{-6} m^2.s^{-1} and 18.4 kJ.mol^{-1} for respectively z^{∞} and E_a are given. For the diffusion coefficient of oxygen in the gel beads, Wijffels et al. (1993) obtained a value of 1.9 * 10^{-6} m^2.s^{-1} for z^{∞} and 17.2 kJ.mol^{-1} for E_a.

Diffusion coefficients of NH_4^+, NO_2^- and NO_3^- in water and biofilms at different temperatures are scarcely found. Therefore, it was not possible to estimate the E_a and z^* values. The diffusion coefficients for these nitrogen compounds in water and biofilms at 7°C were therefore estimated using the temperature dependency of the dynamic viscosity (ω) with the following relation (Newman, 1973)

$$ D\ (T_1)\ .\ \frac{\omega\ (T_1)}{T_1}\ =\ D\ (T_2)\ .\ \frac{\omega\ (T_2)}{T_2} \tag{16} $$

The diffusion coefficients at 7°C thus estimated are $1.1 * 10^{-9}$ $m^2.s^{-1}$ and $1.0 * 10^{-9}$ $m^2.s^{-1}$ for water and biofilm, respectively.

Influence of T on gas-liquid mass transfer. The mass-transfer coefficient for oxygen at the gas liquid interphase is a rather empirical parameter. Influence of bubble size and media composition are difficult to take into account. A value of $4 * 10^{-4}$ $m.s^{-1}$ at 20°C with a temperature dependency of 2.5 % increase per °C is used by Heijnen & Riet (1984). For the gas liquid mass-transfer coefficient (k_{lg}) at 7°C and 30°C a value of $2.7 * 10^{-4}$ $m.s^{-1}$ and $4.4 * 10^{-4}$ $m.s^{-1}$ respectively, were estimated based on this temperature relation. The Henry coefficient (H) for oxygen is 39 [m^3 gas. m^{-3} liquid] at 30°C and 25 [m^3 gas .m^{-3} liquid] at 7°C (Janssen & Warmoeskerken, 1982).

Influence of T on liquid-solid mass transfer. For the mass-transfer coefficient of the liquid-solid interphase an estimation is possible, based on the film-theory. This mass-transfer coefficient depends on the dynamic viscosity and on the diffusion coefficient, which are both temperature dependent. For the mass-transfer coefficient we assume, based on the similar values for the diffusion coefficient, one value for the three nitrogen compounds. For both temperatures it is possible to calculate the mass-transfer coefficient k_{ls} (Wijffels et al.,1991). For that, a value of 1000 and 1008 kg/m^3 is used for the density of water and gel beads, respectively.

Design and initial values for the model. A nitrification process at a low temperature of 7°C in, for example, Norway should have a capacity of $2 * 10^4$ m^3.day^{-1} with an ammonia concentration in the waste water of 2 mM (Ødegaard et al. 1990). This implies an ammonia conversion rate of $4 * 10^4$ mol N.day^{-1}. From this capacity and some initial trials with the model we derived the reactor volumes and dilution rates for all three cases considered here.

The prerequisite of the design was an ammonia conversion at steady state of 75% for the low ammonia cases (LTLA and OTLA) and 95% for the extreme environment case (OTEE). The reactor dimensions, dilution rates, temperatures and influent concentrations are shown in Table II.

Table II *Reactor design*

reactor	volume [m^3]	dilution rate [s^{-1}]	influent NH$_4^+$ [mM]	temperature °C
low temperature (LTLA)	833	$2.8 * 10^{-4}$	2	7
optimal temperature (OTLA)	278	$8.3 * 10^{-5}$	2	30
extreme environment (OTEE)	514	$3.9 * 10^{-6}$	250	30

The model input value for the initial biomass concentration of *N. europaea* and *N. agilis* are the same as used by Hunik et al. (1993), i.e. $4 * 10^{-3}$ and $2 * 10^{-4}$ kg/m^3 gel, respectively. The maximum biomass concentration in the model was set at 8.9 and 3.8 kg/m^3 gel for *N. europaea* and *N. agilis*, respectively. These values are identical to the values of Hunik et al.(1993). A 50 day run of the model was sufficient to reach a steady-state conversion rate of ammonia and nitrite for the three processes.The temperature for the LTLA process was taken 30°C for the first ten days of the experiment; for the rest

of the experiment the temperature was set at 7°C. The optimal temperature of 30°C during the start-up phase was used to accelerate the biomass formation. A steady-state conversion of ammonia within a 50 day run could be achieved with such an increased start-up temperature. The final concentration of 250 mM NH_4^+ in the OTEE process was reached by starting with 50 mM and subsequently increasing it to 100mM at day 6, 150 mM at day 15, 200 mM at day 25 and finally 250 mM NH_4^+ at day 35. This step-wise increase was used to avoid the inhibitory effect of NO_2^- in the start-up phase.

RESULTS & DISCUSSION

For the three nitrification process cases considered, model simulations generated the bulk-phase concentrations of NH_4^+, NO_2^- and NO_3^- and these are shown in Figure 4[a,b,c] as a function of time. The decrease in NH_4^+ concentration and the production of NO_2^- during the first 10 days was caused by the growth of *N. europaea*. The production of NO_3^- and the related growth of *N. agilis* start between day 10 and 20 depending on the process cases. The reactor concentrations of the OTLA case are shown in Figure 4[b]. The temperature step at day 10 for the LTLA case is observed in Figure 4[a]. The step-wise increase in influent ammonia concentration in the OTEE case resulted in a step-wise increase in nitrate concentration as shown in Figure 4[c]. The criteria for the nitrification capacity, at least 75% ammonia removal for the low ammonia cases (LTLA and OTLA) and more then 95% for the high ammonia concentration case (OTEE), were satisfied for all three nitrification cases. The presented data of the model simulations were used in the regime analysis.

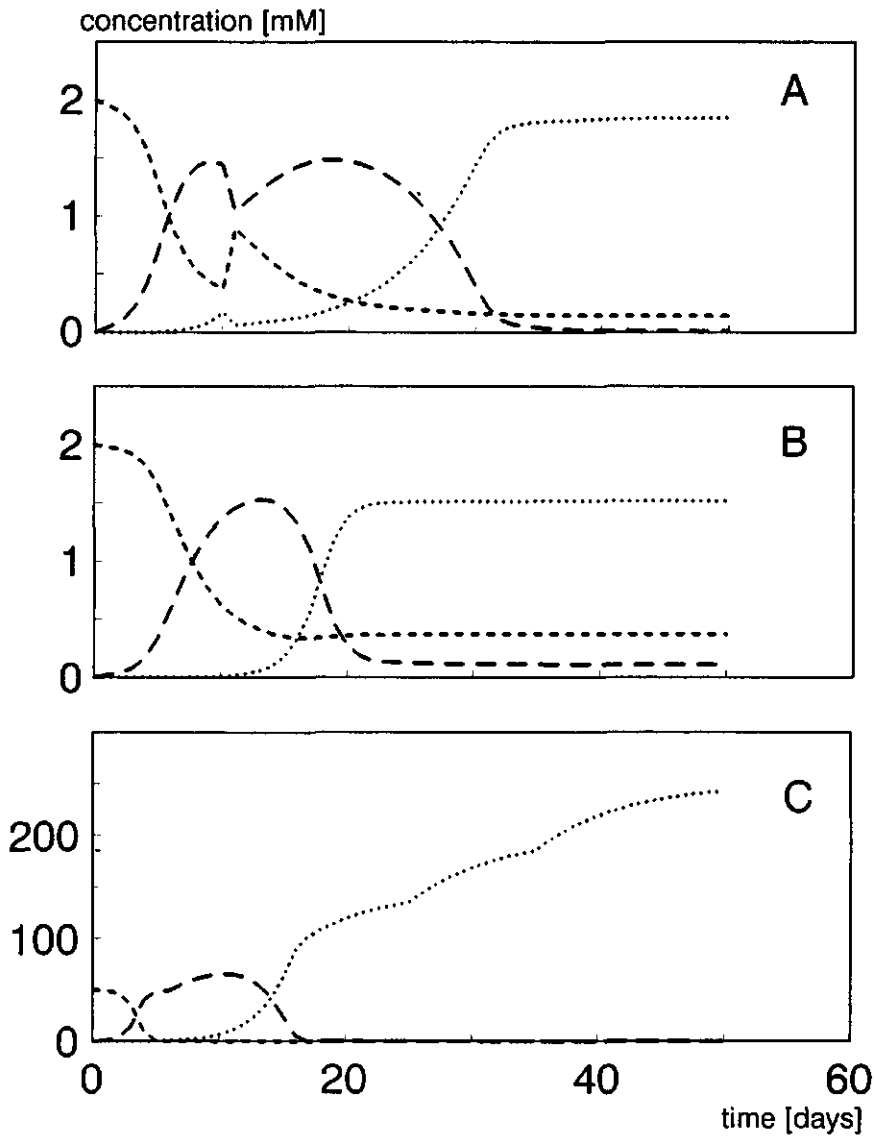concentration [mM]

Figure 4[a,b,c]   Bulk concentrations of NH_4^+ (----), NO_2^- (— —) and NO_3^- (······) as a function of time for the nitrification process predicted by the model at the three cases: (A) LTLA, (B) OTLA and (C) OTEE.

Regime analysis. The values for the gas-phase hold up (ϵ_g) and liquid mixing time (τ_{mix}) depend on the reactor configuration and size. Gas hold up (ϵ_g) values for air-lift loop reactors will be in the range of 0.02-0.05 (Verlaan, 1987; Chisti, 1989). Riet & Tramper (1991) present some data about circulation and mixing times in air-lift loop reactors based on the model of Verlaan (1987). The mixing (180-600 s) and circulation times (45-150 s) they present are for two external air-lift loop reactors with a volume of 265 and 1227 m^3, respectively, a height to riser diameter ratio of 10 : 1 and a ratio between the riser to downcomer diameter of 2 : 1.

Table III *Characteristic times of transport and conversion processes* for the three nitrification processes. The τ_{conv} values are based on the steady-state values at day 50 in Figure 5[a,b,c]

transport phenomena	characteristic time (τ) [s]		
	LTLA (7°C)	OTLA (30°C)	OTEE (250 mM)
τ_{gas}^{rel}	20	20	20
τ_{ex}^{O2}	93	78	78
τ_{lg}^{O2} $(\epsilon_g = 0.02\text{-}0.05)$	181-70	98-38	98-38
τ_{ls}^{O2}	57	35	35
τ_{liq}^{rel}	3600	1200	$2.6 * 10^5$
τ_{ls}^{NH4}	71	42	42
τ_{circ}	40-150	40-150	40-150
conversion processes			
τ_{conv}^{NH4}	30	61	50
τ_{conv}^{NO2}	3.5	26	43
τ_{conv}^{O2}	24	11	19

A difference between mixing and circulation time should be made for loop reactors. Mixing times are useful for pulse-wise addition of a substrate to the reactor and circulation times are more useful for continuous addition of substrates in loop reactors. This latter situation is more applicable and circulation times were therefore used to predict gradients in the reactors.

The characteristic times for all the transport mechanisms in the reactor are independent of the substrate concentrations. This is in contrast to the characteristic time of substrate conversion (τ_{conv}), which depends on the surface concentration of the gel bead. This surface concentration decreased during the start up and finally reached a steady state. The course of τ_{conv} for the three cases is shown in Figure 5[a,b,c]. The regime analysis is based on the steady-state values reached after 50 days of model simulation. The characteristic times for conversion and transport are presented in Table III and discussed below with respect to the substrate involved.

Oxygen. Oxygen depletion of the gas phase depends on the mass transfer of oxygen from gas to liquid phase and amount of oxygen available in the gas phase. With the values for τ_{ex}^{O2} and τ_{ret}^{gas} (Table III) we can conclude that complete exhaustion of the gas bubble is not likely to happen, but a significant decrease in oxygen concentration in the gas bubble will occur. Oxygen exhaustion of gas bubbles in air-lift loop reactors does not become important beneath a reactor height of 15 m, but it also depends on the liquid velocity in the riser.

Oxygen is transported from gas phase via the liquid phase to the solid phase. The rate of this transport is determined by the characteristic times for gas-liquid mass transfer (τ_{lg}^{O2}), liquid-solid mass transfer (τ_{ls}^{O2}) and oxygen conversion (τ_{conv}^{O2}). In Table III the values for τ_{lg}^{O2} (at $\epsilon_g = 0.05$), τ_{ls}^{O2} and τ_{conv}^{O2} are in the same order of magnitude and only trends can thus be indicated. The differences in characteristic times are not sufficient to indicate one step in the process as the only rate-limiting step.
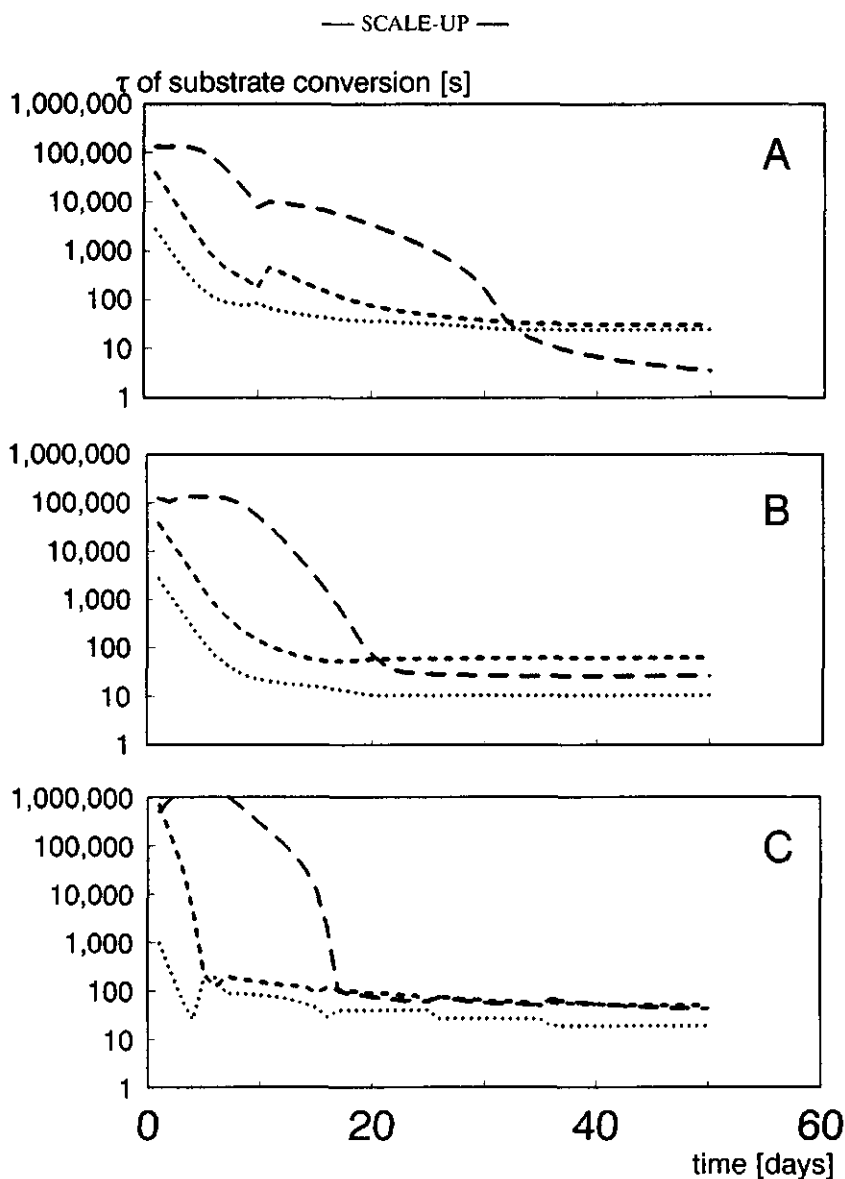
147

Figure 5[a,b,c]   *The characteristic time for substrate conversion (τ_{com}) of the three substrates, NH_4^+ (----) and NO_2^- (——) and O_2 (······) as a function of time for the nitrification process at three different cases (A) LTLA, (B) OTLA and (C) OTEE. Values are obtained from model simulations.*

The values for τ_{lg}^{O2} (at $\epsilon_g = 0.05$), τ_{ls}^{O2} and τ_{conv}^{O2} are decreasing in this order. The fastest process is the oxygen conversion and the higher values for τ_{lg}^{O2} and τ_{ls}^{O2} indicate that transport of oxygen from the gas phase to the gel beads is likely to be rate limiting. With a lower gas hold up (at $\epsilon_g = 0.02$) the value for τ_{lg}^{O2} increases and mass-transfer resistance will even be more important. This is particularly the case for the OTLA case with the lowest value for τ_{conv}^{O2}. The liquid circulation time (τ_{circ}) is in the same order of magnitude as the characteristic times for gas-liquid mass transfer (τ_{lg}^{O2}) and liquid-solid mass transfer (τ_{ls}^{O2}). Gradients in O_2 concentration in the liquid phase can thus be expected. A gel bead, when circulating through the loop reactor, will encounter rapid changes in O_2 concentrations as a consequence of this gradients.

Ammonia and nitrite. The situation for NH_4^+ is restricted to the liquid and solid phase. The liquid phase can be assumed well mixed with respect to NH_4^+ because liquid retention time (τ_{ret}^{liq}) is large compared to the circulation time (τ_{circ}). The characteristic time for NH_4^+ conversion by the immobilized *Ns. europaea* cells (τ_{conv}^{NH4}) is of the same order of magnitude as that for mass transfer (τ_{ls}^{NH4}) between liquid and solid phase. The rate of conversion of NH_4^+ will thus be controlled by both the liquid-solid mass transfer and NH_4^+ conversion by the immobilized cells.

Nitrite is produced within the gel beads by the *Ns. europaea* cells and mass transfer between liquid and solid phase of NO_2^- is thus not important. The value of τ_{conv}^{NO2} for the LTLA case is an order of magnitude smaller than the value for τ_{conv}^{NH4}. This indicates that nitrite conversion is a faster process compared to ammonia conversion and accumulation of NO_2^- is not likely to happen for the LTLA case. This is in contrast with the OTLA and OTEE case where the value of τ_{conv}^{NO2} is close to the value for τ_{conv}^{NH4}. The NO_2^- and NH_4^+ conversion rates are well balanced for the OTLA and OTEE case and distortion of this balance can cause accumulation of NO_2^-. High values for the concentration of toxic NO_2^- in the effluent of a nitrification process are obviously unacceptable.

149

Nitrification. The regime analysis shows that the nitrification process is mainly controlled by mass transfer of the two substrates and to a lesser extent by the conversion rates of them. Accumulation of nitrite is possible at optimal temperature and very unlikely at low temperature. The characteristic time of the NH_4^+ conversion for both the OTLA and OTEE case is considerable longer than that for O_2 conversion. The nitrification for both the OTLA and OTEE is controlled by the O_2 transport and to lesser extent by its conversion.

Design rules. Regime analysis shows that nitrification with immobilized cells is mainly controlled by mass transfer of oxygen. This is an improvement compared to the active sludge process, which is controlled by the slower process of bacterial growth. The design for the OTLA and OTEE case can be further improved with respect to oxygen transport, in particular between gas and liquid phase. This oxygen transport is dependent of k_{lg}, a_{lg}, k_{ls} and a_{ls}. Smaller gas bubbles and gel beads increase these values of k_{lg}, a_{lg}, k_{ls} and a_{ls}. The relation between a_{ls} and gel bead diameter (d_p) is shown in eqs (7) and (8). A decrease in gel bead diameter (d_p) would increase the value a_{ls}. Nevertheless, the minimum gel bead diameter (d_p) is limited by the requirement to keep the gel beads in the reactor. The gas bubble diameter (d_b) is determined by the sparger and the coalescence behaviour of the medium, which is difficult to manipulate. For this reason, it is not useful to produce small bubbles in a coalescent medium because, the advantage of the small bubbles disappears short after the sparger. An increase in gas hold up (ϵ_g) would be beneficial for the oxygen-transfer rate according to eq (3). An increase of solid phase hold up (ϵ_s), i.e. more gel beads in the reactor, is also limited to a maximum of 35%, and as a consequence k_{lg} will be reduced (Verlaan, 1987). For the design of the LTLA case the liquid-solid mass transfer of both oxygen and ammonia could be improved by smaller gel beads and a slightly higher solid-phase hold up.

Sufficient liquid mixing, e.g. prevention of oxygen gradients, should be provided for in all three nitrification processes with immobilized cells. Oxygen gradients in the

reactor can be decreased when the retention time in the non-aerated downcomer is short and the overall circulation time is kept as small as possible. Reactors should therefore have a relatively high riser to downcomer diameter ratio and small height to diameter ratio. The ratio of *N. europaea* and *N. agilis* biomass concentrations is particular important for the optimal temperature processes and probably be controlled with the inoculum of cells during immobilization. This biomass ratio is not important for the LTLA process, because the growth rate of *N. agilis* decreases less with a decrease of temperature than the growth rate of *N. europaea*.

NOMENCLATURE

a_g	=	specific surface area of a gas bubble	$m^2.m^{-3}$ gas phase
a_{lg}	=	surface area of liquid/gas inter phase	$m^2.m^{-3}$ liquid phase
a_{ls}	=	surface area of solid/liquid inter phase	$m^2.m^{-3}$ liquid phase
a_s	=	specific surface area of a gelbead	$m^2.m^{-3}$ solid phase
d_b	=	gas bubble diameter	m
d_p	=	biocatalyst particle diameter	m
E_a	=	activation energy	$J.mol^{-1}$
g	=	gravitational acceleration	$m.s^{-2}$
H	=	Henry coefficient	$m^3.m^{-3}$
$I\!D$	=	diffusion coefficient	$m^2.s^{-1}$
k_{lg}	=	gas/liquid mass transfer coefficient	$m.s^{-1}$
k_{ls}	=	solid/liquid mass transfer coefficient	$m.s^{-1}$
K_S	=	substrate affinity constant	$mol.m^3$
m_s	=	maintenance coefficient	$molN.(kg\ biomassa)^{-1}.s^{-1}$
R	=	gas constant	$J.mol^{-1}.K^{-1}$
S	=	substrate concentration	$mol.m^{-3}$

S_{sur}	=	S at surface of the biocatalyst	$mol.m^{-3}$
S_{bulk}	=	S in bulk phase	$mol.m^{-3}$
Y	=	yield coefficient	$kg.mol^{-1}$
X	=	biomass concentration	$kg.m^{-3}$
Z	=	temperature effected parameter	[-]
z^∞	=	temperature independent parameter	[-]
ϵ_g	=	gas hold up	m^3 gas. m^{-3} liquid
ϵ_s	=	solid phase hold up	m^3 solid. m^{-3} liquid
η^i	=	effectiveness factor	[-]
λ^i	=	molar ionic conductivity	$m^2.S.mol^{-1}$
τ	=	characteristic time	s
τ_g	=	τ for growth	s
τ_{ex}^{O}	=	τ for oxygen exhaustion of gas bubbles	s
τ_{lg}^{O}	=	τ for gas/liquid oxygen transfer	s
τ_{ret}^{liq}	=	τ for the liquid retention time	s
τ_{ret}^{gas}	=	τ for the gas retention time	s
τ_{ls}^{i}	=	τ for solid/liquid transfer of substrate	s
τ_{mix}	=	τ for mixing of liquid phase	s
τ_{circ}	=	τ for liquid circulation in reactor	s
τ_{kin}^{i}	=	τ for substrate conversion	s
τ_{conv}^{i}	=	τ for substrate conversion in biocatalyst	s
μ_{max}	=	maximum specific growth rate	s^{-1}
ω	=	dynamic viscosity	$N.s.m^{-2}$
ρ_l	=	density of liquid phase	$kg.m^{-3}$
ρ_s	=	density of solid phase	$kg.m^{-3}$
i	=	NH_4^+, NO_2^-, NO_3^- and Ns, Nb for *N. europaea*, *N. agilis*, respectively

LITERATURE

Boon B, Laudelout H (1962) Kinetics of nitrite oxidation by *Nitrobacter winogradskyi*. Biochem J 85:440-447.

Bortone G, Piccinini S (1991) Nitrification and denitrification in activated-sludge plants for pig slurry and wastewater from cheese diaries. Bioresouce technology 37:243-252.

Brian PTL, Hales HB (1969) Effects of transpiration and changing diameter on heat and mass transfer to spheres. AIChE J 15:419-425.

Chisti MY (1989) Airlift bioreactors, Elsevier science publishers, Essex, England.

Gooijer CD de, Wijffels RH, Tramper J (1991) Growth and substrate consumption of *Nitrobacter agilis* cells immobilized in carrageenan: Part 1. dynamic modeling. Biotech Bioeng 38:224-231.

Gujer W, Boller M (1989) A mathematical model for rotating biological contactors. In: Proceedings of the technical advances in bioreactors conference, Nice, CFRP-AGHTM Paris, 69-89.

Gullicks HA, Cleasby JL (1990) Cold-climate nitrifying biofilters: design and operation considerations. JWPCF 62:50-57.

Heijnen JJ, Riet K van 't (1984) Mass transfer, mixing and heat transfer phenomena in low viscostiy bubble column reactors. Chem Eng J 28:B21-B42.

Heijnen JJ, Roels JA (1981) A macroscopic model describing yield and maintenance relationships in aerobic fermentation processes. Biotech Bioeng 23:739-763.

Heijnen JJ, Mulder A, Weltevrede R, Hols J, Leeuwen HLJM van (1991) Large scale anaerobic-aerobic treatment of complex industrial waste water using biofilm reactors. Wat Sci Tech, 23:1427-1436.

Helder W, Vries RTP de (1983) Estuarine nitrite maxima and nitrifying bacteria (Ems-Dollard estuary). Netherlands Journal of Sea Reasearch (in English) 17:1-18.

Hunik JH, Bos CG, Hoogen MP van den, Gooijer CD de, Tramper J. (1993) Validation of a dynamic model for substrate conversion and growth of Nitrosomonas europaea and *Nitrobacter agilis* cells immobilized in κ-carrageenan beads. Submitted.(Chapter 6)

Janssen LPBM, Warmoeskerken MMCG (1982) Fysisch technologisch bij-de-hand boek. DUM, Delft, The Netherlands.

Knowles G, Downing AL, Barrett MJ (1965) Determination of kinetic constants for nitrifying bacteria in mixed culture, with the aid of electronic computer. J Gen Microbiol 38:263-278.

Laudelout H, Tichelen L van (1960) Kinetics of the nitrite oxidation by *Nitrobacter winogradskyi*. J Bact 79:39-42.

Laudelout H, Lambert R, Fripiat JL, Pham ML (1974) Effet de la température sur la vitesse d'oxydation de l'ammonium en nitrate par des cultures mixtes de nitrifiants. Ann Microbiol (Inst Pasteur) 125B:75-84.

Laudelout H, Lambert R, Pham ML (1976) Influence du pH et la pression partielle d'oxygène sur la nitrification. Ann Microbiol (Inst Pasteur) 127A:367-382.

Leenen EJTM, Englund G, Tramper J, Wijffels RH (1992) Effluent treatment at low temperatures using artificially immobilized nitrifying bacteria, In: Proceedings of the international conference on Sewage into 2000, Part2: Wastewater treatment. IAWPRC/EWPCA/NVA, Amsterdam, 349-350.

Moser A (1988) Bioprocess technology: kinetics and reactors, Springer-Verlag, New York, USA.

Murphy KL, Sutton PM, Wilson RW, Jank BE (1977) Nitrogen control: design considerations for supported growth systems. J WPCF 49:549-557

Newman JS (1973) Electrochemical systems, Prentice-Hall, Englewood Cliffs, New Jersey.

Ødegaard H, Paulsrud B, Bilstad T, Pettersen JE (1990) Norwegian strategies in the treatment of municipal wastewater towards the reduction of nutrient discharges to the North Sea. In: North Sea pollution, technical strategies for improvement. IAWPRC/EWPCA/NVA, Amsterdam, The Netherlands, 355-366.

Okey RW, Albertson OE (1989) Diffusion's role in regulating rate and masking temperature effects in fixed -film nitrification. J WPCF 61:500-509.

Painter HA (1986) Nitrification in the treatment of sewage and waste-waters. In: Nitrification (ed. Prosser JI) Special publications of the society for general microbiology vol 20, IRL Press, Oxford, UK. 185-211.

Randall CW, Buth D (1984) Nitrite build-up in activated sludge resulting from temperature effects. J WPCF 56:1039-1044.

Riet K van 't, Tramper J (1991) Basic bioreactor design, Marcel Dekker Inc, New York, USA.

Roels JA (1983) Energetics and kinetics in biotechnology, Elsevier Biomedical Press, Amsterdam, The Netherlands.

Schouten GH, Guit RP, Zieleman GJ, Luyben KChAM, Kossen NWF (1986) A comparative study of a fluidized bed reactor and a gas lift loop reactor for the IBE process: Part 1. reactor design and scale down approach. J Cem Tech Biotechnol 36:335-343.

154

St-Arnaud S, Bisaillon J-G, Beaudet R (1991) Microbiological aspects of ammonia oxidation of swine waste. Can J Microbiol 37: 918-923.

Stratton FE, McCarty PL (1967) Prediction of nitrification on the dissolved oxygen balance of streams. Current Research 1:405-410.

Sweere APJ, Luyben KChAM, Kossen NWF (1987) Regime analysis and scale-down: tools to investigate the performance of bioreactors. Enzyme Microb Technol 9:386-398.

Verlaan P (1987) Modelling and characterization of an airlift-loop reactor, PhD Thesis, Wageningen Agricultural University, The Netherlands.

Wanner O, Gujer W (1984) A multispecies biofilm model, Biotech Bioeng 28:314-328.

Weast RC, Astle MJ (eds.) (1980) CRC handbook of chemistry and physics. 60th edition, CRC Press Inc., Boca Raton, Florida, USA, pag F51.

Wijffels RH, Hunik JH, Gooijer CD de, Tramper J (1990) Nitrification with immobilized bacteria in airlift loop reactors modelling and application. In: Proceedings of the 5th European congress on biotechnology, Christiansen C, Munck L, Villadsen J (eds) Copenhagen, Denmark, 392-395.

Wijffels RH, Gooijer CD de, Kortekaas S, Tramper J (1991) Growth and substrate consumption of *Nitrobacter agilis* immobilized in carrageenan: Part 2. Model evaluation. Biotech Bioeng 38:232-240.

Wijffels, R.H., Englund G., Hunik J.H., Leenen E.T.J.M., Bakketun Å., Günther A., Obón de Castro J.M., Tramper J. 1993. Effects of diffusion limitation on immobilized nitrifying organisms at low temperature. Submitted.

Williamson, K., McCarty, P.L. 1976. Verification studies of the biofilm model for bacteria substrate utilization. J. WPCF 48:281-296.

Wise DL, Houghton G (1966) The diffusion coefficients of ten slightly soluble gases in water at 10-60°C. Chem. Eng. Sci. 21:999-1010.

Zevenboom W, Rademaker M, Colijn F (1990) Exceptional algal blooms in dutch north sea waters. In: North Sea pollution, technical strategies for improvement. IAWPRC/EWPCA/NVA, Amsterdam, The Netherlands, 473-486.

8 GENERAL DISCUSSION

T he background of this thesis was a joint research project of the Wageningen Agricultural University, Novem and a manure-treatment company. Integrated nitrification of ammonium from the anaerobically treated manure and from waste gases was the ultimate goal of this project. In chapter 2 and 3 the microbial kinetics at the extreme condition prevailing in such a manure-treatment plant are investigated. A European Community research project of the Wageningen Agricultural University and the Norwegian Institute for Water Research funded the work on the application of nitrification at low temperature. The connection between the extreme conditions prevailing in a manure-treatment plant and at low temperatures is made in chapter 7.

Examples of bench-scale experiments presented in chapter 1 show that nitrification with immobilized cells is a complex process and it is difficult to predict start-up and steady-state conditions from the situation at the beginning of the experiment. An important aspect with respect to this process complexity are the non-uniform conditions within the biofilm and the commensalistic relationship between the two microorganisms involved. In chapter 6 a dynamic model is developed and validated with a technique presented in chapter 5. The dynamic model, based on the microbial kinetics, mass transfer of substrates and air-lift loop reactor properties, is primarily developed for the better understanding of such two-species biofilm processes. For example the occasional substrate and product accumulation in the bench-scale experiments presented in figure 3 and 4 in chapter 1 could be predicted with this dynamic model.

Large volume, low-cost processes like nitrification satisfy the criteria given by Kossen (1992) for processes suitable for optimization studies. The regime analysis presented in chapter 7 provide the tools to optimize the design of large-scale installations at various conditions. The scale-up of the immobilization method, necessary for large-scale applications is presented in chapter 4.

Some questions which arose during the process of writing this thesis and not described in the previous chapters are briefly discussed below.

Microbial kinetics and immobilization. The effects of extreme conditions and low temperature on the kinetic parameters of immobilized cells of *Nitrosomonas europaea* and *Nitrobacter agilis* are assumed to be the same as for suspended cells. The effect of immobilization of these cells on the parameter values is shown by Ginkel et al. (1983) and Tramper & Man (1986). Extrapolation of their results, obtained with various gel bead diameters and cell densities, suggests that the immobilized cells behave as free cells. This observation is confirmed with *Mycobacterium* cells immobilized in alginate (Smith et al. 1993), which where only affected by the calcium ions present in the gel bead but not by the immobilization itself.

Two-substrate limitation. Kinetic parameters for substrate affinity are generally determined with all substrates available in excess except the one for which the substrate affinity is measured. This is not the actual situation for a nitrification process, where in steady-state both substrates are present in very low and therefore limiting amounts. Two-substrate limitation is poorly understood, because it is not easy to measure the conversion rates of the substrates at such low values. The measurement of the oxygen conversion rate requires a highly sensitive oxygen electrode with a short response time. The substrate affinity values for oxygen of *Nitrosomonas europaea* and *Nitrobacter agilis* are within the detection limit of oxygen electrodes. It is therefore possible to measure the oxygen conversion rate in a suspended-cell experiment at substrate concentrations around the substrate affinity values of both substrates. Several methods to describe these two-substrate limitation phenomena are based on: mathematical combinations of two "Monod-like" terms or "most-limiting" substrate (Bader, 1978; Bader, 1982; Mankad & Bungay, 1988; Mankad & Nauman, 1992). The preliminary data (not shown) point in the direction of a "most-limiting" substrate model for the best description of the oxygen conversion rate.

Ion-exchange properties of κ-carrageenan gel. The κ-carrageenan molecule has a negative charge due to the presence of a sulphone group. The gel beads contain 3% w/w κ-carrageenan which means 78 equivalents of negative charge per m^3 of gel (Snoeren, 1976). The negative charge is responsible for ion-exchange properties of the gel, and has a considerable effect on the partition of positive and negative charged ions. The effects on availability of the charged substrates for the immobilized cells and the formation of complexes in the gel beads, sometimes insoluble, are therefore difficult to predict.
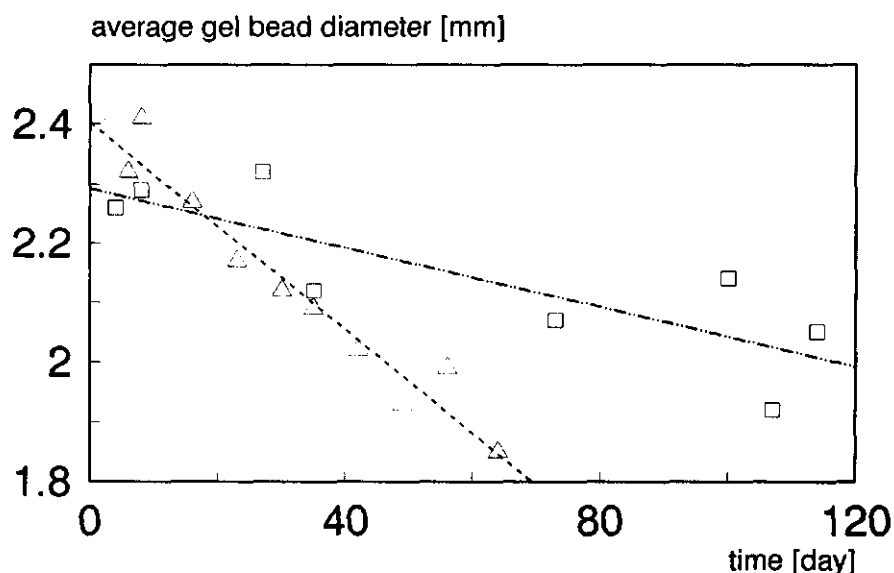
average gel bead diameter [mm]

Figure 1   *The diameter of κ-carrageenan gel beads as function of residence time in the reactor. Air-lift loop reactor of 4 dm^3 (⁻··□⁻··) and 165 dm^3 (– – ◬– –).*

Abrasion. The life-time of the gel beads is important for the economical feasibility of the process. The diameter of the κ-carrageenan gel beads, with growing *Nitrosomonas*

159

europaea and *Nitrobacter agilis* cells, in a 4 and 165 dm³ air-lift loop reactor is shown in Figure 1 as a function of time. The abrasion of the gel beads in the 165 dm³ reactor is faster than in the 4 dm³ reactor. It was not possible to explain the mechanism for this abrasion from the results (not shown) of experiments with gel beads without growing cells in different types of air-lift loop reactors and bubble columns. It was only possible to exclude collision of gel beads as an abrasion mechanism. Obstacles and sharp edges in a reactor can also cause the rapid abrasion of gel beads. This could be responsible for the faster abrasion in the 165 dm³ reactor, which had several obstacles and was not carefully checked for sharp edges.

Applications. Large-scale applications of the nitrification process in air-lift loop reactors are scarce. An air-lift loop reactor for the nitrification of the effluent of anaerobically treated industrial wastewater is presented by Heijnen et al. (1991). They use a solid support with a high density for the attachment of cells. The liquid velocity in the riser should therefore be sufficiently high to keep these cell-covered particles in suspension. As a consequence, their reactor design differs from the design rules given in chapter 7.

CONCLUSIONS

T his thesis provides a set of experimental results and valuable tools for the large-scale application of artificially immobilized nitrifying cells for nitrification of various wastestreams. The next logical step would be application of such an immobilized-cell process under practical conditions.

REFERENCES

Bader FG (1978) Analysis of double-substrate limited growth. Biotech Bioeng 20:183-202.

Bader FB (1982) Kinetics of double-substrate limited growth. In: Microbial population dynamics. Bazin MJ (ed) CRC Press Inc, Boca Raton, Florida, USA. 1-32.

Ginkel CG van, Tramper J, Luyben KChAM, Klapwijk A (1983) Characterization of *Nitrosomonas europaea* immobilized in calcium alginate. Enzyme Microb Technol 5:297-303.

Heijnen JJ, Mulder A, Weltevrede R, Hols J, Leeuwen HLJM van (1991) Large scale anaerobic-aerobic treatment of complex industrial waste water using biofilm reactors. Wat Sci Tech 23:1427-1436.

Kossen NWF (1992) Scale-up in biotechnology. In: Recent advances in biotechnology. Vardas-Sukan F, Sukan ŞS (eds) Kluwer Academic publishers, The Netherlands, 101-136.

Mankad T, Bungay HR (1988) Model for microbial growth with more than one limiting nutrient. J Biotechnol 7:161-166.

Mankad T, Nauman EB (1992) Model of microbial growth under dual limitation. Chem Eng J 48:b9-b11.

Smith MR, Haan A de, Bont JAM (1993) The effect of calcium alginate entrapment on the physiology of *Mycobacterium* sp. strain E3. Appl Microbiol Biotechnol 38:642-648.

Snoeren THM (1976) Kappa-carrageenan, A study on its physico-chemical properties, sol-gel transition and interaction with milk proteins. Dutch Institute for Diary Research (NIZO), Ede, The Netherlands.

Tramper J, Man A de (1986) Characterization of *Nitrobacter agilis* immobilized in calcium alginate. Enzyme Microb Technol 8:472-476.

Summary

S everal aspects of a nitrification process with artificially immobilized cells in an air-lift loop reactor have been investigated and are described in this thesis. In chapter 1 an overview of immobilization methods, suitable reactors, modelling, small-scale applications and scale-up strategy is given. The subjects of chapter 1 provide the starting point of the following chapters. Application of immobilized cells is beneficial for the nitrification process at high product and substrate concentrations and with a process temperature far below the optimal temperature of 30-35°C. In chapter 2 and 3 the kinetics of, respectively, *Nitrosomonas europaea* and *Nitrobacter agilis* cells at high product and substrate concentrations is presented. The results show a severe product inhibition of *Nitrobacter agilis* by nitrite, while *Nitrosomonas europaea* seems to be more sensitive for a high osmotic pressure. In chapter 4 a theoretical background of the immobilization method and further scale-up is presented. For the immobilization method the theory for the break-up of liquid jets, with Newtonian behaviour, is evaluated and a method to apply this theory for non-Newtonian liquids like a κ-carrageenan solution is presented. In chapter 6 a dynamic model for the nitrification with immobilized *Nitrosomonas europaea* and *Nitrobacter agilis* cells is presented. The model includes mass-transfer rates, kinetic behaviour of the microorganisms, and reactor and gel bead properties. Predictions of reactor bulk concentrations of NH_4^+, NO_2^- and NO_3^- (N-compounds) are given by the model together with concentration profiles of N-compounds, oxygen and biomass in the gel beads. A sensitivity analysis of the model parameters shows that the diffusion coefficient of oxygen in the gel beads and the radius of the gel beads are the most important parameters influencing the model output. The model is experimentally validated by means of reactor bulk concentrations and biomass profiles of *Nitrosomonas europaea* and *Nitrobacter agilis* in the gel beads. Predicted and measured values agree very well and the assumptions and equations used in the model seem to be valid. The

biomass profiles of the two microorganisms co-immobilized in the gel beads are determined with immunofluorescence and a stereological method (chapter 5). The immunofluorescence technique was used to separate the *Nitrosomonas europaea* and *Nitrobacter agilis* colonies in the beads. From the position and diameter of the colonies it is possible to determine the spatial distribution of the two microorganisms in the gel beads. In chapter 7 the model is used as a tool to develop a strategy to scale-up the nitrification process with immobilized cells. A design for a large-scale application should be optimized with respect to the transport of oxygen to the immobilized cells in the gel beads. This is an advantage over the nitrification process with suspended cells, which is limited by the growth rate of the nitrifying bacteria. The growth of nitrifying bacteria is a slower process than the transport of oxygen to the cells. Some interesting aspects, which were not treated elsewhere in this thesis, are discussed in the general discussion in chapter 8.

Samenvatting

I n dit proefschrift worden de verschillende aspecten van het onderzoek naar het nitrificatie proces met geïmmobiliseerde cellen in een air-lift loop reactor beschreven. Hoofdstuk 1 bevat een overzicht van immobilisatiemethoden, geschikte reactoren, modellering, kleinschalige toepassingen en de aanpak voor schaalvergroting van het proces. De onderwerpen uit hoofdstuk 1 vormen het startpunt voor de volgende hoofdstukken. Het gebruik van geïmmobiliseerde cellen is een voordeel bij hoge substraat- en produktconcentraties en bij een procestemperatuur ver onder de optimale temperatuur van 30-35°C. In hoofdstuk 2 en 3 wordt het onderzoek naar de relevante kinetische parameters van, respectievelijk, *Nitrosomonas europaea* en *Nitrobacter agilis* beschreven. De resultaten laten zien dat *N. agilis* sterk geremd wordt door het produkt, nitraat, terwijl *N.europaea* meer gevoelig is voor een hoge osmotische druk. De theoretische achtergrond van de immobilisatie methode en verdere schaalvergroting hiervan worden beschreven in hoofdstuk 4. De theorie voor het opbreken van een vloeistofstraal met Newtonse eigenschappen wordt hierin besproken, evenals een methode om deze theorie toe te passen op niet-Newtonse vloeistoffen. In hoofdstuk 6 wordt een dynamisch model voor de nitrificatie met geïmmobiliseerde cellen van *N. europaea* en *N. agilis* gepresenteerd. Het model omvat stofoverdrachtssnelheden, kinetiek van de micro-organismen en reactor- en eigenschappen van de gelbolletjes. In dit hoofdstuk worden ook modelvoorspellingen gepresenteerd van de concentraties stikstof- verbindingen in de reactorbulk en de concentratieprofielen van de stikstofverbindingen, zuurstof en biomassa in de gelbolletjes. Een gevoeligheidsanalyse van de modelparameters laat zien dat de diffusiecoëfficiënt van zuurstof in de gel en de straal van de bolletjes de parameters zijn die de modelvoorspellingen het sterkst beïnvloeden. Het model is experimenteel gevalideerd met behulp van reactor bulkconcentraties en biomassaprofielen in de bolletjes. De voorspelde en gemeten waarden komen goed

overeen en de veronderstellingen die gemaakt zijn bij het opstellen van het model lijken dus juist te zijn. De biomassaprofielen van de twee samen geïmmobiliseerde micro-organismen in de gelbolletjes zijn gemaakt met behulp van immunofluorescentie en een stereologische methode (hoofdstuk 5). De immunofluorescentietechniek wordt gebruikt voor het onderscheidt tussen de *N. europaea* en de *N. agilis* kolonies in de gelbolletjes. Met de bepaling van de positie en de diameter van de kolonies is het mogelijk om de ruimtelijke verdeling van de beide micro-organismen in de bolletjes te beschrijven. In hoofdstuk 7 wordt het model gebruikt bij het ontwikkelen van een strategie voor de schaalvergroting van nitrificatieprocessen met geïmmobiliseerde cellen. Er blijkt dat een ontwerp voor een dergelijke grootschalige toepassing geoptimaliseerd moet worden voor het zuurstoftransport naar de geïmmobiliseerde cellen in de gelbolletjes. Dit is in tegenstelling tot een nitrificatieproces met gesuspendeerde cellen, waar de nitrificatie-snelheid wordt beperkt door de groeisnelheid van de micro-organismen. Deze groeisnelheid is een aanzienlijk trager proces dan het transport van zuurstof.

Enkele interessante onderwerpen die in de voorafgaande hoofdstukken zijn blijven liggen worden in hoofdstuk 8 kort bediscussieerd.

Curriculum vitae

11-9-1958   Jan Hendrik Hunik geboren te Rotterdam.

1970-1979   Nijmeegse Scholen Gemeenschap te Nijmegen afgesloten met achtereenvolgens MAVO, HAVO en Atheneum-B diploma.

1979-1987   Doctoraal examen in de Milieuhygiëne aan de Landbouw Universiteit te Wageningen. Met de afstudeervakken: Microbiologie, Fysische Chemie en Waterzuivering. Stages bij Bavaria B.V. en Montana State University, Montana, Verenigde Staten.

1988-1992   Assistent in Opleiding bij de sectie Proceskunde, Landbouw Universiteit Wageningen.

1993   Post-doc onderzoek bij de sectie Proceskunde, Landbouw Universiteit Wageningen.

1993   Werkzaam bij Unilever Research Laboratorium Vlaardingen, sectie Bioprocessing.